EXPOSURE POTENTIAL OF SULFURIC ACID MIST AT PHOSPHATE FERTILIZER FACILITIES

By

YU-MEI HSU

A DISSERTATION PRESENTED TO THE GRADUATE SCHOOL
OF THE UNIVERSITY OF FLORIDA IN PARTIAL FULFILLMENT
OF THE REQUIREMENTS FOR THE DEGREE OF
DOCTOR OF PHILOSOPHY

UNIVERSITY OF FLORIDA

2008

To my parents, sisters and brother for their constant love, understanding, and support.

ACKNOWLEDGMENTS

I am grateful for Dr. Chang-Yu Wu (my supervisory committee chair) for his patience, guidance, and encouragement. I also sincerely thank Dr. Chang-Yu Wu for giving me the opportunity to study at UF, and letting me learn how to be a good professor and to be patient with others. He is not only my advisor, but also the paragon in my life.

I would like to express my deeply appreciation to Dr. Dale A. Lundgren for his invaluable research experience and his inspiration. My grateful appreciation would also go to Dr. Jean M. Andino and Dr. Wesley E. Bolch for their warmth, kindness and their good-natured support. They have generously given their time and expertise to improve this dissertation.

This study was funded by Florida Institute of Phosphate Research (FIPR). I would also like to express my gratitude to Dr. Brian K. Birky, Research Director for Public Health, for his valuable guidance, advice and comments.

I am grateful to Tom McNally, Robert Ammons, and J. Wesley Nall from the Polk County Health Unit in Winter Haven, Florida for carrying out the pre-sampling and all persons at the phosphate fertilizer plants to help for the field sampling and they are Alan A. Pratt, Melody Foley, Martin St. John, Debra Waters, Paul D. Holewski, Tara Crews, Todd W Smith, and Foster Thorpe.

I thank Dr. Eric Allen for his knowledgeable instruction, and Cheng-Chuan Wang, Hsing-Wang Li, and Shu-Hau Hsu for assisting me in the field sampling, and Joshua Kollet and Katherine Wysocki for helping me with the lab experiments.

Many thanks go to my good friends, Ying Li, Jianmei Liu, Jin-Hwa Lee, Anadi Misra, and Ian Liu, for their patience, kindness, love and warmth. I thank my labmates, Alex Theodore, Jenkins Charles, Danielle Hall, Nathan Topham, Charles Michael Jenkins, Myung-Heui Woo, Lindsey Riemenschneider, and Qi Zhang, who kindly assisted my research.

TABLE OF CONTENTS

LIST OF TABLES

LIST OF FIGURES

Abstract of Dissertation Presented to the Graduate School
of the University of Florida in Partial Fulfillment of the
Requirements for the Degree of Doctor of Philosophy

EXPOSURE POTENTIAL OF SULFURIC ACID MIST AT PHOSPHATE FERTILIZER FACILITIES

By

Yu-Mei Hsu

August 2008

Chair: Chang-Yu Wu
Major: Environmental Engineering Sciences

Strong inorganic acid mists containing sulfuric acid (H_2SO_4) were identified as a "known human carcinogen" in a recent report on carcinogens by the National Toxicology Program where phosphate fertilizer manufacture was listed as one of many occupational exposures to strong acids. To properly assess the occupational exposure to H_2SO_4 mists in modern facilities, the objective of this study was to characterize the true H_2SO_4 mist concentration levels.

Three sets of experiments were conducted. Firstly, field sampling using dichotomous samplers, silica gel tubes and cascade impactors was conducted to collect the $PM_{2.5}/PM_{10}$ H_2SO_4 mist concentration, total H_2SO_4 mist concentration, and size-resolved H_2SO_4 mist concentration, respectively, at phosphate fertilizer plants.

The H_2SO_4 concentrations were found to vary significantly among these plants with H_2SO_4 pump tank areas having the highest concentration level. When high aerosol mass concentrations were observed, the H_2SO_4 mist had its mode size in the 3.8—10 μm range that would deposit in the upper respiratory region.

Secondly, SO_2 adsorption and sulfur(IV) oxidation were investigated under various sampling times, SO_2 concentrations and sampling flowrates. Experimental results verified that the collecting medium can adsorb SO_2 gas and the extraction procedure of NIOSH Method 7903

aids the transformation of SO_2 into sulfate to cause a positive artifact. The experimental data were also fitted into a deactivation model for estimating the artifact sulfate concentration.

Thirdly, a honeycomb denuder system and the deactivation model were applied to minimize the artifact sulfate of NIOSH Method 7903 in a field sampling campaign. Both the system and the model were shown to effectively reduce the artifact sulfate concentration. However, the concentration thus determined was still higher than that measured by a cascade impactor which had no artifact. One possible reason is the residual sulfate in the collecting medium.

CHAPTER 1
INTRODUCTION

Sulfuric Acid Mist and Its Health Effects

Strong inorganic acid mists containing sulfuric acid (H_2SO_4) have been reported to correlate with the incidence of lung and laryngeal cancers in humans [*Blair and Kazerouni*, 1997; *Sathiakumar et al.*, 1997; *Steenland*, 1997] and are identified as a "known human carcinogen" as reported by the U.S. National Toxicology Program (NTP) [*USDHHS*, 2005]. Sulfuric acid is typically present in the air as a mist. Its chemical characteristics include low volatility, high acidity, high reactivity, high corrosivity, and high affinity for water. Sulfuric acid also irritates the human airways, and this irritation may potentially damage pulmonary epithelium, causing subsequent carcinogenic effects from other inhaled substances.

Although the carcinogenetic mechanism of sulfuric acid mist is not known [*Blair and Kazerouni*, 1997], a low pH environment has been reported to induce chromosomal aberrations, gene mutation and cell transformation. Depurination, which is the removal of a purine (adenine or guanine) from a DNA molecule, and deamination of cytidine in DNA molecules, which is the replacement of the amine functional group by the ketone group, has been shown to be enhanced by exposure to sulfuric acid mist [*Swenberg and Beauchamp*, 1997]. In a case study of workers engaged in the manufacture of sulfuric acid, significant increases were observed in the incidences of genotoxic effects, including sister chromatid exchange (an exchange of segments between the sister chromatids of a chromosome), micronucleus formation, and chromosomal aberration in peripheral lymphocytes [*Meng et al.*, 1995; *Meng and Zhang*, 1997]. As exposure to chemical fumes is suspected to be one of the reasons for lung cancer formation, information regarding the concentration levels of the acid mists is of seminal importance.

Sulfuric Acid Regulations

The current Occupational Safety & Health Administration (OSHA) 8-hour time-weighted average (TWA) of permissible exposure level (PEL) for sulfuric acid mist is currently set at 1 mg/m^3 with its 15-min short-term exposure level (STEL) set at 3 mg/m^3 [*CFR*]. It is well known that the deposition of an aerosol in the respiratory system depends on its aerodynamic behavior. Aerosols with an aerodynamic diameter larger than 1 μm mainly deposit in the extrathoracic airways, and ultrafine aerosols with particle sizes less than 0.01 μm predominantly deposit in the tracheobronchial region by Brownian motion, whereas aerosols of intermediate diameter deposit in the alveolar regions [*Hinds*, 1999]. In considering the effects of aerosol size, the American Conference of Governmental Industrial Hygienists (ACGIH) has adopted a threshold limit value-time-weighted average (TLV-TWA) of 0.2 mg/m^3 for the thoracic particulate fraction of sulfuric acid mist [*ACGIH*, 2004].

Sulfuric Acid Mist in Manufacturing Facilities

Several studies have reported sulfuric acid concentrations in worker environments. In a sulfuric acid plant in Sweden [*Englander et al.*, 1988], the concentration was at 0.1 to 3.1 mg/m^3 for samples taken in 1979–1980. In a Finnish sulfuric acid plant [*Skyttä*, 1978], the concentration was measured within the range of 0 to 1.7 mg/m^3. The concentration in a Russian plant [*Petrov*, 1987] was found to be higher, ranging from 1.8 to 4.6 mg/m^3. Samples taken in a sulfuric acid plant at a U.S. copper smelter in 1984 showed lower concentrations ranging form 0.15 to 0.24 mg/m^3. Limited information regarding the mist size distribution in sulfuric acid production plants is available [*Muller*, 1992]. It is reported that the size of mist particles ranged from about 0.1 μm to greater than 10 μm.

There are no current reports characterizing sulfuric acid mist in the fertilizer manufacturing industry. Studies cited in the NTP report were all carried out a few decades ago.

Increased rates of lung cancer in correlation with exposure to chemical fumes in some of these studies are the reason for recent concerns. A historical cohort study [*Hagmar et al.*, 1991] on workers employed in a Swedish fertilizer factory was carried out for two cohorts (1236 men in 1906–62 and 2131 men in 1963–85). Significant excesses were found for cancers of the respiratory tract and lung cancers. The results from U.S. studies, on the other hand, showed different trends. A cohort study was carried out for men who worked in Florida phosphate processing facilities during 1949–1978 [*Checkoway et al.*, 1985a; 1985b]. Lung cancer mortality was higher than that found in for the entire U.S. population although this rate was insignificant when compared to the Florida population. Internal comparison for mortality rates from lung cancer was also conducted for the same population. For workers in sulfuric and phosphoric acid production, no consistent increase in relative risk for lung cancer was found. National Institute for Occupational Safety and Health (NIOSH) researchers conducted an investigation at a phosphate fertilizer production facility in Polk County [*Stayner et al.*, 1985]. Three major acids identified by the personal and area samplings were fluorides (mean: 3.39 mg/m^3), sulfuric acid (mean: 0.11 mg/m^3) and phosphoric acid (mean: 0.25 mg/m^3). A total of 3199 subjects who had worked at the plant from 1953–1976 were studied. Overall mortality and morbidity from all cancers were lower than expected, and the risk for lung cancers increased only slightly. Another study [*Block et al.*, 1988] carried out for male workers in another Florida phosphate company between 1950 and 1979 showed a significant excess of lung cancer deaths among white workers in comparison to both U.S. rates and Florida rates. However, when an internal comparison of job categories was made with respect to lung cancer, no increase was found for workers exposed to chemical fumes (sulfuric acid, sulfur dioxide and fluorides).

Limited information on acid mist concentrations in the phosphate fertilizer manufacturing industry is available. In U.S. facilities, the mean sulfuric acid mist concentration ranges from 0.07 to 0.571 mg/m^3 [*Apol et al.*, 1987; *Cassady et al.*, 1975; *Stephenson et al.*, 1977]. The concentration reported in a Finnish study [*FIOH*, 1990] was 8.3 mg/m^3 (1951 data). A Russian study [*Tadzhibaeva and Gol'eva*, 1976] also reported a high sulfuric acid mist concentration, 2.7 to 9.2 mg/m^3. Compared to foreign facilities, sulfuric mist concentrations in U.S. plants were low, and the OSHA standard of 1 mg/m^3 was met. Size distribution related to sulfuric acid mist emission in the fertilizer manufacture industry, however, is not available.

Manufacturing Processes in Fertilizer Manufacturing Facilities

Phosphate rock, which is the main useful product of phosphate ore, consists of calcium phosphate mineral apatite ($Ca_5(PO_4)_3(OH, F, Cl)$) with gangue constituents including silica (SiO_2), fluoride (F), calcite ($CaCO_3$), dolomite ($CaMg(CO_3)_2$), clay, and iron-aluminum oxide (Fe_2O_3, Al_2O_3). Several chemical formulas are commonly used for phosphate rock which includes fluorapatite ($Ca_5(PO_4)_3F$), chlorapatite ($Ca_5(PO_4)_3Cl$) and hydroxyapatite ($Ca_5(PO_4)_3(OH)$). The United States is the principal producer of chemical fertilizer using phosphate rock [*Hodge*, 1994].

The final products from phosphate fertilizer plants in Florida are mainly diammonium phosphate (DAP), monoammonium phosphate (MAP), and concentrated sulfuric acid solution. Wet process using sulfuric acid to react with phosphate rock is commonly used by the phosphate fertilizer industry in Florida to produce phosphoric acid. Figure 1-1 shows the manufacturing process flow, which can be divided into three stages.

In the first stage, phosphate rock reacts with sulfuric acid at the attack tank to produce phosphoric acid with 30-55 wt% P_2O_5. The simplified reactions of the wet process at the attack tank (also called as reactor) are shown in Reaction 1-1 [*Palm*, 1992]. Sulfuric acid of 93% is fed

into the attack tank. The violent reaction between phosphate rock and sulfuric acid causes heat release in the form of vapor, which is evacuated from the attack tank with other gaseous effluents. A cooling system is needed to maintain the temperature at 70–80 °C in this process [*Becker*, 1989].

$$Ca_{10}(PO_4)_6F_2 + 10H_2SO_4 + 20H_2O \rightarrow 10CaSO_4 \cdot 2H_2O + 6H_3PO_4 + 2HF \quad (1\text{-}1)$$

At the second stage, the reaction product from the first stage passes through a rotating table filter or belt filter to separate phosphoric acid from its byproduct phosphogypsum (calcium sulfate dihydrate, $CaSO_4 \cdot 2H_2O$). A cooling system is applied to maintain the temperature at 70–75 °C in this process [*Becker*, 1989]. Some H_3PO_4 is lost to phosphogypsum from this process.

At the third stage, the final product, MAP or DAP, is produced by reacting phosphoric acid of 30-55% P_2O_5 (by weight) with ammonia at the granulator, as shown in Reaction 1-2 and 1-3. When poor product quality is detected, weak sulfuric acid is used to scrub the granulator.

$$H_3PO_4 + NH_3 \rightarrow (NH_4)H_2PO_4 \quad (1\text{-}2)$$

$$H_3PO_4 + 2NH_3 \rightarrow (NH_4)_2HPO_4 \quad (1\text{-}3)$$

The manufacturing process of sulfuric acid can also be divided into three stages:

(1) The production of sulfuric acid starts from the combustion of elemental sulfur (S) to produce sulfur dioxide (SO_2). Elemental sulfur is pumped into the sulfur burner and is burned with dry combustion air to form SO_2. Sulfur dioxide and excess air leave the burner at 700–1,000 °C which need to be cooled to 425 °C to protect the converter in the next stage [*Muller*, 1992].

(2) At the second stage, SO_2 is subsequently oxidized to form sulfur trioxide (SO_3) when passing through a series of catalytic converters. The reaction proceeds as Reaction 1-4 which is

an exothermic reaction. This equilibrium equation is controlled by the concentrations of SO_2, SO_3 and temperature. High SO_3 concentration and temperature can favor the reverse reaction. The temperature is 180–250 °C when gas leaves the converter [*Muller*, 1992].

$$SO_{2(g)} + \frac{1}{2}O_2 \leftrightarrow SO_{3(g)} \qquad (1\text{-}4)$$

$\Delta H \approx$ - 41,400 Btu/lb·mol

(3) Sulfur trioxide can quickly combine with water vapor to produce sulfuric acid at the sulfuric acid pump tank. The reaction is shown as Reaction 1-5, which is also an exothermic reaction [*Ridler*, 1959].

$$SO_{3(g)} + H_2O_{(g)} \rightarrow H_2SO_{4(l)} \qquad (1\text{-}5)$$

The produced sulfuric acid is stored in tanks. Some plants produce more sulfuric acid than needed and sell excess sulfuric acid solution to other companies. Trucks are used for the transportation of sulfuric acid solution. The loading and unloading of sulfuric acid solution is carried out through a nozzle at a truck station.

Sulfuric Acid Mist Measurement

Sulfuric acid exists in the mist form which can be collected by filtration. NIOSH Method 7903 is an OSHA approved method which employs a silica gel tube to collect acid mist. The silica gel tube consists of one section of glass fiber filter plug and two sections of silica gel. The glass fiber filter and the silica gel are designed to collect aerosols and acid gases, respectively. NIOSH Method 7903 is the method commonly applied for personal sampling in the workplace due to its convenience. However, both the glass fiber filter and silica gel can adsorb SO_2 [*Chow*, 1995; *Lee and Mukund*, 2001] that will lead to an overestimate of sulfate.

Phosphate Fertilizer Manufacture in NTP Report

Although phosphate fertilizer manufacture was listed in the NTP report [*USDHHS*, 2005] as one of many occupational exposures to strong inorganic acids, the occupational exposures to inorganic acid mists containing sulfuric acid existing at levels equal to or greater than the PEL used by the International Agency for Research on Cancer (IARC) are based on results obtained during the period 1951 to 1976. In addition, all of the results greater than the PEL for sulfuric acid are from outside the U.S. [*USDHHS*, 2005]. The significant improvement of health and safety measures in the US fertilizer industry in the past decades is expected to have significantly lowered current levels. Excessive respiratory protection may be costly and stressful and still not provide any beneficial reduction in exposure. Thus, characterization of the true exposure level at modern facilities is a necessary step to the establishment of the best policy for worker protection.

Research Objectives

Five objectives were set in this doctoral research study to accurately characterize sulfuric acid mist at phosphate fertilizer facilities. The first objective is to characterize the major water soluble ionic species of $PM_{2.5}$ and $PM_{2.5-10}$ at phosphate fertilizer facilities. The location with high chemical species concentrations can be identified as well. The characterization can be applied for the establishment of the best policy for worker protection.

The second objective is to determine the sulfuric acid mist concentrations with size-resolved information by a cascade impactor and the total sulfuric acid mist concentration using NIOSH Method 7903. The study also seeks to determine the correlation between these two samplers at the phosphate fertilizer facilities.

The third objective is to determine the chemical characteristics of mist aerosols in the current phosphate facilities with size-resolved information and to estimate the aerosol hydrogen ion concentration at the phosphate fertilizer facilities using a thermodynamic model.

The fourth objective is to verify and quantify the effect of SO_2 interference on the artifact sulfate in NIOSH Method 7903. The oxidation of sulfur(IV) into sulfate and SO_2 adsorption following the NIOSH protocol were also investigated in this study.

The fifth objective is to investigate the effectiveness of two methods, a deactivation model and a honeycomb denuder system, to minimize the artifact sulfate in a field sampling at the phosphate fertilizer facilities.

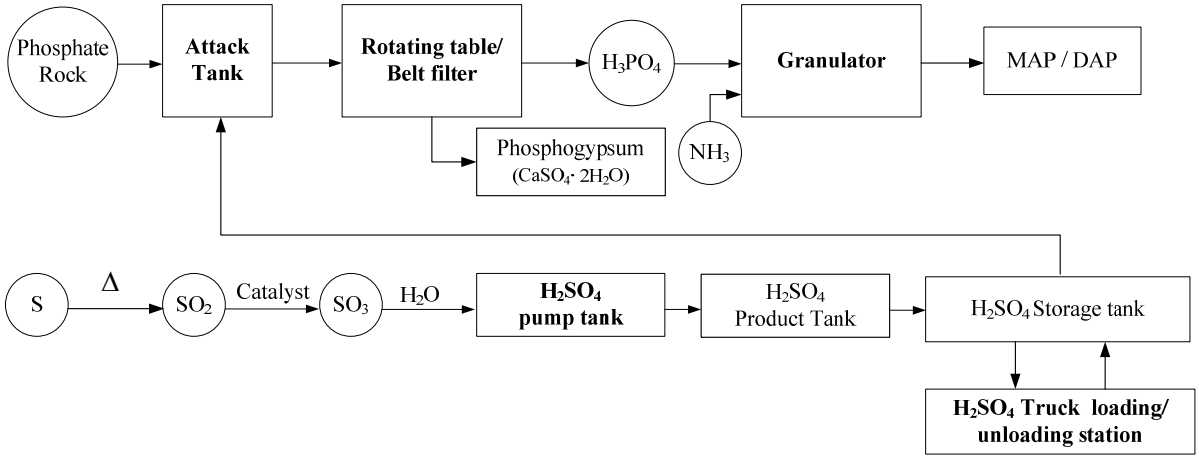

Figure 1-1. Monoammonium phosphate and diammonium phosphate manufacturing process

CHAPTER 2
CHEMICAL CHARACTERISTICS OF AEROSOL MISTS IN PHOSPHATE FERTILIZER MANUFACTURING FACILITIES*

Background

Phosphate products are widely used around the world for fertilizer (90%), detergents (4.5%), animal feed (3.3%), and food and beverages (0.7%) [*Becker*, 1989]. The United States is the second largest producer of phosphate fertilizers in the world [*Bhaskaran et al.*, 2004]. The manufacturing process flow of phosphate fertilizer is shown in Figure 2-1. In Florida, phosphoric acid is usually produced by a wet process by reacting H_2SO_4 with naturally occurring phosphate rock in a reactor that is referred to in the industry as the "attack tank". Phosphogypsum is a byproduct of this process. The simplified reactions of the wet process are as Reaction 2-1 [*Becker*, 1989]:

$$Ca_{10}(PO_4)_6F_2 + 10H_2SO_4 + 20H_2O \rightarrow 10CaSO_4 \cdot 2H_2O + 6H_3PO_4 + 2HF \quad (2\text{-}1)$$

Rotating table filters and belt filters are used to separate phosphoric acid and phosphogypsum. Phosphoric acid of 30-55% P_2O_5 (by weight) reacts with ammonia to produce MAP or DAP in the granulator, as shown in Reaction 2-2 and Reaction 2-3 [*Hodge and Popovici*, 1994].

$$H_3PO_4 + NH_3 \rightarrow (NH_4)H_2PO_4 \quad (2\text{-}2)$$

$$H_3PO_4 + 2NH_3 \rightarrow (NH_4)_2HPO_4 \quad (2\text{-}3)$$

In these facilities, H_2SO_4 used for digestion of phosphate ores is produced by sulfur combustion [*Hodge and Popovici*, 1994]. The sulfuric acid production process initiates in a sulfur burner. The resulting combustion gas consists primarily of SO_2 that is routed to a series of

* Reprinted with permission from Hsu, Y.-M., Wu, C.-Y., Lundgren, D. A., Nall, J. W., Birky, B. K., 2007. Chemical Characteristics of Aerosol Mists in Phosphate Fertilizer Manufacturing Facilities. *J. Occup. Environ. Hyg*. 4, 17-25.

catalytic converters to transform the sulfur dioxide into SO_3. By mixing with water, sulfur trioxide quickly forms sulfuric acid that is moved from pump tanks to storage tanks for use in the production of phosphoric acid. Some facilities produce more sulfuric acid than needed and sell the excess to others.

Reduced pH environments are known to enhance the depurination (i.e. removing a purine (adenine or guanine) from a DNA molecule) rate of DNA and the deamination (that is, replacing the amine functional group by the ketone group) rate of cytidine [*USDHHS*, 2005], which can cause DNA damage or mutation. Sulfuric acid also irritates the human airway, and this irritation may potentially damage the epithelium, causing subsequent carcinogenic effects of other substances [*ACGIH*, 2004].

Phosphate fertilizer manufacture was listed in the report as one of many occupational exposures to strong inorganic acids. However, the occupational exposures to inorganic acid mists containing sulfuric acid existing at levels equal to or greater than PEL used by the IARC are based on results obtained during 1951-1976 [1992]. In addition, all of the results used by the IARC greater than the PEL for sulfuric acid were from outside the United States [*Tadzhibaeva and Gol'eva*, 1976]. In U.S. facilities, the sulfuric acid mist mean concentration ranged from 0.07 to 0.57 mg/m^3 [*Apol et al.*, 1987; *Cassady et al.*, 1975; *Stephenson et al.*, 1977]. The significant improvement of environmental, health, and safety measures in the U.S. fertilizer industry in the past is expected to have greatly lowered current levels.

The objective of this chapter was to characterize the thoracic particulate fraction of chemical species concentration level at phosphate fertilizer facilities in Florida. The chemical species concentration level would be applied to estimate the required sampling time for a cascade impactor sampling. The information is critical for health risk assessment, is useful in identifying

the key sources. Such characterization is a necessary step in the establishment of the best policy for worker protection.

Methods

Sampling Locations

Due to the different manufacturing process designs among these phosphate fertilizer plants, the aerosol emission sources at each plant are different. Two to five locations at each plant were selected where sulfuric acid mists may exist. These locations included the top of sulfuric acid pump tank, attack tank (reactor), filtration floor, sulfuric acid truck loading/unloading station, and granulator on a scrub day (Figure 2-1 and Table 2-1). In total, there were 24 sampling locations in eight plants and two background locations included in this study. The geographic locations of these sampling sites are shown in Figure 2-2. Winter Haven, FL and Gainesville, FL, were employed as the background locations. Gainesville is located between the plant in north FL and the plants in central FL. Winter Haven is located at the east of the plants in central FL. The distance between Gainesville and the nearest plant in north FL is approximately 60 miles; the distance between Winter Haven and the nearest plant in central FL is approximately 20 miles. Three samples were obtained at each location. Due to the low particulate concentration at the background locations, sampling was carried out for 24 h.

The sulfuric acid pump tank is where the newly produced sulfuric acid is distributed to sulfuric acid storage tanks. The leakage of SO_3 from ducting can bind with moisture to form fine aerosols. Gas duct leaks in the sulfuric acid production plant are normally repaired quickly and are extremely difficult to sample. The sampling location chosen in the sulfuric acid production plants was on top of the sulfuric acid pump tank because the pump tank is vented to atmosphere and has a large throughput.

The attack tank is where sulfuric acid reacts with phosphate rock. The strong reaction between sulfuric acid and phosphate rock causes the production of gaseous species that attach to existing aerosols or form aerosols by reacting with other gaseous species. Therefore, in the phosphoric acid production plants, sampling locations were chosen near the attack tanks.

Two different types of product filters are used in these plants, including a belt filter and a rotating table (commonly the Bird type) filter where the reaction products are filtered and washed under vacuum to separate phosphoric acid and phosphogypsum. The rotating table filter is a circular table with pie-shaped filter pans that rotate in a circular motion while filtering out the phosphogypsum. The individual pan tilts and dumps the washed phosphogypsum into a hopper for pumping to a phosphogypsum storage mound. The belt filter is a continuous belt that washes the phosphogypsum at different sections along the belt and dumps the gypsum at the end of the belt into a hopper for distribution to the phosphogypsum storage area. Sampling locations were selected adjacent to both types of filters.

The sulfuric acid truck station (an outdoor location) is where trucks load or unload sulfuric acid. Sampling was conducted near the loading nozzle as this location is where sulfuric acid is most likely to enter the atmosphere.

The last sampling location was at the granulator on a "scrub" day when the product line is shut down to clean the piping and ductwork by spraying a mixture of process water and small amounts of sulfuric acid. This solution is recirculated from open-top tanks during the scrub cycle. Sampling was conducted adjacent to these tanks.

Sampling and Analysis Methods

Dichotomous samplers (model SA241 CUM; Anderson Instruments, Atlanta, GA) were used to separate aerosols into two sizes: fine mode (aerodynamic diameter smaller than 2.5 μm

or $PM_{2.5}$) and coarse mode (aerodynamic diameter ranges from 2.5 to 10 μm or $PM_{2.5-10}$). The reason for using dichotomous samplers is because PM_{10} curve is similar to the thoracic fraction. The sampling flow rates were 1.67 and 15 Lpm for the fine and coarse mode, respectively. The sampling time in the production facilities was 12 h. Three samples were obtained at each location. The total sample numbers (plants) at the pump tank area, rotating table/belt filter floor, attack tank area, truck station, and the granulator (on a scrub day) were 27(8), 27(8), 6(2), 9(3), and 2(1), respectively.

Zefluor, or backed Teflon, membrane filters (P5PJ001, 8 × 10 inches, 2.0 μm, Pall Corp., Ann Arbor, MI) were used to collect the aerosol. Zefluor membrane filters provide high collection efficiency and low reactivity with acidic gases [*Baron and Willeke*, 2001; *Chow*, 1995]. A microbalance (model MC 210 S, Sartorius Corp., Edgewood, N.Y.; readability 10 μg) was used for weighing the particle mass. Filters were placed in a desiccator at room temperature for pre- and post-conditioning for 24 h before weighing the filters. The vapor pressures of sulfuric acid mist and phosphoric acid are low and they remain in the mist form at this condition. An ion chromatography (IC) system (Dionex ICS 1500; Dionex Corp., Atlanta, GA) was used to analyze the soluble ions of the samples. The analysis conditions are shown in Table 2-2. Fluoride, chloride, nitrate, sulfate, phosphate, sodium, potassium, calcium, and magnesium were analyzed and the IC's detection limit for each ion is listed in Table 2-3.

Using this analysis method, it is impossible to distinguish whether the sulfate measured is from sulfuric acid or other sulfates (e.g., ammonium sulfate, calcium sulfate). Consequently, all particulate sulfate was assumed to be sulfuric acid mist in this study [*NIOSH*, 1994]. The conversion of sulfuric acid mist concentration from sulfate concentration follows Equation 2-4 listed below:

$$\left[H_2SO_4\right]\ \left(\mu g/m^3\right)=\left[SO_4^{2-}\right]_{\text{measured by IC}}\left(\mu g/m^3\right)\times\frac{98(\text{M.W. of } H_2SO_4)}{96(\text{M.W. of } SO_4^{2-})} \quad (2\text{-}4)$$

Results and Discussion

Background Sites

Table 2-4 shows the median ion species concentrations at the two background sites. The median $PM_{2.5}$ and $PM_{2.5\text{-}10}$ concentrations (N = 3) in Gainesville were 15.0 and 11.2 μg/m^3, and the maximum PM_{10} concentration was 29.7 μg/m^3. The median $PM_{2.5}$ and $PM_{2.5\text{-}10}$ concentrations (N = 3) in Winter Haven were 26.2 and 13.7 μg/m^3, and the maximum PM_{10} (the sum of $PM_{2.5}$ and $PM_{2.5\text{-}10}$) concentration was 50.9 μg/m^3. The mass concentrations in Winter Haven were slightly higher than in Gainesville. The mass concentrations of the fine mode were higher than the coarse mode. Overall, the mass concentrations at both locations were not high. The major species of the $PM_{2.5}$ in Gainesville were sulfate (median: 5.05 μg/m^3) and ammonium (median: 4.24 μg/m^3), and the concentrations of all other species were low. The major species in Winter Haven was ammonium. The median concentration was 5.10 μg/m^3 for $PM_{2.5}$ and 7.78 μg/m^3 for $PM_{2.5\text{-}10}$. Phosphate concentrations were lower than the detection limit at both locations; however, low fluoride concentrations were observed in Winter Haven (0.086- 0.149 μg/m^3). The major fluoride emission source is fertilizer facilities in central Florida [*USEPA*, 1995]. Hence, the particulate fluoride might come from these facilities.

Mass Concentrations Measured in the Facilities

The aerosol mass concentrations at 24 locations are summarized in Figure 2-3 with their maximum, minimum, mean, and median at each type of location. As shown, the mass concentration varied significantly from one location to the other and within each type of location. There are various factors that may affect the concentration level, such as production activity

level and types of processes. Weather and ambient aerosols may also affect outdoor locations like the sulfuric acid pump tank and the sulfuric acid truck station.

The rotating table/belt filter floor had a high aerosol mass concentration due to mechanical agitation and gas species condensation. The median values (range) of the fine mode and the coarse mode were 77.8 (27.8–381) and 79.5 (25.7–338) $\mu g/m^3$, respectively. Among the various locations, the attack tank had the highest fine mode aerosol mass concentration. The median value (range) of the fine mode was 389 (98.6–894) $\mu g/m^3$ and its coarse mode mass concentration (range) was 58.1 (13.6–266) $\mu g/m^3$. At the attack tank, the strong reaction of sulfuric acid and phosphate rock releases heat and some species that have high vapor pressures. In general, the attack tank and the rotating table/belt filter floor are the two major emission sources of aerosol in these facilities whereas the aerosol mass concentrations are lower at the sulfuric acid pump tank, the truck loading/unloading station and granulator on a scrub day.

Ion Concentrations Measured in the Facilities

The results of ion analysis are presented in Figure 2-4 to Figure 2-7 for the sulfuric acid pump tank area, the attack tank area, the filter floor, and the truck station, respectively. At the sulfuric acid pump tank area (Figure 2-4), sulfate was the dominant species, and the median (minimum and maximum) concentrations were 15.3 (1.33 and 77.0) and 5.1 (0.501 and 104) $\mu g/m^3$ for the fine mode and the coarse mode, respectively. The maximum PM_{10} sulfate concentration, 181 $\mu g/m^3$, is equivalent to a maximum sulfuric acid mist concentration of 185 $\mu g/m^3$, which is lower than 0.2 mg/m^3, the TLV-TWA of the thoracic particulate fraction of sulfuric acid recommended by ACGIH.

In the sulfuric acid manufacturing process, SO_3 is present in the ductwork of the plant before being absorbed into the acid stream. Any leak from the duct can release SO_3 that can

readily react with moisture in the air to produce H_2SO_4 mist [*Finlayson-Pitts and Pitts*, 2000]. The temperature at the pump tank is about 110 °C, which is not high enough to evaporate H_2SO_4 (boiling point around 330 °C) [*Weast*, 1988]. The leakage of SO_3 from surrounding ductwork is likely to be the main source that causes higher relative sulfuric acid mist concentrations at the sulfuric acid pump tank area. In addition to the SO_3 emission rate, the other important factor that can influence the aerosol size of the mist is humidity. High humidity assists the condensational growth of sulfuric acid mist, whereas a high emission rate aids the nucleation of ultrafine sulfuric acid mist. Ammonium was also the dominant species, and the median (minimum and maximum) concentrations were 8.7 (1.40 and 22.1) and 2.5 (0.428 and 25.9) $\mu g/m^3$ for the fine mode and the coarse mode, respectively.

The fast reaction of ammonia gas and sulfuric acid mist to form ammonium sulfate ($(NH_4)_2SO_4$) is likely the mechanism responsible for the ammonium concentration. Although this location is not expected to have ammonia gas emissions, ammonia comes from other locations in these plants and also commonly exists in ambient air. The presence of ammonia gas can neutralize the acidity of sulfuric acid or acidic aerosol. Regarding other ions such as fluoride, chloride, phosphate, sodium, potassium, magnesium and calcium, these outdoor locations have generally low concentrations.

At the attack tank area (Figure 2-5), fluoride was the dominant species, and the median (minimum and maximum) concentrations were 105 (7.25 and 455) and 21.2 (1.22 and 85.9) $\mu g/m^3$ for the fine mode and the coarse mode, respectively. The maximum PM_{10} fluoride concentration was 541 $\mu g/m^3$; the TWA-PEL of fluoride is 2 mg/m^3. The attack tank is where sulfuric acid reacts with phosphate rock that mainly contains calcium, phosphate, and fluoride. The reaction products are phosphoric acid and phosphogypsum, which will precipitate.

The violent reaction also produces heat and water vapor from this process, and gaseous fluorides (silicon tetrafluoride (SiF_4) and hydrogen fluoride (HF)) are the byproducts from this process [*Mann*, 1992]. In the weak phosphoric acid production of 30% P_2O_5, SiF_4 is the major fluoride form to volatilize because of its higher vapor pressure. The molar ratio of HF to SiF_4 is less than 2 when the phosphoric acid is below 50% P_2O_5. Increasing the concentration of P_2O_5 to 50% makes more HF escape from liquid phase [*Denzinger et al.*, 1979]. In the presence of atmospheric moisture, fluorosilicic acid (H_2SiF_6), hydrogen fluoride and silicon oxide are created (Reaction 2-5 to Reaction 2-8) [*Hodge and Popovici*, 1994]. The gaseous fluorides adsorption process is dependent on the surface area of water droplet. Therefore, the size distribution of water droplets may influence the partitioning of fluoride.

$$SiO_2 + 4\ HF \rightarrow SiF_4 + 2\ H_2O \quad (2\text{-}5)$$

$$3\ SiF_4 + 2\ H_2O \rightarrow 2\ H_2SiF_6 + SiO_2 \quad (2\text{-}6)$$

$$SiO_2 + 6\ HF \rightarrow H_2SiF_6 + 2\ H_2O \quad (2\text{-}7)$$

$$H_2SiF_6 \rightarrow SiF_4 + 2\ HF \quad (2\text{-}8)$$

For the rotating table/belt filter floor, fluoride was the dominant species for the fine mode (median: 3.9 $\mu g/m^3$; range: 0.173–106 $\mu g/m^3$), whereas phosphate, sulfate, and ammonium were also important. The rotating table and belt filters are open systems used to filter intermediate products to obtain 30% phosphoric acid. The temperature of this process is about 100 °C. Because it is an open system operating at high temperature, water, gaseous fluoride, and phosphoric acid evaporate to form fine mist aerosols. Ammonia gas is easily absorbed into the acid mist to neutralize the acid. Phosphate was the major constituent for the coarse mode (median: 22.3 $\mu g/m^3$; range: 2.33–122 $\mu g/m^3$), whereas sulfate and ammonium were also important. For PM_{10}, phosphate was the major species and its highest concentration was 170

$\mu g/m^3$. Filter cake formed in this filtration process, which mainly consists of phosphogypsum, contributes to the loading of the coarse particles due to mechanical agitation. As shown, the calcium concentration of the coarse mode is higher than the fine mode. The vaporized acids can also condense on these mechanically agitated wet particles. Therefore, they were also present in the coarse mode.

At the sulfuric acid truck loading and unloading stations, ammonium and sulfate were the dominant species for the fine mode (median: 9.5 and 4.2 $\mu g/m^3$, respectively) and the concentration ranges of ammonium and sulfate were 4.77–32.9 and 0.613–9.74 $\mu g/m^3$, respectively. Phosphate, ammonium and sulfate were the dominant species for the coarse mode (median: 8.5, 5.2 and 3.3 $\mu g/m^3$) and their ranges were 1.26–48.4, 0.3–13.6, and 1.36–12.8 $\mu g/m^3$. For this outdoor location, the possible period to release sulfuric acid is when trucks load and unload sulfuric acid, which is usually 2-3 h/day. This emission is not a continuous source. Hence, most of the time, the aerosol loading was greatly influenced by the ambient condition and likely the aerosols were from other locations in the plant. In summary, the concentrations of all species were low.

Sampling for the granulator on a scrub day was conducted in one facility only. The median concentrations (N = 2) are shown in Table 2-5. For the fine mode, fluoride and ammonium were the dominant species; for the coarse mode, phosphate, fluoride, and ammonium were the major ones. In normal operation, 30% phosphoric acid is present in this system. In this plant, the period of scrubbing was about 4 h, and a weak sulfuric acid solution was used to scrub the piping and ductwork. Nevertheless, sulfate concentration was low at this location.

Aerosol Acidity

The hydrogen ion plays an important role in the carcinogenetic mechanism and skin irritation. Therefore, hydrogen ion concentration in the aerosol provides very useful data for assessing the health risk. Assuming that charge balance of those ions exists in the aerosols in this study, hydrogen ion concentration can be estimated by Equation 2-9:

$$[H^+] (\mu eq/m^3) = [Anion] - [Cation] \quad (2\text{-}9)$$

Anion species include phosphate, fluoride, sulfate, chloride, and nitrate; cation species include ammonium, sodium, potassium, calcium, and magnesium. The statistics of hydrogen ion concentrations at each location are shown in Table 2-6. Fine mode aerosol at the attack tank area had the highest hydrogen ion concentration, 20.7 $\mu eq/m^3$ or 20.7 $\mu g/m^3$ with a median of 4.4 $\mu eq/m^3$, indicating they were strongly acidic. On the other hand, the average hydrogen ion concentration at sulfuric acid pump tank areas (fine mode) and sulfuric acid truck stations were negative (i.e., the aerosol had excess OH^-), which indicated that the aerosol was somewhat basic.

The relationship of cation equivalent weight and anion equivalent weight is shown in Figure 2-8, which can be used to determine the acidity of the aerosol. The key factors that can control the acidity of the aerosol are the amounts of basic or acidic species. The acidic species in these plants include fluoride, sulfate, and phosphate. The only basic gas in the plant that can neutralize all acid species (i.e., sulfuric acid, gaseous fluoride, and phosphoric acid) is ammonia. In Figure 2-8, the cation and anion equivalent weights can be divided into two regions: smaller than 3 and larger than 3 $\mu eq/m^3$. In the case of low acid species loading, the aerosol acidity can be influenced by the presence of basic species; however, at high acid species loading, the limited amount of basic species may not be enough to neutralize the aerosol acidity. At the rotating table/belt filter floor and the attack tank, the main acidic gases such as gaseous fluoride and

phosphoric acid are emitted from the process, and there is no source of ammonia in these indoor locations. Therefore, the aerosols remain acidic.

On the other hand, both the sulfuric acid pump tank area and truck loading/unloading station are outdoor locations. Wind assists in the mixing of the aerosols with ambient air. For the sulfuric acid pump tank, the high surface area of the fine mode aerosol is easier for mass transfer of basic gases, while the coarse mode aerosol needs a longer time to reach neutralization [*Meng and Seinfeld*, 1996]. The truck loading/unloading station does not have any significant sulfuric acid emission source, and aerosols at this location come mainly from other locations. Hence, the aerosol acidity depends on the wind strength/direction and aerosol emission source. The results also imply that the aerosol becomes less hazardous as it moves away from the emission source due to atmospheric dilution and neutralization by basic species.

Summary

Aerosol sampling using dichotomous samplers was carried out at five types of locations in eight fertilizer facilities. The highest sulfate concentration was obtained at the sulfuric acid pump tank area. The maximum sulfuric acid concentration measured in PM_{10}, including fine mode and coarse mode, was 0.185 mg/m^3. At the attack tank area where phosphoric acid is produced by reacting sulfuric acid with phosphate rock, fluoride was the dominant species. The maximum fluoride concentration in PM_{10} was 462 $\mu g/m^3$. At the rotating table/belt filter floor, phosphoric acid is separated from phosphogypsum by rotating table/belt filter and the high temperature is favorable for the evaporation of fluoride and phosphoric acid, which can subsequently form fine aerosol or condense on phosphogypsum aerosol created by mechanical agitation. The maximum phosphate concentration in PM_{10} was 170 $\mu g/m^3$. On a scrub day, a weak sulfuric acid solution is used to clean the piping and ductwork of the granulator for an

average of 4 h per day. Particulate sulfate concentrations were low during the scrubbing activity. At the truck loading/unloading station, the possible emission period is around 2–3 h/day, and this emission is not continuous. The concentration levels at the loading/unloading station were low and were greatly influenced by outdoor conditions.

The PM_{10} concentrations of sulfuric acid mist at these facilities were lower than the TLV-TWA standard of 0.2 mg/m^3 recommended by ACGIH for the thoracic fraction of sulfuric acid aerosol. The maximum PM_{10} of sulfuric acid mist was observed at the sulfuric acid pump tank area and was close to but found to be lower than the TLV-TWA. If monitoring of personal exposures to sulfuric acid mist is to be required, these efforts should focus on workers with activities in this area.

Table 2-1. Sampling locations at phosphate fertilizer plants in Florida

Location	Sulfuric Acid Pump Tank	Filter Floor (Rotating Table)	Filter Floor (Belt)	Granulator (on a Scrub day)	Truck Station	Attack Tank
Plant A	X	X	X	X		X
Plant B	X X		X		X	
Plant C	X	X			X	
Plant D	X	X				
Plant E	X	X				
Plant F	X	X				
Plant G	X	X			X	X
Plant H	X	X				
Total sample number	27	21	6	2	9	6

Table 2-2. Analysis conditions for soluble ions

Dionex ICS-1500	Cation	Anion
Analyzable species	K^+, Na^+, Ca^{2+}, Mg^{2+}, NH_4^+	F^-, Cl^-, NO_3^-, SO_4^{2-}, PO_4^{3-}
Extraction solution volume (D.I. water)	10 ml	10 ml
Analytical column	IonPac CS12A	IonPac AS9-HC
Guard column	IonPac CG12A	IonPac AG9-HC
Suppressor	ASRS-ULTRA II	CSRS-ULTRA II
Eluent	18 mM methanesulfonic acid	9.0 mM sodium carbonate
Flow rate	1.0 ml/min	1.0 ml/min
Injection volume	50 μl	50 μl
Analysis time	20 min	30 min

Table 2-3. Detection limit of ion chromatography (ICS 1500)

Anion	ppm	Cation	ppm
F^-	0.10	Na^+	0.05
Cl^-	0.02	NH_4^+	0.12
NO_3^-	0.07	K^+	0.05
PO_4^{3-}	0.06	Mg^{2+}	0.04
SO_4^{2-}	0.12	Ca^{2+}	0.08

Table 2-4. Median concentration (μg/m^3) of ion species at background sites

	Mass	F^-	Cl^-	PO_4^{3-}	SO_4^{2-}	Na^+	NH_4^+	K^+	Mg^{2+}	Ca^{2+}
					Gainesville, FL					
Fine	15.0	<DL*	<DL	<DL	5.05	0.20	4.24	0.15	0.03	0.23
Coarse	11.2	<DL	0.03	<DL	0.22	0.60	1.50	0.02	0.10	1.16
					Winter Haven, FL					
Fine	15.0	0.06	<DL	<DL	2.58	0.98	5.10	0.17	0.22	0.29
Coarse	15.0	<DL	0.30	<DL	0.41	0.90	7.78	0.14	0.07	0.60

<DL*: lower than detection limit.

Table 2-5. Median concentration ($\mu g/m^3$) of aerosol chemical composition at the granulator on a scrub day

	F^-	Cl^-	NO_3^-	PO_4^{3-}	SO_4^{2-}	Na^+	NH_4^+	K^+	Mg^{2+}	Ca^{2+}
Mean (Fine mode)	14.1	2.11	2.53	1.93	3.75	0.389	8.77	0.2	0.064	0.391
Mean (Coarse mode)	8.69	1.31	1.46	37.0	4.75	1.22	10.1	0.238	0.527	1.16

Table 2-6. Statistics of hydrogen ion concentrations (μeq/m^3) at each location

Location	Filter floor		H_2SO_4 pump tank area		Attack tank area		H_2SO_4 truck station	
Mode	Fine	Coarse	Fine	Coarse	Fine	Coarse	Fine	Coarse
Maximum	4.8	4.2	0.6	3.3	20.7	4.7	-0.1	0.3
Minimum	-1.5*	-1.2	-1.2	-0.9	-2.1	0.0	-1.2	-0.7
Median	0.2	0.5	0.0	0.0	4.4	1.3	-0.3	-0.2

*: A "-" sign indicates OH^- concentration.

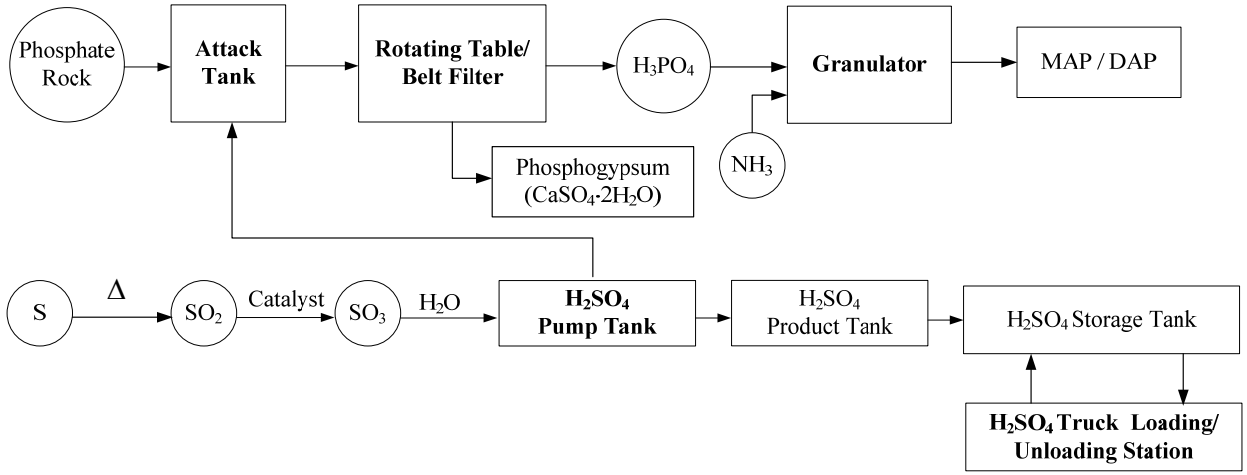

Figure 2-1. Manufacturing processes at fertilizer facilities

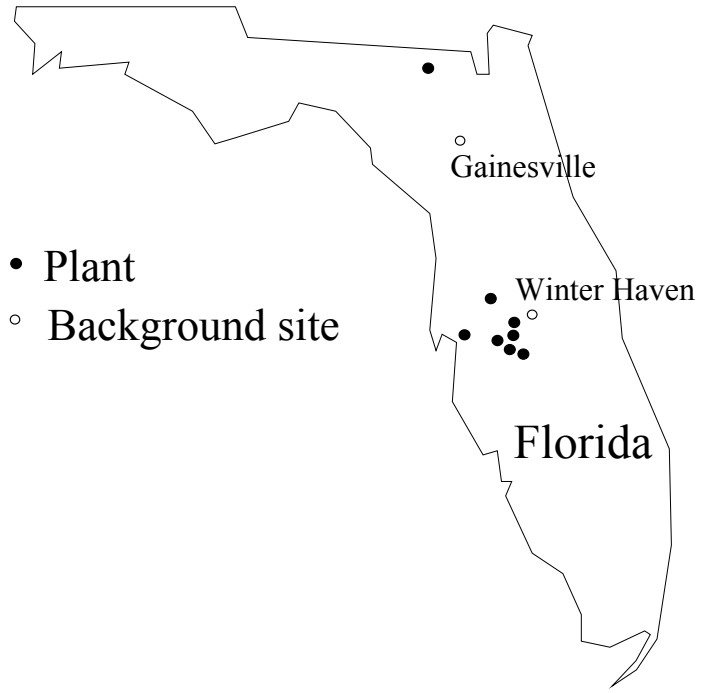

Figure 2-2. Geographic locations of sampling sites

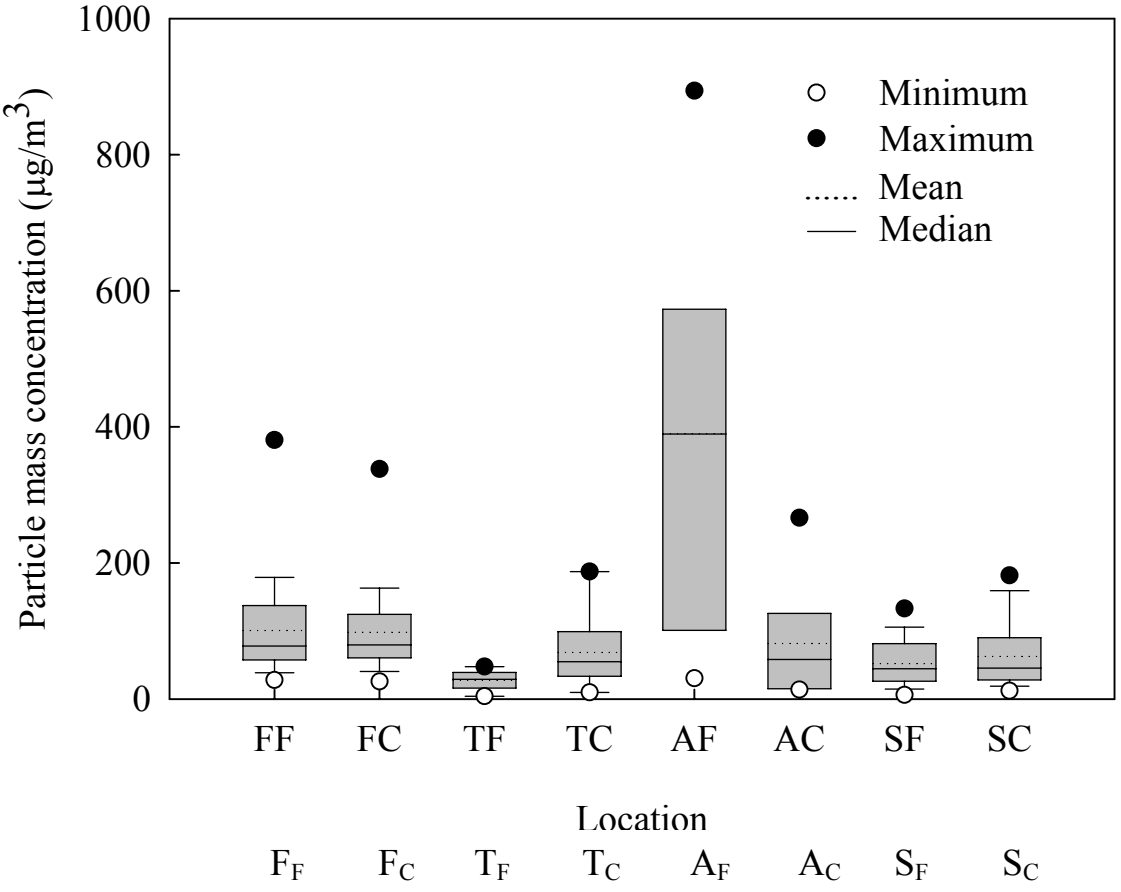

Figure 2-3. Fine mode and coarse mode aerosol mass concentrations at various locations. The first letter denotes location: F- filter (rotating table or belt filter) floor, T- truck loading/unloading station, A- attack tank area and S- sulfuric acid pump tank area. The subscript denotes particle size: F- fine mode ($PM_{2.5}$), C- coarse mode ($PM_{2.5-10}$)

A

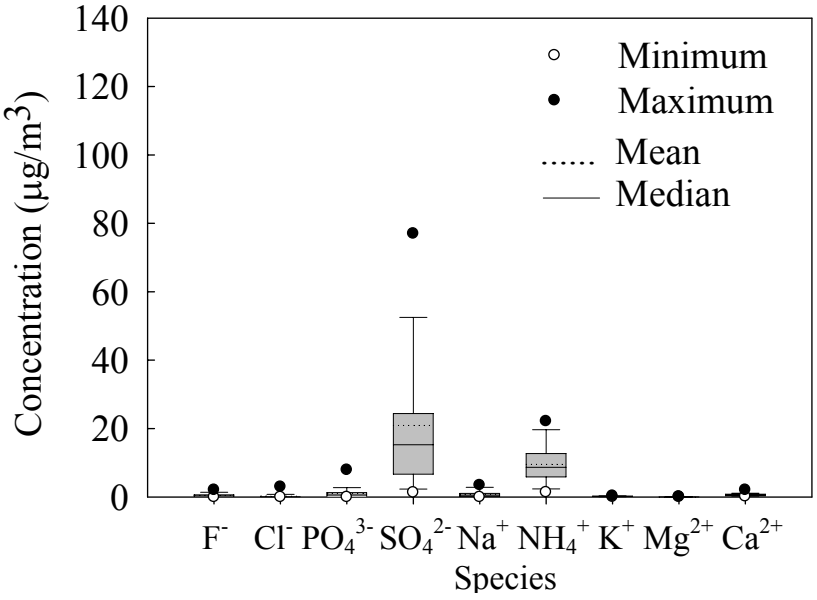

B

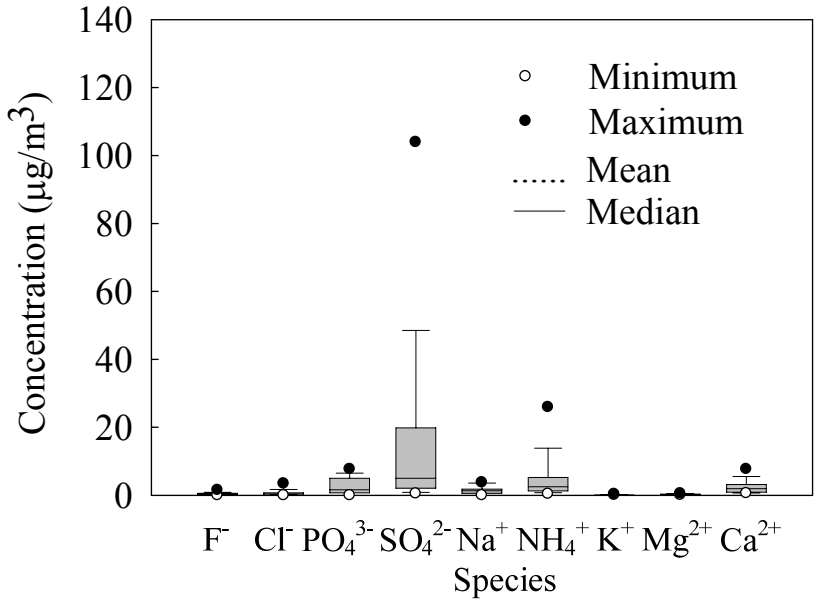

Figure 2-4. Aerosol chemical species at the sulfuric acid pump tank area. A) For fine mode. B) For coarse mode

A

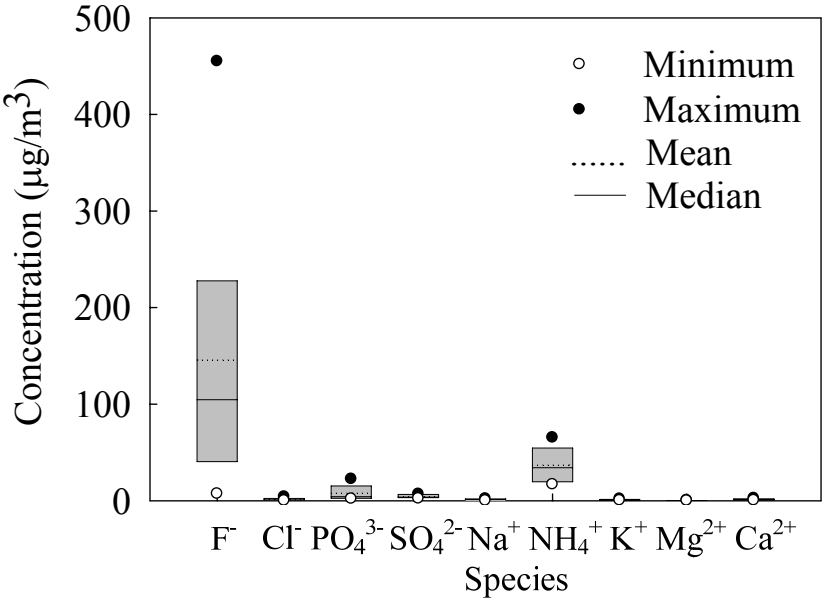

B

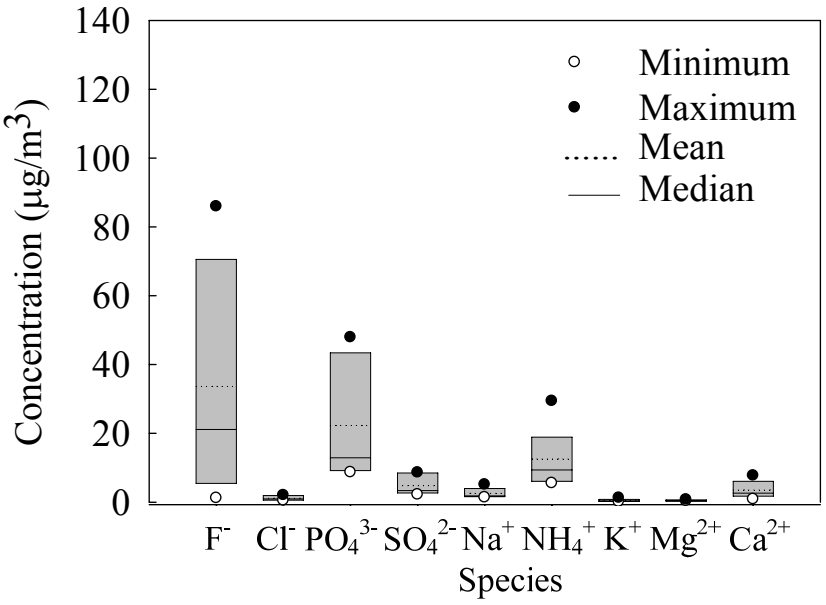

Figure 2-5. Aerosol chemical species at the attack tank area. A) For fine mode. B) For coarse mode

A

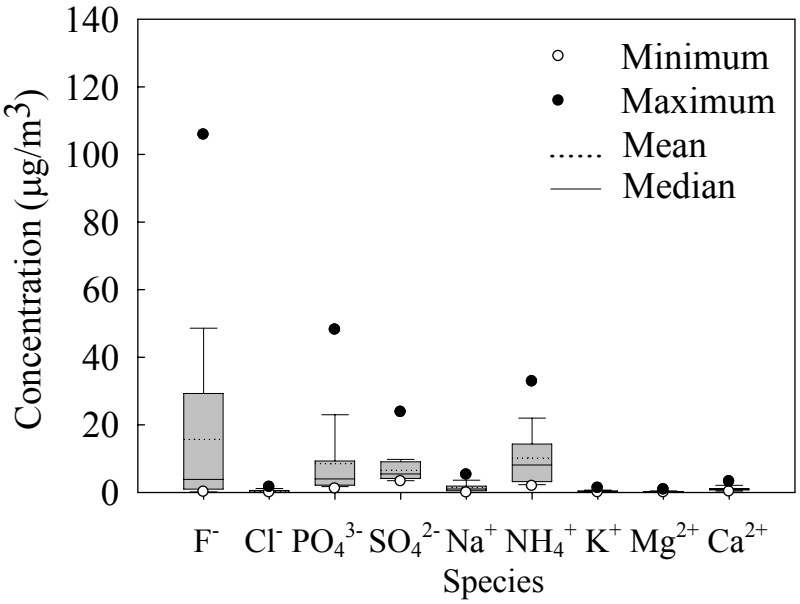

B

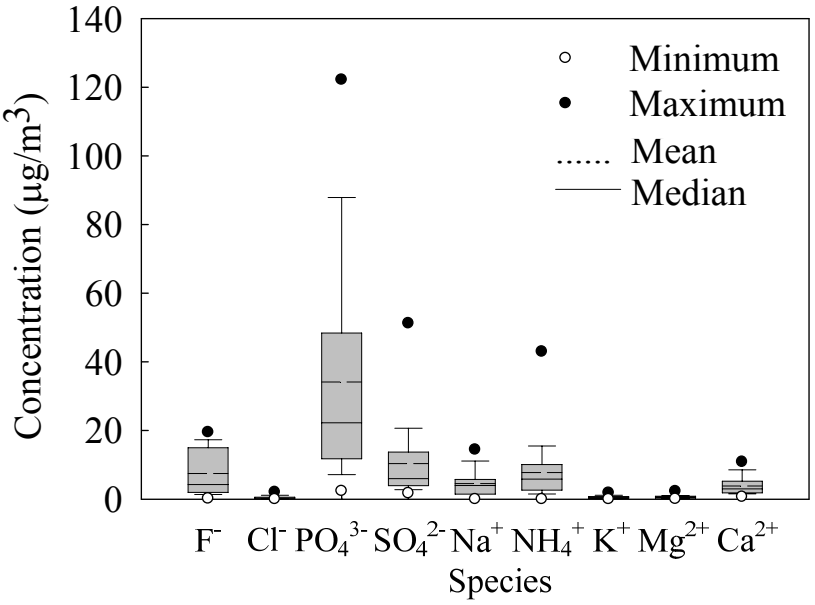

Figure 2-6. Aerosol chemical species at the rotating table/belt filter floor. A) For fine mode. B) For coarse mode

A

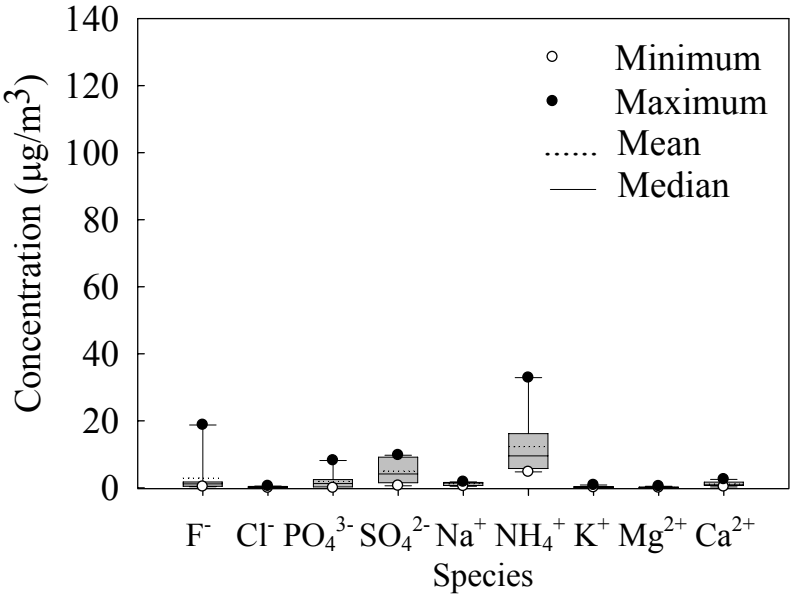

B

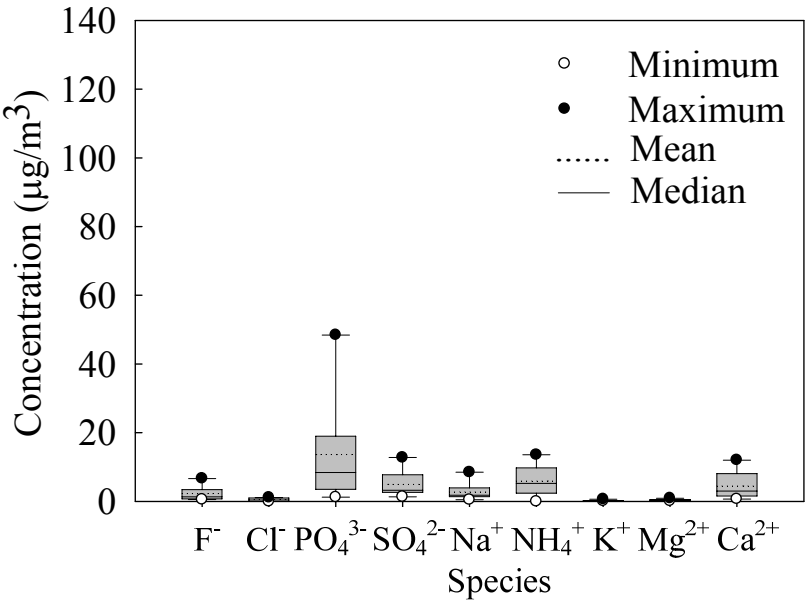

Figure 2-7. Aerosol chemical species at the sulfuric acid truck loading/unloading station. A) For fine mode. B) For coarse mode

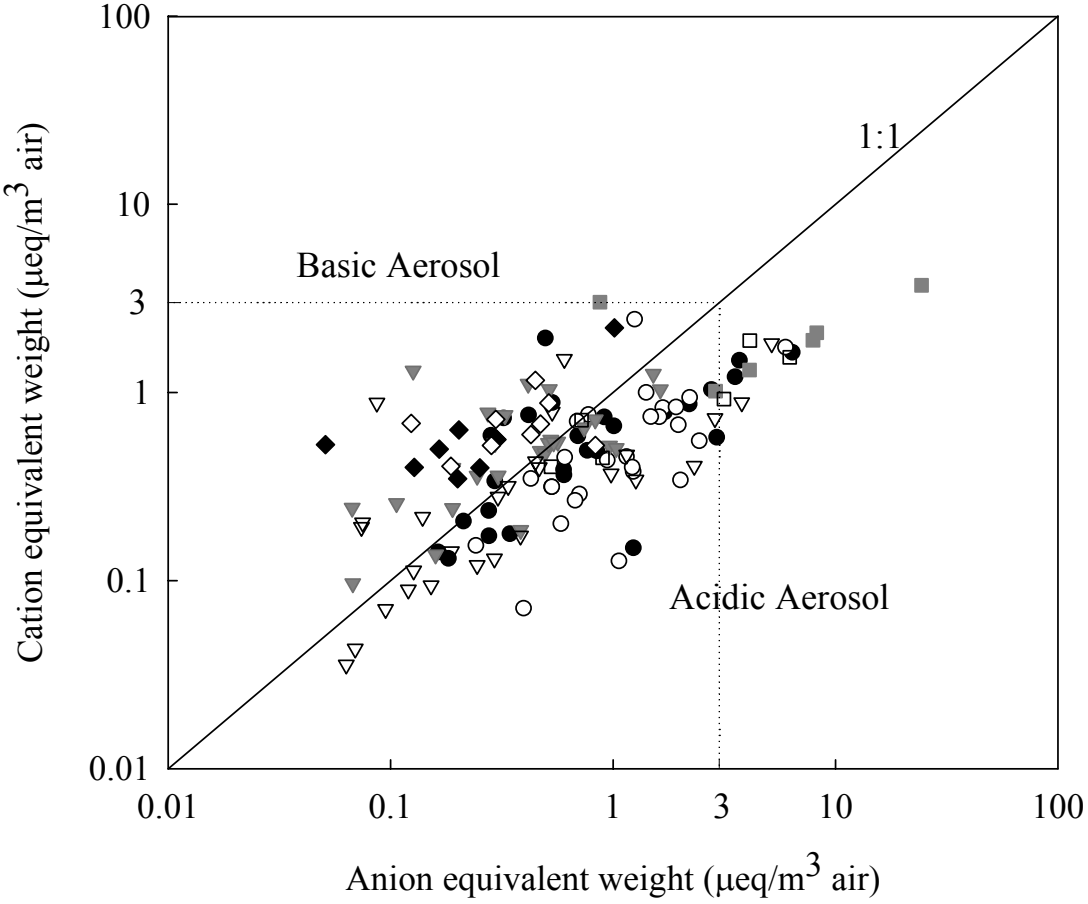

Figure 2-8. Relationship of cation equivalent weight and anion equivalent weight

- ● Belt / rotating table filter floor (fine)
- ○ Belt / rotating table filter floor (coarse)
- ▼ H_2SO_4 pump tank area (fine)
- ▽ H_2SO_4 pump tank area (coarse)
- ■ Attack tank area (fine)
- □ Attack tack area (coarse)
- ◆ H_2SO_4 truck station (fine)
- ◇ H_2SO_4 truck station (coarse)

CHAPTER 3
SIZE-RESOLVED SULFURIC ACID MIST CONCENTRATIONS AT PHOSPHATE FERTILIZER MANUFACTURING FACILITIES IN FLORIDA*

Background

Strong inorganic acid mists containing sulfuric acid have been reported to correlate with lung and laryngeal cancer in humans [*Blair and Kazerouni*, 1997; *Sathiakumar et al.*, 1997; *Steenland*, 1997] and are identified as a human carcinogen as reported by the NTP [*USDHHS*, 2005]. Sulfuric acid is typically present in the air in the mist form. Its chemical characteristics include low volatility, high acidity, high reactivity, high corrosivity and high affinity for water.

Phosphate fertilizer manufacture is listed in the NTP report as one of the industries that has sulfuric acid mist exposure potential. The OSHA has established an 8 h TWA of PEL of sulfuric acid mist at 1 mg/m^3. It is well known that the deposition of an aerosol in the respiratory system depends on its aerodynamic behavior. Considering the effects of aerosol size, the ACGIH has adopted a TLV-TWA of 0.2 mg/m^3 for the thoracic particulate fraction of sulfuric acid mist [*ACGIH*, 2004].

NIOSH Method 7903 is an OSHA-approved method that is commonly used by the health and safety staff in industries to measure the total sulfuric acid mist concentration. The sampler of NIOSH Method 7903 is a silica gel tube consisting of one section of glass fiber filter plug followed by two sections of silica gel (commercially available: ORBO-53 tube, Supelco, and SKC silica gel tube, SKC). The glass fiber filter plug is designed to filter out the majority of acid aerosols while the silica gel sections are used mainly to adsorb acid gases. The collected samples are desorbed in eluent and the aliquots are analyzed by IC. NIOSH researchers who developed the method reported ~90% collection efficiency for acidic aerosols with 0.4 μm

* Reprinted with permission from Hsu, Y.-M., Wu, C.-Y., Lundgren, D. A., Birky, B. K., 2007. Size-Resolved Sulfuric Acid Mist Concentrations at Phosphate Fertilizer Facilities in Florida. *Ann. Occup. Hyg.* 51, 81-89.

volume median diameter (94.8 ± 4.8% for H_3PO_4 and 86 ± 4.6% for H_2SO_4) when the samples collected on the glass fiber section and the front silica gel section (400 mg) were combined [*Cassinelli*, 1986; *Cassinelli and Taylor*, 1981].

Cascade impactors are commonly used for characterizing aerosol size distribution [*Dibb et al.*, 2002; *Swietlicki et al.*, 1997]. Large particles are collected on a substrate by inertial impaction, while small particles can better follow the changes in the flow direction of a curved air stream. By adopting a series of impactor stages with increasing flow velocities, the aerosol size distribution can be classified.

The approved NIOSH method only provides total sulfuric acid mist concentration, but not size-dependent information. The comparison of the total mist concentration with the size-fractionated measurement by the cascade impactor may provide a convenient tool for correlating exposure levels based on the simpler NIOSH method. This information can be applied to develop informed policies with respect to respiratory protection in the workplace.

To properly assess the occupational exposure of workers to sulfuric acid mist in phosphate fertilizer manufacturing facilities, the objectives of this chapter were to determine the total sulfuric acid mist concentrations using the approved NIOSH method and to characterize the size distributions of sulfuric acid mist by cascade impactor sampling. All other chemical species will be reported in next chapter. Furthermore, the feasibility of using a correlation factor between these two measurements was examined.

Methods

Sampling Sites

The final products of phosphate fertilizer facilities are MAP, DAP, phosphoric acid and sulfuric acid. The manufacturing processes have been described in Hsu *et al*. [2007a]. Five types of locations with the potential of H_2SO_4 exposure corresponding to the manufacturing

process were selected for sampling. These locations (the number of the sampling sites) include the sulfuric acid pump tank area (9), rotating table/belt filter floor (9), attack tank area (2), truck station for loading/unloading sulfuric acid (3), and the granulator on a "scrub" day (1). Sampling was carried out at eight plants. Seven of them are located in central Florida, and one of them is located in north Florida. In addition, Gainesville, FL, and Winter Haven, FL, were chosen as the background sites.

Sampling and Analysis Methods

A University of Washington Source Test cascade impactor (Mark III) was used as an area sampler to sample mist aerosols for the size distribution. The inlet of the cascade impactor was set at 1.5 m from the floor. The impactor was operated at 25 Lpm with aerodynamic cut sizes (d_{50}) of 0.20, 0.48, 0.98, 1.8, 3.8, 10 and 23 μm for the seven stages, respectively. The impactor with glass fiber filter can provide high collection efficiency for aerosols; however, glass fiber filter is well known to adsorb acidic gas, such as sulfur dioxide [*Chow*, 1995; *Lee and Mukund*, 2001]. Therefore, Teflon membrane filters (Zefluor^{TM}, 8 × 10 inches, pore size: 2 μm, Pall Corp., Ann Arbor, MI) that provide high collection efficiency and low reactivity with acidic gases [*Chow*, 1995; *Lee and Mukund*, 2001] were applied for the collection substrate. Those filters were cut to fit onto the impactor stages. The collection efficiencies of the cascade impactor for liquid (substrate: a glass fiber filter) and solid aerosols (substrate: an aluminum foil with silicone coating) were 97.2 ± 11.9 and 94.1 ± 17.3%, respectively [*Pauluhn*, 2005]. Droplet break-up in this instrument is negligible for large droplets (10 and 25 μm) even when a high sampling flow rate (28.3 Lpm) is applied [*Horton and Mitchell*, 1989]. A final Teflon filter (Zefluor^{TM}, 47 mm, pore size: 2 μm, Pall Corp., Ann Arbor, MI) was placed after the impactor to collect penetrating aerosols. Filters were placed in a desiccator at room temperature for pre- and

post-conditioning for 24 h before weighing to reduce the effect of water collected by the filter. The vapor pressure of sulfuric acid mist is low and it remains in the mist form under these conditions. The lower limit of particle size collected on the final filter was assigned to be 0.03 μm, a typical value of those employed in other research studies [*Divita et al.*, 1996; *Howell et al.*, 1998; *Wagner and Leith*, 2001]. The aerodynamic diameters of collected particles were from 0.03 to 23 μm. PM_{23} is the aerosol mass concentration with an aerodynamic diameter smaller than 23 μm, which was the largest aerosol size collected using this methodology. PM_{23} sulfuric acid mist concentration was used to compare the total sulfuric acid mist concentration provided by NIOSH Method 7903.

NIOSH Method 7903 was applied for the sampling of total sulfuric acid mist concentration using a commercially available silica gel tube (ORBO 53 tube, Supelco). The sampling flow rate was 0.45 Lpm for 72 sets of samples. Six sets of samples were also collected at 0.3 Lpm in order to verify whether the results were the same at different flow rates in the recommended range (0.2 – 0.5 Lpm) [*Cassinelli*, 1986; *Cassinelli and Eller*, 1979; *Cassinelli and Taylor*, 1980; *NIOSH*, 1994].

Gravimetric measurement for sample mass was carried out using a microbalance (model MC 210 S, Sartorius Corp., Edgewood, NY; readability 10 μg), and the analysis of sulfate concentration was accomplished by using an IC system (Dionex ICS 1500, Dionex Corp., Atlanta, GA). The analytical columns of anion species [nitrate (NO_3^-), sulfate (SO_4^{2-}), fluoride (F^-), phosphate (PO_4^{3-}), and chloride (Cl^-)] and cation species [potassium (K^+), calcium (Ca^{2+}), magnesium (Mg^{2+}), sodium (Na^+), and ammonium (NH_4^+)] are IonPac AS9-HC (Dionex Corp., Atlanta, GA) and IonPac CS12A (Dionex Corp., Atlanta, GA), respectively. The detection limit for sulfate was determined to be 0.12 ppm for this system.

The sampling time was 24 h and three successive samples were obtained for each sampler at each site. Totally, there were 72 sets of impactor samples and 78 silica gel tube samples in those plants. In background locations, there were six sets of impactor samples and six silica gel tube samples.

Calculation of Fine Mode

Because 2.5 μm was not one of the cascade impactor cut-sizes, $PM_{2.5}$ was determined by interpolating the size bin that covers 2.5 μm (i.e., 1.81 and 3.76 μm). Assuming a uniform distribution in this size range in log-scale, $PM_{2.5}$ can be obtained according to the following relationship:

$$\frac{\log(2.5)-\log(1.81)}{\log(3.76)-\log(1.81)}=\frac{PM_{2.5}-PM_{1.81}}{PM_{3.76}-PM_{1.81}} \quad (3\text{-}1)$$

Rearranging the formula, $PM_{2.5}$ can be derived as:

$$PM_{2.5}=0.44\times[\,PM_{3.76}-PM_{1.81}\,]+PM_{1.81} \quad (3\text{-}2)$$

Calculation of Sulfuric Acid Mist Concentration

According to NIOSH Method 7903, sulfuric acid mist concentration is converted from the sulfate concentration determined by IC. Although the sulfate may not necessarily come from sulfuric acid (i.e., it can be ammonium sulfate or calcium sulfate), any sulfate determined by this method is conservatively assumed to be sulfuric acid. In this study, the same protocol was followed for all samples from the fertilizer plants.

Results and Discussion

Background Site

In general, the mass concentrations and sulfate concentrations were low at both background locations. The PM_{23}, PM_{10} and $PM_{2.5}$ were 20.6–53.2, 18.7–36.9 and 15.1–26.4 $\mu g/m^3$ in Gainesville, and 19.1–27.0, 16.3–27.0 and 11.5–22.8 $\mu g/m^3$ in Winter Haven. The

corresponding sulfate concentrations were 5.4–8.6 (PM_{23}), 5.2–7.1 (PM_{10}) and 5.0–6.3 ($PM_{2.5}$) $\mu g/m^3$ in Gainesville, and they were lower in Winter Haven: 3.0–3.2 (PM_{23}), 2.7–2.8 (PM_{10}) and 2.4–2.5 ($PM_{2.5}$) $\mu g/m^3$. The ratios of sulfate concentration to the sum of all ionic species concentrations (NO_3^-, SO_4^{2-}, F^-, PO_4^{3-}, Cl^-, K^+, Ca^{2+}, Mg^{2+}, Na^+, and NH_4^+) were 0.44–0.46 in Gainesville and 0.16–0.39 in Winter Haven.

For NIOSH method samples, the total sulfate concentrations ranged from 6.81 to 10.5 $\mu g/m^3$ in Gainesville and much higher in Winter Haven, 31.2–46.0 $\mu g/m^3$. Compared to the cascade impactor results, the measurements were closer in Gainesville than those in Winter Haven. The ratio of sulfate from the impactor to sulfate from the NIOSH method sampler ranged from 0.67 to 0.82 in Gainesville and from 0.069 to 0.096 in Winter Haven. It should also be noted that while the impactor results showed higher sulfate concentrations in Gainesville than in Winter Haven, the NIOSH method measurements showed the opposite. It is suspected that the NIOSH Method 7903 might have interferences from SO_2 gas. This will be further discussed in later sections.

Plants: Cascade Impactor Samples

The sampling results of the cascade impactor at all locations are shown in Figure 3-1A. The highest median sulfuric acid mist concentration was observed at the sulfuric acid pump tank areas where two sulfuric acid mist concentrations from the cascade impactor were higher than the OSHA standard, 1 mg/m^3. The size information at each type of location will be discussed as follows.

Attack tank area

Sampling for the attack tank area was carried out at two plants. The aerosol and sulfuric acid PM_{23}, PM_{10} and $PM_{2.5}$ mass concentrations are listed in Table 3-1. Aerosols at the attack

tank areas had high mass loadings but low sulfuric acid concentrations. The violent reaction in the attack tank releases heat and causes a significant amount of volatile species to evaporate. These species, such as fluoride gases, condense on existing aerosols when they encounter cooler ambient air, thus resulting in high aerosol mass concentrations. However, the temperature in the process was not high enough for the evaporation of sulfuric acid or sulfate salt that has lower vapor pressure. Hence, sulfuric acid mist concentrations were low at this location.

Sulfuric acid pump tank area

Sampling at the sulfuric acid pump tank area was carried out at all eight plants. The PM_{23}, PM_{10} and $PM_{2.5}$ mass concentrations are listed in Table 3-2. The geometric mean PM_{23}, PM_{10} and $PM_{2.5}$ sulfuric acid concentrations (±geometric standard deviation) were 41.7 (±5.5), 37.9 (±5.8), and 22.1 (±4.5) $\mu g/m^3$. The highest geometric mean sulfuric acid concentration from cascade impactor measurement among all types of locations was indeed observed at the pump tank area. The large geometric standard deviation implies that the sulfuric acid concentrations at these nine sulfuric acid pump tank areas differed greatly. The geometric mean ratios of sulfate concentration to all ionic species were greater than 0.50, which indicated that sulfate was the predominant ion accounting for the aerosol mass at this type of location.

The aerosol mass size distributions and sulfuric acid size distributions are shown in Figure 3-2. They are plotted in two ranges: larger than and smaller than 100 $\mu g/m^3$. The size distribution maintained the same pattern at a given site, but not from site to site. It should also be noted that most of the sulfuric acid size distributions resemble the aerosol mass size distributions at the same site. At plants B1, D, H and B2, Figure 3-2A, both the aerosol mass concentrations and sulfuric acid mass concentrations were higher than 100 $\mu g/m^3$, and the aerosols were predominantly supermicron particles. The sulfate/aerosol mass ratios were greater than 0.5 (Table 3-3). The high ratios indicate that sulfuric acid was the major species and that

these locations might have sulfuric acid emission sources. At the pump tank area, the possible sulfuric acid emission source is the leakage of SO_3 that will quickly combine with water molecules to form H_2SO_4.

At other plants, Figure 3-2B, the sulfuric acid concentrations were lower than 100 $\mu g/m^3$ and their sulfuric acid aerosols were mainly in the submicron range or presented no specific pattern. In the case of a very low aerosol mass loading, the sulfuric acid aerosols could very likely be affected by the ambient aerosols at this outdoor location. The geometric mean sulfuric acid concentration at Plant F was 6.8 $\mu g/m^3$ (Table 3-3), which is as low as that at the background sites.

Belt or rotating table filter floor

Sampling at the belt or rotating table filter floor area was carried out at all eight plants. The aerosol mass concentrations were high: the PM_{23}, PM_{10} and $PM_{2.5}$ mass concentrations ranged from 57.4 to 2535, 54.0 to 1857 and 28.3 to 358 $\mu g/m^3$, respectively; their geometric mean concentrations (±geometric standard deviation) were 225.3 (±2.3), 187.0 (±2.2) and 94.7 (±1.8) $\mu g/m^3$, respectively. PM_{23}, PM_{10} and $PM_{2.5}$ sulfuric acid concentrations were 7.1−575, 4.9–419 and 2.4–60.0 $\mu g/m^3$; the geometric mean sulfuric acid concentrations (±geometric standard deviation) of PM_{23}, PM_{10} and $PM_{2.5}$ were 17.9 (±2.7), 14.4 (±2.7) and 6.6 (±2.1) $\mu g/m^3$.

The ratios of sulfate to all ions ranged from 0.07 to 0.32 (geometric mean: 0.16). The low ratios indicate that sulfuric acid was not a major compound at the filter floor area. The fractional size distributions of aerosol mass and sulfuric acid at nine belt/rotating table filter floors are shown in Figure 3-2C. Sulfuric acid was dominantly present in the coarse mode. During this process, gypsum is filtered out by belt or rotating table filter, and the aerosols are formed by

mechanical agitation. The similarity in sulfuric acid and aerosol mass size distributions indicates that the chemical might be from the residual content in the product.

Sulfuric acid truck loading/unloading station

Sampling at the truck loading/unloading station was conducted at three plants. The aerosol mass concentrations were low and their PM_{23}, PM_{10} and $PM_{2.5}$ ranged from 19.9 to 174, 15.8 to 131, and 10.0 to 69.7 $\mu g/m^3$. Sulfuric acid was the major species (the ratios of sulfate to total ion mass: 0.28–0.42, median: 0.36); the concentrations ranged from 3.9 to 24.5 (PM_{23}), 3.5 to 23.9 (PM_{10}) and 3.1 to 20.6 ($PM_{2.5}$) $\mu g/m^3$, which were close to the measurements at the background locations. All size distributions of sulfuric acid were similar: the mode size was 0.48–0.98 μm. During loading and unloading, sulfuric acid is transferred from the storage tank in liquid form to the truck. The only possible pathway that workers can be exposed to sulfuric acid is the spray of sulfuric acid from the truck loading nozzle. Normally, the connection is well sealed and the workers are well protected to avoid contact with liquid sulfuric acid. The measurements verified that the sulfuric acid concentrations were very low.

Granulator on a scrub day

The mass concentrations ranged from 126 to 835 (PM_{23}), 90.2 to 578 (PM_{10}) and 59.7 to 303 ($PM_{2.5}$) $\mu g/m^3$. The sulfuric acid concentration ranges were 7.63–87.9 (PM_{23}), 5.73–59.7 (PM_{10}) and 3.85–51.6 ($PM_{2.5}$) $\mu g/m^3$. The source of sulfuric acid mists is the spray from the scrubbing process (a weak acid solution) which is not a steady operation. Hence, the concentrations varied significantly, but they were all below the standards.

Plants: NIOSH Method Samples

Sampling results of the NIOSH samples at five types of locations are shown in Figure 3-1B. Generally, the sulfuric acid pump tank area had the higher concentrations. However, the

maximum sulfuric acid concentration (11225 μg/m^3) measured by the NIOSH method for all locations was obtained at the filter floor area. The largest geometric mean sulfuric acid concentration was obtained at the pump tank area (143.2 μg/m^3), followed by the granulator on a scrub day (122.4 μg/m^3) and then at the filter floor (108.7 μg/m^3). The geometric mean concentrations at the granulator on a scrub day and sulfuric acid truck loading/unloading stations were at lower levels.

Comparisons of the Results from the Cascade Impactor and the NIOSH Method

The paired measurements of PM_{23} sulfuric acid concentrations from the cascade impactor and total sulfuric acid concentrations from the NIOSH method at all sampling locations are shown in Figure 3-3. As shown, 71 out of 72 impactor samples had a lower concentration than the NIOSH method measurement. The ratios of sulfuric acid mist concentrations from the NIOSH to the cascade impactor were 1.5–229.0 for 71 impactor samples. The largest difference was over two orders of magnitude, and many of the NIOSH measurements were more than 10 times larger the impactor results. The substantial difference was quite unexpected. To quantitatively compare these two measurements and evaluate their correlation, three ratios were used which are defined as Equation 3-3 to Equation 3-5:

$$R_{23} = \frac{\mathrm{PM}_{23}}{\mathrm{C_N}} \tag{3-3}$$

$$R_{10} = \frac{\mathrm{PM}_{10}}{\mathrm{C_N}} \tag{3-4}$$

$$R_{2.5} = \frac{\mathrm{PM}_{2.5}}{\mathrm{C_N}} \tag{3-5}$$

where PM_{23}, PM_{10} and $PM_{2.5}$ are sulfuric acid concentrations from the cascade impactor and C_N the sulfuric acid concentration by NIOSH Method 7903.

Table 3-4 displays the R_{23}, R_{10} and $R_{2.5}$ at five types of sampling locations. A large variation at each type of location is observed, e.g., from 0.00 to 0.67 at the filter floor areas for R_{23}. A strong relationship between methods would be indicated by a constant correlation factor; the wide variation of the ratios does not allow any meaningful correlation of these two types of measurements. The much higher values by the NIOSH method also prompted further investigation of the data.

In examining the data, it was found that in many cases the silica gel sections collected more sulfuric acid than the glass fiber section (see examples in Table 3-5). The results of the NIOSH method imply that sulfuric acid as well as sulfate is partially measured as a gas. In the ambient condition, there is no known sulfate species (inorganic) that exists in the gas phase. Even sulfuric acid exists in the condensed phase because it has a high boiling point of 330 ^{o}C and a very low vapor pressure at room temperature (< 0.001 mmHg) [*Weast*, 1988]. Furthermore, the hygroscopic sulfuric acid will rapidly pick up moisture in the air and remain in the aerosol phase. It should be noted again that according to Ortiz and Fairchild [1976] the majority of the aerosol mass is collected on the glass fiber filter plug. Chen *et al*. [2002] reported that aerosol penetration across the filter section of the silica gel tube (SKC 226-10-03 tube) at the most penetrating size was lower than 5%. The collection efficiency of large particles (> 3 μm) is higher than 99%. Sulfuric acid mists mainly exist as coarse aerosols at the pump tank area (Figure 3-2A); hence, aerosol penetration cannot explain the high sulfuric acid concentration sampled by silica gel. Thus, the situation that more sulfuric acid mist is collected in the silica gel section than the glass fiber section is highly unlikely. The adsorption of a significant amount of interfering gases by the silica gel is therefore suspected to be the reason for the observed phenomenon.

Another unexpected phenomenon was observed when comparing the results obtained from the NIOSH method at different sampling flow rates. In the recommended range of sampling flow rate (0.2–0.5 Lpm), concentrations should be similar when different flow rates are used. Two different flow rates, 0.3 and 0.45 Lpm, were employed for six sets of the NIOSH method sampling, and the results are shown in Table 3-5. These paired samples were taken concurrently (e.g., #1-low and #1-high were taken at the same time), and three consecutive samples were carried out (i.e., #1 followed by #2 and then by #3). As shown, sulfuric acid concentrations at the lower flow rate (0.3 Lpm) were higher than those at the higher flow rate (0.45 Lpm). Most of the ratios ($C_{@\ 0.3\ Lpm}/\ C_{@\ 0.45\ Lpm}$) were larger than 1, and they were much higher in the silica gel section than those in the glass tube section. The concentrations at two different flow rates do not exhibit any direct proportion between the gas phase and the particulate phase. Hence, systemic errors can be neglected. The collection mechanism of acid gases on the silica gel is diffusion, and its efficiency decreases as the flow rate increases (due to shorter residence time). The observations support the hypothesis that the higher measurement in the silica gel section is probably from the collection of gas.

Silica gel, a high surface area material, can adsorb SO_2 [*Kopac and Kocabas*, 2002; *Stratmann and Buck*, 1965]. The hydrophilic property of silica gel can effectively attract moisture which can enhance the absorption of soluble species, such as SO_2 [*Tsai et al.*, 2001]. The adsorbed or absorbed SO_2 can be further oxidized to form sulfate [*Lunsford*, 1979] that causes overestimation.

Annual SO_2 concentrations (2003) were monitored by the state of Florida [*FDEP*, 2003] and the results indicated that central FL had higher SO_2 concentrations (~2–6 ppb) than north FL (~2–3 ppb) . If the above hypothesis is true, this might explain why sulfate concentrations in

Winter Haven measured by the NIOSH method were much higher than those in Gainesville but the impactor results did not exhibit such a pattern.

Limited SO_2 concentrations in fertilizer facilities are available in the literature. The SO_2 concentration in a fertilizer factory in India was 41.7 mg/m^3 [*Yadav and Kaushik*, 1996] while those in China and Sweden were 0.34–11.97 and 3.6 mg/m^3, respectively [*Englander et al.*, 1988; *Meng and Zhang*, 1990]. Atmospheric dispersion can quickly reduce the concentration to a much lower level as reported in a study near a fertilizer factory in Zimbabwe [*Jonnalagadda et al.*, 1991]. If the hypothesis holds true, the sulfuric acid concentration in the fertilizer facilities can be expected to be overestimated when SO_2 is present in the studied facilities. Further investigation of this subject is warranted.

Comparisons of Sulfuric Acid Mist Concentrations with OSHA and ACGIH Regulations

The number of samples with concentrations higher than the OSHA regulation (total sulfuric acid mist concentration < 1 mg/m^3) was 7 of the 78 samples collected. According to the cascade impactor sampling, 90% of the samples were lower than the ACGIH standard and 97% of the samples were lower than the OSHA regulation. The results of the NIOSH method samples obtained concurrently with the impactor samples had a smaller percentage of samples with concentrations lower than the OSHA regulation. The only location where the sulfuric acid mist concentrations from the cascade impactor exceeded both the OSHA and ACGIH standards was the sulfuric acid pump tank area. For the NIOSH method samples, the locations included sulfuric acid pump tank areas, belt/rotating table filter floors and the granulator on a scrub day.

Summary

In this study, the total sulfuric acid mist concentration and sulfuric acid mist size distributions at modern phosphate fertilizer manufacturing facilities in Florida were characterized

by using NIOSH Method 7903 and a cascade impactor, respectively. Sampling was carried out at five types of locations in eight facilities and two background sites.

Based on cascade impactor sampling, sulfuric acid pump tank areas had higher sulfuric acid mist concentrations than other types of locations and sulfuric acid was the dominant chemical species. When high sulfuric acid concentrations were identified, the aerosols were dominantly in the coarse mode. The most likely cause of high sulfuric acid concentrations at this location is the leakage of SO_3. Constant inspection of the tubing around this location and immediate repair may provide an effective measure to further lower the concentrations. According to the impactor sampling results, seven samples (total: 72) exceeded the ACGIH standard (0.2 mg/m^3, thoracic fraction), and two samples (total: 72) were above the OSHA regulation (1 mg/m^3, total concentration). Meanwhile, there were seven samples (total: 78) by the NIOSH method that exceeded the OSHA regulation. It should be noted at these locations, workers typically stay for about 1–2 h per day and respirators for sulfuric acid mist are required in this area. Consequently, the real time-weighted exposure to sulfuric acid mist is likely to be lower than the concentrations from the stationary sampling conducted in this study.

The results from the cascade impactor and the NIOSH method were compared to determine if a correlation factor could be established. The sulfuric acid mist concentrations from the NIOSH method were higher than those from the cascade impactor for the dominating majority of samples. No specific trend of systemic error was observed between these two methods. In many cases, the silica gel section collected more "sulfuric acid" than the glass fiber filter plug. This is highly unlikely because sulfuric acid or sulfates are not known to exist in the gas form in the ambient condition, and should not be collected in the silica gel section. Moreover, the sulfuric acid concentrations at 0.30 Lpm were higher than the concentrations at

0.45 Lpm in the NIOSH method sampling, indicating the influence of diffusing gases. The possible reason for the variation is the interaction between SO_2 and silica gel/glass fiber filter. Further investigation has been verified the causes and is discussed further in Chapter 5.

Table 3-1. PM_{23}, PM_{10} and $PM_{2.5}$ mass and sulfuric acid concentrations at the attack tank areas

$\mu g/m^3$	Sample number	min	max	Geometric mean	Geometric standard deviation
PM_{23}					
Mass[a]	6	86.2	1853	341.3	3.9
Mass (IC)[b]	6	62.7	414.6	152.8	2.3
Sulfuric acid[c]	6	6.7	19.0	10.1	1.5
PM_{10}					
Mass[a]	6	76.1	1767	308.3	4.1
Mass (IC)[b]	6	59.4	397	139.6	2.3
Sulfuric acid[c]	6	6.3	12.5	8.7	1.3
$PM_{2.5}$					
Mass[a]	6	64.6	720	187.0	2.9
Mass (IC)[b]	6	41.6	182	90.1	1.8
Sulfuric acid[c]	6	2.3	7.6	5.5	1.6

Mass[a]: mass concentration from weighing the mass.
Mass (IC)[b]: the sum of all ionic species concentrations measured by IC.
Sulfuric acid[c]: all sulfate is conservatively assumed to be sulfuric acid.

Table 3-2. PM_{23}, PM_{10} and $PM_{2.5}$ mass and sulfuric acid concentrations at the sulfuric acid pump tank areas

$\mu g/m^3$	Sample number	min	max	Geometric mean	Geometric standard deviation
PM_{23}					
Mass[a]	27	20.4	1644	121	3.3
Mass (IC)[b]	27	9.4	1268	69.5	3.8
Sulfuric acid[c]	27	2.1	1187	41.7	5.5
Sulfate/ Mass (IC)	27	0.22	0.98	0.588	1.52
PM_{10}					
Mass[a]	27	14.7	1625	105	3.5
Mass (IC)[b]	27	8.7	1221	61.9	4.0
Sulfuric acid[c]	27	2.0	1155	37.9	5.8
Sulfate/ Mass (IC)	27	0.23	0.98	0.600	1.52
$PM_{2.5}$					
Mass[a]	27	12.1	648	56.4	2.8
Mass (IC)[b]	27	6.5	548	35.0	3.2
Sulfuric acid[c]	27	1.8	558	22.1	4.5
Sulfate/ Mass (IC)	27	0.25	1.00	0.619	1.47

Mass[a]: mass concentration from weighing the mass.
Mass (IC)[b]: the sum of whole ionic species concentrations measured by IC.
Sulfuric acid[c]: all sulfate is conservatively assumed to be sulfuric acid.

Table 3-3. Mass, sulfuric acid concentrations and sulfate/mass[a] ratios of the impactor samples at the sulfuric acid pump tank areas

Plant	Mass (μg/m^3)		Sulfuric acid (μg/m^3)		Sulfate/ Mass[a]	Sample size
	Geometric mean	Geometric standard deviation	Geometric mean	Geometric standard deviation	Mean	
D	905.9	1.8	643.3	1.8	0.96	3
B1	550.8	3.0	298.3	3.8	0.84	3
H	177.9	2.1	114.0	2.6	0.88	3
B2	95.7	1.9	37.7	2.0	0.57	3
E	64.9	1.7	33.1	2.0	0.71	3
C	76.4	1.3	11.8	1.8	0.41	3
A	71.5	1.9	21.4	1.5	0.46	3
G	50.4	1.4	8.0	1.5	0.45	3
F	37.4	2.5	6.8	4.5	0.42	3

Mass[a]: mass concentrations combining all ionic species concentrations

Table 3-4. Statistics of R_{23}, R_{10} and $R_{2.5}$ at five types of sampling location

		Sample number	Min	Max	Geometric mean	Geometric standard deviation
Sulfuric acid pump tank area	$PM_{2.5}$	27	0.04	0.58	0.15	2.21
	PM_{10}	27	0.06	2.65	0.26	2.22
	PM_{23}	27	0.06	2.74	0.30	2.20
Belt/rotating table filter floor	$PM_{2.5}$	27	0.00	0.41	0.06	2.81
	PM_{10}	27	0.00	0.64	0.13	2.52
	PM_{23}	27	0.00	0.67	0.17	2.55
Truck station	$PM_{2.5}$	9	0.05	0.36	0.10	1.93
	PM_{10}	9	0.08	0.42	0.15	1.81
	PM_{23}	9	0.10	0.44	0.18	1.81
Attack tank area	$PM_{2.5}$	6	0.02	0.10	0.06	1.93
	PM_{10}	6	0.02	0.22	0.09	2.08
	PM_{23}	6	0.03	0.23	0.11	2.07
Granulator on a scrub day	$PM_{2.5}$	3	0.03	0.28	0.13	3.88
	PM_{10}	3	0.03	0.40	0.16	4.25
	PM_{23}	3	0.04	0.54	0.21	3.87

Table 3-5. Sulfuric acid concentrations and the ratios measured at two flow rates at the rotating table filter floors using NIOSH Method 7903

Sampler section	$[H_2SO_4]^a$ ($\mu g/m^3$)						$C_{@\ 0.3\ Lpm} / C_{@\ 0.45\ Lpm}$		
	Low flow rate (@ 0.3 Lpm)			High flow rate (@ 0.45 Lpm)					
	#1	#2	#3	#1	#2	#3	#1	#2	#3
Total [b]	90.3	141.0	118.8	80.8	87.2	89.8	1.12	1.62	1.32
Glass fiber	36.7	44.3	44.3	35.7	37.7	46.7	1.03	1.17	0.95
Silica gel	53.6	96.7	74.5	45.1	49.5	43.2	1.19	1.95	1.73

$[H_2SO_4]^a$: paired samples at two flow rates taken concurrently.
Total[b]: the sum of the results from the glass fiber section and the silica gel section.

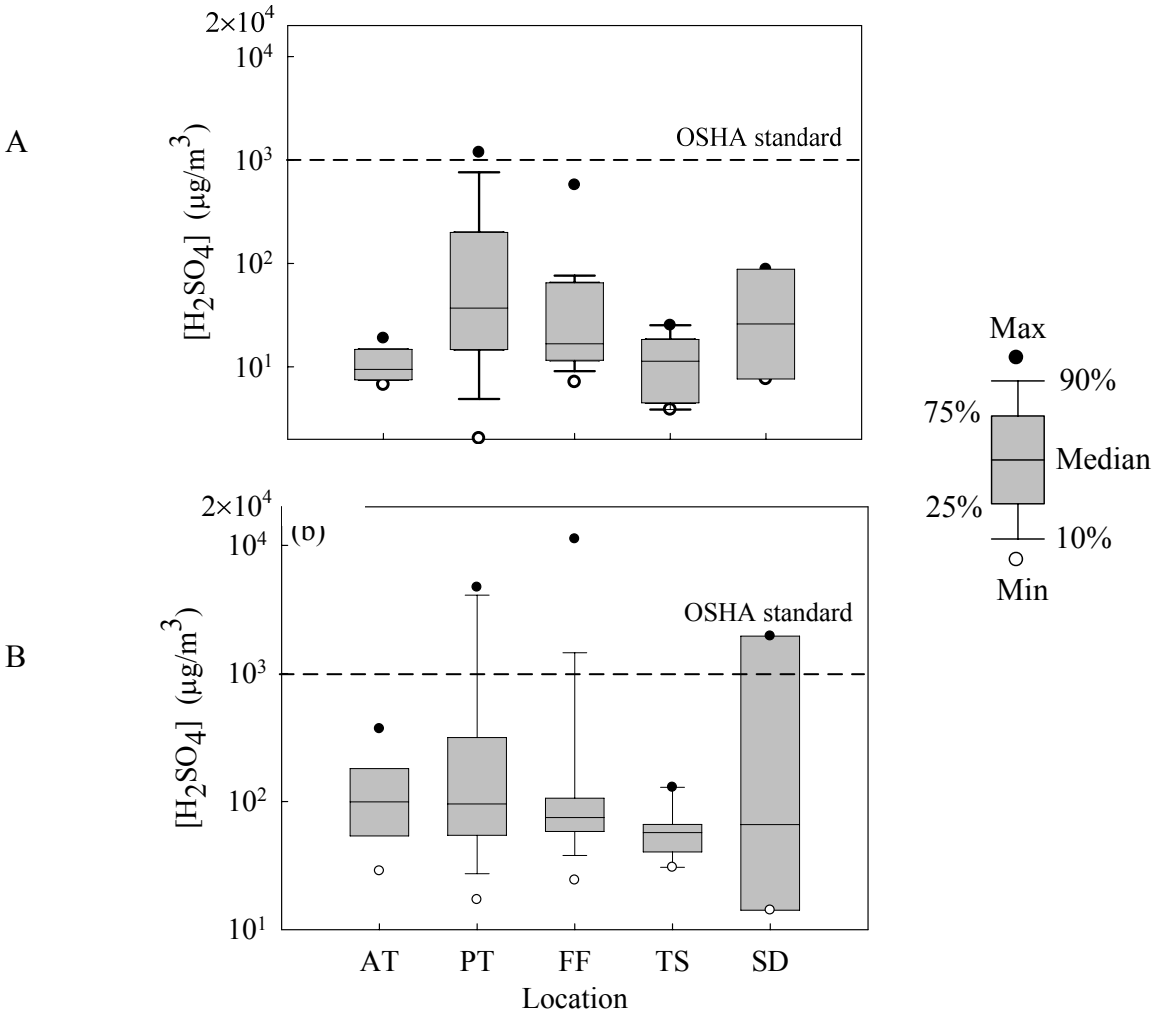

Figure 3-1. Sulfuric acid concentrations at 5 types of locations. Locations: AT- attack tank, PT- sulfuric acid pump tank, FF- filter (rotating table or belt filter) floor, and TS- truck station for sulfuric acid loading/unloading. Sampling methods: A) PM_{23} sulfuric acid by cascade impactor, and B) Total sulfuric acid by NIOSH Method 7903

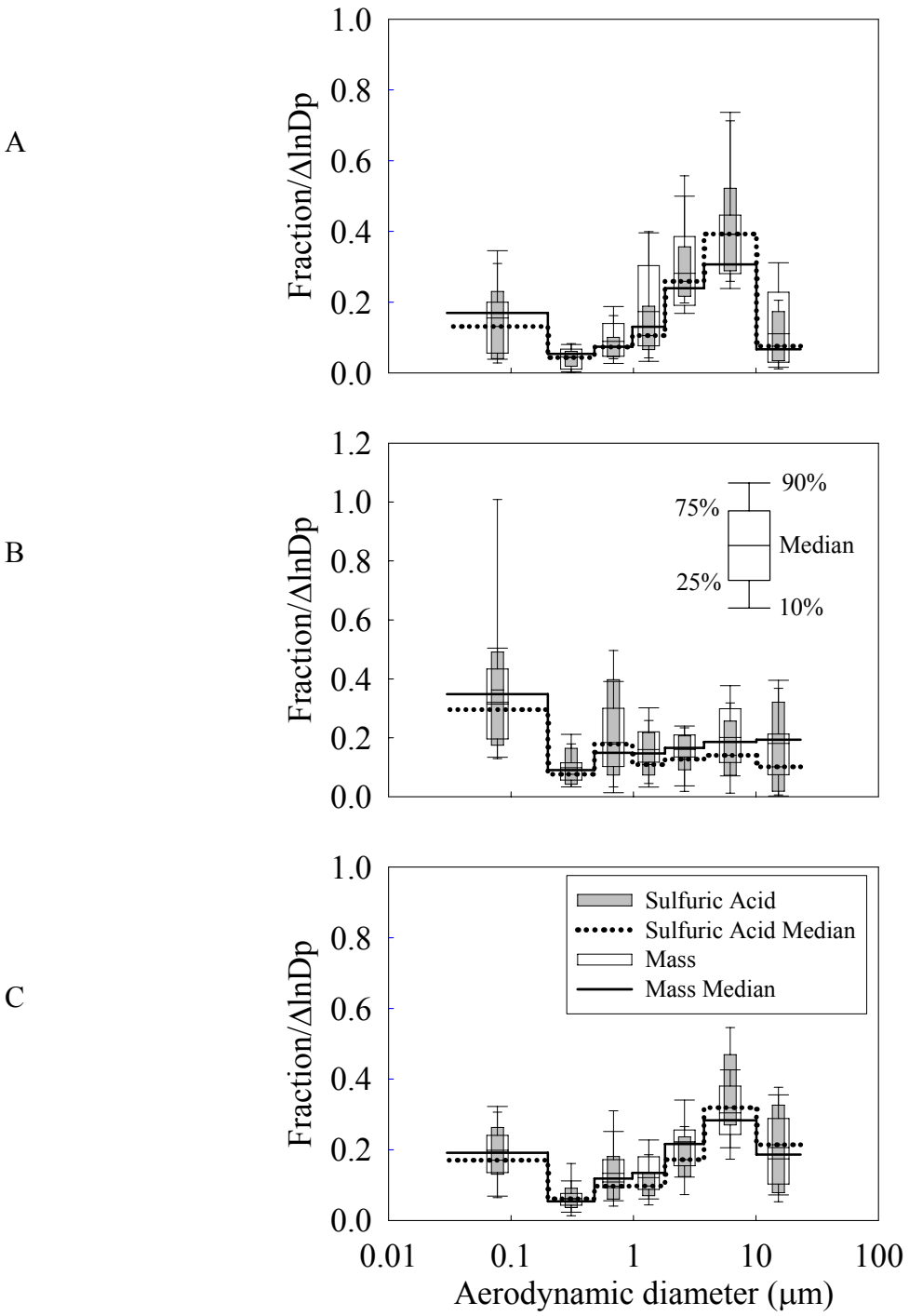

Figure 3-2. Sulfuric acid mist and aerosol mass size distributions. A) Sulfuric acid pump tank areas, high aerosol mass loading (> 100 μg/m3). B) Sulfuric acid pump tank areas, low aerosol mass loading (< 100 μg/m3). C) Belt/rotating table filter floors

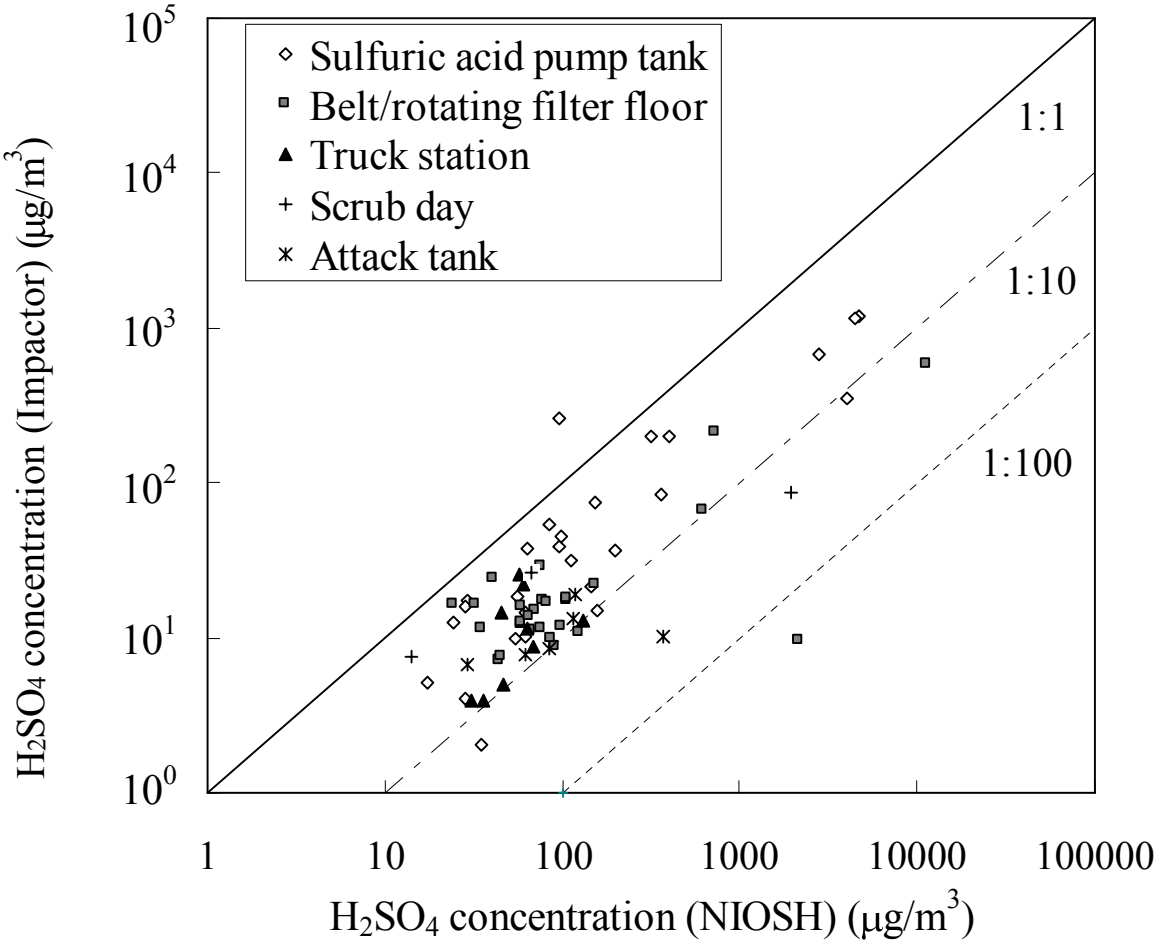

Figure 3-3. Comparison of PM_{23} sulfuric acid concentrations from the cascade impactor and total sulfuric acid concentrations from the NIOSH method

CHAPTER 4
SIZE DISTRIBUTION, CHEMICAL COMPOSITION AND ACIDITY OF MIST AEROSOLS IN FERTILIZER MANUFACTURING FACILITIES IN FLORIDA*

Background

Strong inorganic acid mists containing sulfuric acid have been reported to correlate well with lung and laryngeal cancers in humans [*Blair and Kazerouni*, 1997; *Sathiakumar et al.*, 1997; *Steenland*, 1997]. Phosphate fertilizer manufacturing facilities, where sulfuric acid is used to digest phosphate rock to form H_3PO_4, have been listed by the NTP [*USDHHS*, 2005] as one of many occupational exposures to strong acid. The current OSHA 8 h TWA of PEL of H_2SO_4 and H_3PO_4 mists is set at 1 mg/m^3. The carcinogenic mechanism of strong inorganic acid mists containing sulfuric acid is not clearly understood yet [*Blair and Kazerouni*, 1997]. However, reduced pH environments are known to enhance the depurination rate of DNA and the deamination rate of cytidine [*Swenberg and Beauchamp*, 1997; *USDHHS*, 2005], which can cause DNA damage or mutation. Furthermore, studies have found that adverse pulmonary health effects are related to the hydrogen ion (H^+) rather than sulfate [*Ostro et al.*, 1991; *Schlesinger*, 1984, 1989; *Schlesinger et al.*, 1990a; *Schlesinger et al.*, 1990b] and that the biological response is a function of the total concentration of H^+ deliverable to the cells or the total extractable H^+ per particle [*Schlesinger and Chen*, 1994].

The aerosol acidity is an important factor that affects the amount of the extractable H^+, i.e., strong acid can release more H^+. In phosphate fertilizer facilities, H_3PO_4 and H_2SO_4 mists are the major acid species [*Hsu et al.*, 2007a]. These two strong acids can contribute a significant amount of the extractable H^+. Currently, no method is available to directly measure the aerosol acidity; nevertheless, several ambient aerosol thermodynamic models have been developed to

* Reprinted with permission from Hsu, Y.-M., Wu, C.-Y., Lundgren, D. A., Birky, B. K., 2007. Size Distribution, Chemical Composition and Acidity of Mist Aerosols in Fertilizer manufacturing Facilities in Florida. *J. Aerosol Sci.* doi:10.1016/j.jaerosci.2007.10.008.

estimate the aerosol acidity [*Yao et al.*, 2006, 2007]. However, particulate phosphate species have not been included in those aerosol models because the concentrations of those species are too low to be detected in the ambient aerosols.

The hazard of aerosol depends on the chemical compositions and the sites where the aerosol deposits. It is well known that the deposition of an aerosol in the respiratory system is related to its aerodynamic behavior. Meanwhile, relative humidity and chemical characteristics of the aerosol may affect its size. Sulfuric acid is hydrophilic, and the size of the mist can increase significantly when it encounters moisture [*Seinfeld and Pandis*, 1998; *Wu and Biswas*, 1998] in the respiratory system.

In considering the effects of aerosol size on human health, the ACGIH has adopted a TLV-TWA of 0.2 mg/m^3 for the thoracic particulate fraction of sulfuric acid mist [*ACGIH*, 2004]. Although the acid mist size distribution is an important parameter in evaluating health effects, in the past very little data was available for the particle size distribution of phosphoric acid mists at phosphate fertilizer facilities. The objectives of this chapter are to characterize the chemical characteristics of mist aerosols in the current phosphate facilities with size-resolved information and to establish an aerosol thermodynamic model to estimate aerosol acidity.

Methods

Sampling Sites

Five types of locations which might have high acid mist concentrations were selected, including H_2SO_4 pump tank areas, product filter floors, attack tank areas, truck stations for loading/unloading H_2SO_4, and a granulator on a scrub day. Sampling was conducted at seven plants in central FL and one plant in north FL. Totally, there were 24 sampling locations at eight fertilizer plants. The type and number of sampling locations at each plant have been described in detail in Hsu *et al*. [2007a] and Chapter 2 of this dissertation.

Sampling and Analysis Methods

A University of Washington Source Test cascade impactor (Mark III) was used to collect mists for the size distribution. The impactor was operated at 25 Lpm and the corresponding d_{50} was 0.20, 0.48, 0.98, 1.8, 3.8, 10, and 23 μm for the seven stages, respectively. Aerosol bounce from the impaction plates can result in mass loss and thus distort the sample's true size distribution. However, a previous study [*Pauluhn*, 2005] showed that the mean mass recoveries from cascade impactor analyses were 97.2 ± 11.9% and 94.1 ± 17.3% for liquid and solid aerosols, respectively; therefore, aerosol bounce problems of the cascade impactor can be neglected.

The collection substrate used in this study was Zefluor™, or backed Teflon membrane filter (pore size: 2 μm, Pall Corp.), which provides high collection efficiency and low reactivity with acidic gases [*Chow*, 1995; *Lee and Mukund*, 2001]. A final filter (Zefluor™, 47 mm, pore size: 2 μm, Pall Corp.) was placed after the impactors to collect any penetrating aerosols. The lower limit of particles collected on the final filter was assigned to be 0.03 μm, a value commonly used in similar cascade impactor sampling studies [*Divita et al.*, 1996; *Howell et al.*, 1998; *Wagner and Leith*, 2001]. The sampling time was 24 h and three successive samples were obtained at each location. Totally, there were 72 sets of impactor samples in those plants. A microbalance (model MC 210 S, Sartorius Corp.; readability: 10 μg) was used for weighing the aerosol mass. In order to reduce the interference of water vapor, all filters were placed in a desiccator at room temperature for pre- and post-conditioning for 24 h before weighing the filters. After weighing the filter, water soluble species were extracted from the filter using deionized (DI) water in an ultrasonic bath (Bath ultrasonic timer, Fisher scientific) for 1 h. A Nanopure Diamond system (Barnstead International) provided the DI water with a conductivity

of 18.2 megohm. The water soluble ion species concentrations were analyzed by an IC system (Dionex ICS 1500, Dionex Corp.). Two analytical columns, IonPac CS12A (Dionex Corp.) and IonPac AS9-HC (Dionex Corp.), were applied to analyze cations, including K^+, Na^+, Ca^{2+}, Mg^{2+}, and NH_4^+, and anions, including F^-, Cl^-, NO_2^-, NO_3^-, SO_4^{2-}, and PO_4^{3-}, respectively.

Aerosol Thermodynamic Model

A thermodynamic model of multicomponent aerosols was developed to estimate the acidity of aerosols with high sulfuric acid (200 μg/m^3) or high phosphoric acid (500 μg/m^3) concentration. The important parameters of the model—chemical components, the aerosol water amount (AWA), equilibrium reactions, reaction constants, and the activity coefficient calculations—are described in this section.

Five chemical species larger than 1% (mass) based on the chemical analysis in this study were selected: Ca^{2+}, NH_4^+, Na^+, SO_4^{2-}, and PO_4^{3-}. Liquid components include H^+, Ca^{2+}, NH_3, NH_4^+, Na^+, SO_4^{2-}, HSO_4^-, H_2SO_4, $H_2PO_4^-$, H_3PO_4, $H_5P_2O_8^-$, H_2O, Na_3PO_4, and $(NH_4)_3PO_4$; solid components include $Ca_3(PO_4)_2$, $CaHPO_4$, $NH_4H_2PO_4$, $(NH_4)_3PO_4$, Na_3PO_4, NaH_2PO_4, Na_2HPO_4, $CaSO_4 \cdot 2H_2O$, NH_4HSO_4, $(NH_4)_2SO_4$, $NaHSO_4$, and Na_2SO_4. AWA (μg/m^3 air) was calculated by Equation 4-1:

$$AWA = AMC - IMC \quad (4\text{-}1)$$

where AMC is the total aerosol mass concentration (μg/m^3 air) and IMC the total ionic species mass concentration (μg/m^3 air).

Chemical equilibrium reactions and equilibrium constants are listed in Table 4-1 for 20 reactions. The equilibrium constant is expressed as a function of temperature. It should be noted that the sampling was conducted for 24 h and temperature varied during the sampling.

Therefore, the rate constants under the standard condition, 298.15 K, were applied in the modeling work.

The activity of ionic species in aqueous phase (a_i) is defined as Equation 4-2:

$$a_i = r_i \times m_i \tag{4-2}$$

where r_i is the activity coefficient of species *i* and m_i is the molal concentration of species *i* (mole solute/kg solvent).

Multicomponent activity coefficients were calculated following the Kusik and Meissner method [*Kim et al.*, 1993], which is based on binary activity coefficients:

$$\log r_{12} = \frac{z_2}{(z_1+z_2)I} \times \left[m_2 \left(\frac{z_1+z_2}{2} \right)^2 \log r_{12}^0 + m_4 \left(\frac{z_1+z_4}{2} \right)^2 \log r_{14}^0 + \ldots \right]$$

$$+ \frac{z_1}{(z_1+z_2)I} \times \left[m_1 \left(\frac{z_1+z_2}{2} \right)^2 \log r_{12}^0 + m_3 \left(\frac{z_3+z_2}{2} \right)^2 \log r_{32}^0 + \ldots \right] \tag{4-3}$$

where r_{12} is the activity coefficient of a 1-2 ion pair in the multicomponent solution, z_i is the absolute number of unit charges of ion species *i*, and *I* is the ionic strength of the solution, which is

$$I = \sum_i \frac{1}{2} m_i z_i^2 \tag{4-4}$$

r_{ij}^o is the mean ionic activity coefficient of the single solute solution with *i-j* ion pair.

To calculate multicomponent activity coefficients, binary activity coefficients need to be available. They were calculated by a polynomial regression method [*Bassett and Seinfeld*, 1983] for the ionic strength smaller than 30 mole/kg and the Kusik and Meissner method [*Kim et al.*, 1993] for that larger than 30 mole/kg. The polynomial regression method is shown in Equation 4-5.

$$\ln r_{12}^{o} = \frac{-AI^{1/2}}{1+BI^{1/2}} + \sum_{i=1} a_i I^i \tag{4-5}$$

where A, B, and a_i are parameter values which are available in Bassett and Seinfeld [1983].

The Kusik and Meissner method is shown in Equation 4-6 and q values used in this model are listed in Kim *et al*. [1993].

$$r_{12}^{o} = \left(\left[1 + B(1+0.1I)^{q} - B \right] \times \exp\left(-\frac{0.5107 I^{1/2}}{1+CI^{1/2}} \right) \right) \tag{4-6}$$

where $B = 0.75 - 0.065 \times q$ and $C = 1 + 0.055 \times q \times \exp(-0.023 \times I^3)$

Currents ambient aerosol thermodynamic models have not included phosphate species, including H_3PO_4, $H_2PO_4^-$ and $H_5P_2O_8^-$. However, phosphate species should be considered in this study due to high particulate phosphate concentrations and the activities were calculated by Pitzer's equation shown in Equation 4-7 to Equation 4-9 [*Jiang*, 1996].

$$\ln r_1 = z_1^2 f^r + \sum_a m_a \left[2B_{1a} + \left(\sum mz \right) C_{1a} \right] + \sum_c m_c \left[2\theta_{1c} + \sum_a m_a \psi_{1ca} \right]$$
$$+ \sum_c \sum_a m_c m_a \left[z_1^2 B'_{ca} + |z_1| C_{ca} \right] + \sum_a \sum_{a'} m_a m_{a'} \psi_{1aa'} \tag{4-7}$$

$$\ln r_2 = z_2^2 f^r + \sum_c m_c \left[2B_{c2} + \left(\sum mz \right) C_{c2} \right] + \sum_a m_a \left[2\theta_{1a} + \sum_c m_c \psi_{2ac} \right]$$
$$+ \sum_c \sum_a m_c m_a \left[z_2^2 B'_{ca} + |z_2| C_{ca} \right] + \sum_c \sum_{c'} m_c m_{c'} \psi_{cc'2} \tag{4-8}$$

$$\ln r_{12} = \frac{\left(v_1 \ln r_1 + v_2 \ln r_2 \right)}{v_1 + v_2} \tag{4-9}$$

where $f^r = -0.392 \left[\frac{I^{1/2}}{1+1.2I^{1/2}} + \frac{2}{1.2} \ln\left(1+1.2I^{1/2}\right) \right]$

$$B_{ij} = \beta_{ij}^{(0)} + \frac{\beta_{ij}^{(1)}}{2I} \times \left[1 - \left(1 + 2I^{1/2}\right)\exp\left(-2I^{1/2}\right)\right]$$

$$B_{ij}^{'} = \frac{\beta_{ij}^{(1)}}{2I^2} \times \left[-1 + \left(1 + 2I^{1/2} + 2I\right)\exp\left(-2I^{1/2}\right)\right]$$

$$C_{ij} = \frac{C_{ij}^{\phi}}{2\sqrt{z_i z_j}}$$

$$\theta_{ij}^{'} = \frac{\partial \theta_{ij}}{\partial I}$$

ν_1 and ν_2 are the number of moles of ion species 1 and 2 per mole of 1-2 ion pair species dissociating completely. The parameters $\beta_{ij}^{(0)}, \beta_{ij}^{(1)}, C_{ij}^{\phi}$ and ψ are listed in Jiang [1996] and $\theta_{ij}^{'}$ can be neglected for most cases [*Kim et al.*, 1993].

Results and Discussion

Aerosol Chemical Species

Sulfuric acid mists, phosphoric acid mists, and particulate fluoride were the major species observed in the phosphate fertilizer plants. Their concentrations at all locations are shown in Figure 4-1. The highest mass concentrations of these species were 1163, 1589 and 388 μg/m^3, and they were obtained at the sulfuric acid pump tank area, the belt/rotating table filter floor, and the attack tank area, respectively. Major chemical species concentrations and their size nformation at each location are discussed in the following sections. All ion concentrations at the truck station were very low (max: 64 μg/m^3) and are therefore not discussed further.

Sulfuric aid pump tank areas

The size distribution of sulfuric acid in this area has been reported previously [*Hsu et al.*, 2007b], and only the major results are summarized here. The median mass concentrations (±standard deviation) were 98 (±430), 71 (±424) and 52 (±149) μg/m^3 for PM_{23}, PM_{10} and $PM_{2.5}$

(aerosol aerodynamic diameter smaller than 23, 10 and 2.5 μm), respectively. The major mode was 3.8–10 μm when high sulfuric acid mist concentration was observed. Sulfuric acid was the dominant species in this area, and its size distribution was similar to the aerosol mass size distribution at this location.

For other species at the sulfuric acid pump tank areas, ammonium had the highest concentration, second only to sulfuric acid, followed by calcium. The sulfuric acid pump tank area is an outdoor location where the emitted aerosols can mix with the ambient air. The relations between sulfate and two major cations, calcium and ammonium, are shown in Figure 4-2. In the case of sulfate and ammonium, the ratios of sulfate to ammonium were close to 1 for small particles (< 1.8 μm, including the impactor stages of 0.03–0.20, 0.20–0.48, 0.48–1.0, 1.0–1.8 μm) when sulfate concentrations were low (< 50 neq/m^3). Regarding the relation between calcium and sulfate, it was the large particles (> 1.81 μm) that had calcium/sulfate ratios close to 1 when sulfate concentrations were low (< 50 neq/m^3). The relation between sulfate and both basic species is shown in Figure 4-2C. It is interesting to note that both size ranges had a similar trend where the concentrations of the two basic species were combined. Furthermore, the combined concentrations were higher than sulfate concentrations when sulfate concentrations were lower (< 50 neq/m^3). There is a transition range between 50 and 500 neq/m^3. Above 500 neq/m^3, sulfate concentrations were higher than those of the two basic species. Clearly demonstrated, calcium and ammonium play a critical role in neutralizing the acid, and they dominate in separate size ranges: ammonium for fine aerosols and calcium for coarse aerosols. However, if the acid emission is high, there may not be sufficient cations in the air to balance the acids.

Product filter floors

Phosphoric acid was the major species at the product filter floors and particulate fluoride was the species of the next importance. The median mass concentrations (±standard deviation) of PM_{23}, PM_{10}, and $PM_{2.5}$ were 201 (±514), 178 (±372), and 95 (±68) μg/m^3, respectively. The median concentrations of phosphoric acid were 35 (PM_{23}), 26 (PM_{10}), and 5 ($PM_{2.5}$) μg/m^3 and those of particulate fluoride were 19 (PM_{23}), 17 (PM_{10}), and 11 ($PM_{2.5}$) μg/m^3. Phosphoric acid mists and aerosol mass size distributions are shown in Figure 4-3, and both had a similar trend. It can be clearly seen that predominantly the phosphoric acid was present in the coarse mode (3.8–10 μm). The boiling point of pure phosphoric acid is 217 °C [*Weast*, 1988]. However, the boiling point of phosphoric acid solution decreases as the concentration of phosphoric acid in the solution decreases [*Messnaoui and Bounahmidi*, 2005]. The boiling point is only 108 °C when phosphoric acid concentration is 36 wt% P_2O_5, which is the designated concentration in the manufacturing process. This temperature is close to the operating temperature (100 °C) in the manufacturing process at the plants. Hence, it is possible that phosphoric acid vaporizes at this operating condition and then condenses to form aerosols when it encounters cooler air. The species that had the second highest median concentration was fluoride and the size distributions at the product filter floor areas are displayed in Figure 4-3C. The major mode size of fluoride was 3.8–10 μm. The minor mode size of fluoride was 0.03–0.2 μm. Because the product filter floors are semi-open space, no major cations are available to neutralize the phosphoric acid and fluoride. The inside air does not mix well with ambient air. Therefore, the aerosol emission controls the aerosol chemical species concentrations at this type of location.

Attack tank areas

Sampling was carried out at two attack tank areas and six samples were obtained. Particulate fluoride was the major species at the attack tank areas. The median concentrations of fluoride were 67 (PM_{23}), 64 (PM_{10}), and 60 ($PM_{2.5}$) $\mu g/m^3$, which indicated most fluoride existed in small aerosols. Phosphate rock, which is the main useful product of phosphate ore, consists of calcium phosphate mineral apatite with gangue constituents, which include silica, fluoride, calcite, dolomite, clay and iron-aluminum oxide [*Hodge and Popovici*, 1994]. The attack tank is where phosphate rock reacts with sulfuric acid. The violent reaction causes strong heat release in the form of vapor, which is evacuated from the attack tank with other gaseous effluents. Fluoride can be evaporated as gaseous fluoride, e.g., silicon tetrafluoride [*Parish*, 1994]. Fluoride has strong affinity with silica, and therefore fluoride generated from the process tends to combine with silica. The high affinity of fluoride with silica causes fluorosilicic acid to remain in phosphoric acid solution or fluorosilicate (SiF_6^{2-}) to precipitate. Particulate fluoride size distributions at the attack tank areas are shown in Figure 4-4. Two types of size distribution were observed. When fluoride concentrations were high (two samples: 320 and 388 $\mu g/m^3$), the mode size was 3.8–10 μm. This occurred at a plant where the attack tank was not a closed system. At this location with high fluoride concentrations, moisture was also high. Therefore, the possible explanation for the size distribution is that gas phase fluoride and water were evaporated and then condensed on existing aerosols. For the other plant where the attack tank is a closed system, the fluoride concentrations and humidity were lower (four samples: 25–85 $\mu g/m^3$), and the mode size was 0.03–0.2 μm.

Ammonium had the second highest concentration, and its median concentrations were 22 (PM_{23}), 20 (PM_{10}) and 18 ($PM_{2.5}$) $\mu g/m^3$. The relation between these two major species, fluoride

and ammonium, is shown in Figure 4-5. The results indicated that there was not enough ammonium to neutralize fluoride when high fluoride concentrations were observed (> 250 neq/m^3).

Granulator on a scrub day

Table 4-2 displays the median concentrations of PM_{23}, PM_{10} and $PM_{2.5}$ of all species at the granulator on a scrub day. Particulate fluoride, phosphate, sulfate and ammonium had higher concentration levels than others. Nonetheless, there was no clear trend in terms of the dominating species due to significant variation among the samples. Scrubbing is an intermittent maintenance activity and it usually takes 3-4 h for one scrubbing. Therefore, the aerosol emission was not stable.

Aerosol Acidity

Although the carcinogenic mechanism of strong inorganic acid mists containing sulfuric acid is not clear yet, aerosol acidity may play a key factor. To estimate the aerosol acidity, the charge balance method and the aerosol thermodynamic model were applied in this study.

Charge balance method

Sulfuric acid and phosphoric acid were the major species at the pump tank areas and the product filter floors, respectively. Assuming that charge balance of those ions analyzed in this study exists in the aerosols, hydrogen ion concentration can be estimated by the difference between cation and anion equivalent weights. The relationships of cation equivalent weight and anion equivalent weight of PM_{10-23}, $PM_{2.5-10}$, and $PM_{2.5}$ at these locations are shown in Figure 4-6. The aerosol acidity was high at the sulfuric acid pump tank areas for $PM_{2.5-10}$ and $PM_{2.5}$. When anion concentration was higher than 500, 500, and 1000 neq/m^3 for PM_{10-23}, $PM_{2.5-10}$, and $PM_{2.5}$, respectively, most aerosols were acidic.

Whether the location is in an outdoor environment or an indoor setting affects the acidity. In general, the major acid species can be neutralized by the abundant ammonia around the area in the outdoor location; in contrast, there is not enough mixing with the ambient air in the indoor location and the amount of ammonia is insufficient. A good example is the aerosol at the product filter floor. All product filters are indoor locations. It can be clearly seen that most aerosols are acidic in this type of location regardless of their particle size. In addition to indoor/outdoor location, the other important factor is the acid loading. This can be best illustrated using the samples at the sulfuric acid pump tank areas. At this area, the PM_{10-23} aerosol had a low acid loading (< 500 neq/m^3) and the aerosol was more or less neutral. Regarding $PM_{2.5}$ and $PM_{2.5-10}$ aerosols, the same can be said for low anion loading cases (< 1000 and 500 neq/m^3), while the aerosols were acidic at high loadings (> 1000 and 500 neq/m^3). In the case of high aerosol loadings, the aerosol remains acidic because of the limited amount of basic species available to neutralize the particles in a short period of time after emission. In $PM_{2.5-10}$, 9 of 27 samples showed high acidity because sulfuric acid mists were dominant in this size range. The sampling location for the granulator on a scrub day was an outdoor location where the air could mix with ambient air. The aerosols from this location were close to neutral, even though their concentrations were high. The major species to neutralize the aerosol acidity was ammonium from the granulator where phosphoric acid reacted with ammonia to produce the final products, diammonium phosphate or monoammonium phosphate.

Aerosol thermodynamic model

An aerosol thermodynamic model has been established in this study to calculate the acidity of aerosols with high sulfuric acid and phosphoric acid mist concentrations. Sulfuric acid is a stronger acid than phosphoric acid. Also, the former is hygroscopic in nature while the latter is

not. These two factors have strong influences on the aerosol's characteristics in a humid environment, e.g., equilibrium size and aerosol H^+ concentration.

Four samples with sulfuric acid concentrations higher than 200 μg/m^3 were selected and two samples with phosphoric acid concentrations higher than 500 μg/m^3 were selected as representatives. Particulate fluoride concentrations were lower than 2.5 mg/m^3, the OSHA regulation. Furthermore, aerosol fluoride can exist as H_2SiF_6, which could not be discriminated in this study. Therefore, the samples with high fluoride concentration at the attack tank area were not investigated.

The results for aerosols with high sulfuric acid mist concentrations are displayed in Figure 4-7A. The modes of H^+ concentration were 1.8–3.8 μm and 3.8–10 μm. The highest H^+ concentration was 170 mole/kg (molality) and its mode was 1.8–3.8 μm. The hygroscopic sulfuric acid can quickly pick up moisture to form larger mist particles in the respiratory system and the actual location where mists deposit can vary. Several assumptions were made to estimate the deposition site of aerosols and the time to reach its equilibrium size: (1) the relative humidity of the sampling locations and the human respiratory system were 40% and 95%, respectively; (2) the geometric mean size (2.6 μm for 1.8–3.8 μm and 6.2 μm for 3.8–10 μm) was considered as the representative size; (3) the cross-sectional area of human nose inlet is 2 cm^2; (4) the air volume of one inhalation is 0.5 L; (5) the time for one inhalation is 1 s; (6) the distance from nose inlet to the laryngeal region is 10 cm. The Zdanovskii–Stokes–Robinson (ZSR) equation [*Jacobson*, 1999] shown in Equation 4-10 was used to calculate the equilibrium aerosol size at a given relative humidity, and Equation 4-11 [*Hinds*, 1999] was used to determine the time for reaching the new equilibrium size.

$$m_a = Y_0 + Y_1 a_w + Y_2 a_w^2 + Y_3 a_w^3 + Y_4 a_w^4 + Y_5 a_w^5 + Y_6 a_w^6 + Y_7 a_w^7 \quad (4\text{-}10)$$

where m_a is the molality of solute x, a_w the water activity (relative humidity expressed as a fraction), and *Y*'s the polynomial coefficients [*Jacobson*, 1999].

$$d_p \frac{d(d_p)}{dt} = \frac{4D_v M}{R\rho} \times \frac{p_\infty}{T_\infty} \times \phi \text{, } d_p > \lambda \tag{4-11}$$

where d_p is the aerosol size, t the time, D_v the diffusion coefficient of vapor, M the molecular weight of the liquid, R the gas constant (8.314 $J \cdot K^{-1} \cdot mol^{-1}$), ρ the density of the liquid, p_∞ the partial pressure of vapor in the gas surrounding the droplet, T_∞ the temperature away from the droplet surface, λ = 0.066 μm, and

$$\phi = \frac{2\lambda + d_p}{d_p + 5.33\left(\frac{\lambda^2}{d_p^2}\right) + 3.42\lambda}\text{, Fuch's correction factor}$$

The hydrogen ion size distributions at RHs of 40% and 95% for the sample with sulfuric acid mist concentration of 653 $\mu g/m^3$ are shown in Figure 4-7B. As the relative humidity increases, H^+ concentration decreases while the mode size slightly increases. The time required to grow to the equilibrium size is only 0.014 s, which is smaller than the aerosol traveling time of 0.04 s for 10 cm. As shown, the inhaled mist aerosol can grow large enough to deposit in the upper respiratory tract.

The International Commission on Radiological Protection (ICRP) model has been developed to predict total and regional deposition of inhaled aerosol [*ICRP*, 1994]. Three simplified ICRP equations, Equation 4-12 to Equation 4-14, were also applied in this study to determine the deposition fraction (DF) for monodisperse spheres of standard density at standard conditions [*Hinds*, 1999]. For the head airways, DF_{HA},

$$DF_{HA} = IF\left[\frac{1}{1+\exp\left(6.84+1.183\ln d_p\right)}+\frac{1}{1+\exp\left(0.924-1.885\ln d_p\right)}\right] \quad (4\text{-}12)$$

where IF is the inhalable fraction given as

$$IF = 1 - 0.5\left(1-\frac{1}{1+0.00076d_p^{2.8}}\right) \quad (4\text{-}13)$$

For the tracheobronchial region, DF_{TB},

$$DF_{TB} = \left(\frac{0.00352}{d_p}\right)\left[\exp\left(-0.234\left(\ln d_p+3.40\right)^2\right)+63.9\exp\left(-0.819\left(\ln d_p-1.61\right)^2\right)\right] \quad (4\text{-}14)$$

For the alveolar region, DF_{AL},

$$DF_{AL} = \left(\frac{0.0155}{d_p}\right)\left[\exp\left(-0.416\left(\ln d_p+2.84\right)^2\right)+19.11\exp\left(-0.482\left(\ln d_p-1.362\right)^2\right)\right] \quad (4\text{-}15)$$

Three cases were considered, and the results are shown in Table 4-3. In Cases 1a and 2a, the geometric mean sizes for the 2 modes discussed previously were used. These particles were assumed to maintain their original sizes since the ICRP model does not allow consideration of particle growth. As shown, the larger 6.2 μm particles had a higher DF in the head airways than the smaller 2.6 μm particles. It should be noted, however, that the IF of 6.2 μm particles was slightly lower than 2.6 μm particles. In Case 3, 11.8 μm is the equilibrium size of 6.2 μm. Due to the much lower IF, the DF of 11.8 μm particles was actually lower than the smaller 6.2 μm particles!

Since the growth to the equilibrium size takes much shorter time than the aerosol traveling time as previously discussed, the equilibrium size was used to determine the deposition in Cases 1b and 2b. Different outcomes were observed! Compared with the no-growth cases, the DF greatly increased. The results show that sulfuric acid mists sampled in this study mainly deposit

in the upper respiratory tract, which is consistent with epidemiological evidence of a correlation between H^+ concentration and laryngeal cancer. The results also demonstrate the importance of considering particle growth for hygroscopic components in assessing the particle's deposition in the respiratory system. However, it must be noted that extensive epidemiological studies of phosphate industry workers have concluded "no relation was found between acid mist exposures and laryngeal cancer" [*Checkoway et al.*, 1996].

Hydrogen ion size distributions for high phosphoric acid mist concentrations are shown in Figure 4-7C. The mode size of hydrogen ion concentration was 1.8–3.8 μm and the highest H^+ concentration was 37.4 mole·kg^{-1}. Compared to the sulfuric acid cases discussed previously, clearly the hydrogen ion concentration of the phosphoric acid cases was lower even when its concentration, 1589 μg/m^3, was higher than sulfuric acid mist concentration. The results show that sulfuric acid plays the dominant role in contributing extractable H^+ and phosphoric acid is not as important as sulfuric acid in supplying extractable H^+.

Summary

In phosphate fertilizer facilities, phosphoric acid and sulfuric acid mists were the major aerosol components for the product filter floors and the sulfuric acid pump tank areas, respectively. The median concentration and the standard deviation of sulfuric acid at the sulfuric acid pump tank areas were 37 ± 322 μg/m^3. The median concentration ± one standard deviation for phosphoric acid was 35 ± 326 μg/m^3, and it mainly existed in the coarse mode. The possible source of phosphoric acid was evaporation and then condensation when it encountered cooler air. The attack tank area had highest fluoride concentration, which was 25–388 μg/m^3 at this area. The current OSHA 8-h TWA–PEL of phosphoric acid and sulfuric acid mist set at 1 mg/m^3 was not exceeded on average, but could be exceeded at the product filter floors and the pump tank

areas, respectively, under conservative assumptions that all phosphoric acid and sulfuric acid came from phosphate and sulfate, respectively. It should be noted that workers spend much less than 8 hours per day in the area, and thus the true time-weighted exposure level can be expected to be lower.

Calcium and ammonium were the major species to neutralize the aerosol acidity at the sulfuric pump tank areas when acid loading was low. The aerosol thermodynamic model showed the modes of aerosol H^+ concentration in 1.8–3.8 μm and 3.8–10 μm for the aerosols with high sulfuric acid mist concentrations. These hygroscopic acid mists can grow in the high humidity conditions of the upper respiratory system, and aerosols with high H^+ concentrations mainly deposit in the upper respiratory system. Sulfuric acid was found to play a much more prominent role than phosphoric acid and fluoride. The respiratory deposition projection of sulfuric acid mists is consistent with that of H^+ and both components mainly deposit in the extrathoracic airways of the head and neck. However, extensive epidemiological studies of phosphate industry workers have not shown an increased incidence of any type of cancer.

Table 4-1. Equilibrium relations and constants

Equilibrium Relation	Equilibrium Constant Expression	Equilibrium Constant Keq (298.15 K)	Units	Source
$H_2SO_{4(aq)} \longleftrightarrow HSO_{4(aq)}^- + H_{(aq)}^+$	$\frac{\left[H^+\right]\left[HSO_4^-\right]r_{H^+}r_{HSO_4^-}}{\left[H_2SO_4\right]r_{H_2SO_4}}$	1.000×10^{3}	mole/kg	Jacobson [1999]
$HSO_{4(aq)}^- \longleftrightarrow SO_{4(aq)}^{2-} + H_{(aq)}^+$	$\frac{\left[H^+\right]\left[SO_4^{2-}\right]r_{H^+}r_{SO_4^{2-}}}{\left[HSO_4^-\right]r_{HSO_4^-}}$	1.020×10^{-2}	mole/kg	Jacobson [1999]
$H_3PO_{4(aq)} \leftrightarrow H_{(aq)}^+ + H_2PO_{4(aq)}^-$	$\frac{\left[H^+\right]\left[H_2PO_4^-\right]r_{H^+}r_{H_2PO_4^-}}{\left[H_3PO_4\right]r_{H_3PO_4}}$	6.918×10^{-3}	mole/kg	Jiang [1996]
$H_2PO_{4(aq)}^- + H_3PO_{4(aq)} \leftrightarrow H_5P_2O_{8(aq)}^-$	$\frac{\left[H_5P_2O_8^-\right]r_{H_5P_2O_8^-}}{\left[H_2PO_4^-\right]\left[H_3PO_4\right]r_{H_2PO_4^-}r_{H_3PO_4}}$	1.263	$mole^{-1}\cdot kg$	Jiang [1996]
$NH_{4(aq)}^+ \longleftrightarrow NH_{3(aq)} + H_{(aq)}^+$	$\frac{\left[NH_3\right]\left[H^+\right]r_{NH_3}r_{H^+}}{\left[NH_4^+\right]r_{NH_4^+}}$	5.623×10^{-10}	mole/kg	Benjamin [2002]
$H_2O \longleftrightarrow H_{(aq)}^+ + OH_{(aq)}^+$	$\frac{\left[H^+\right]\left[OH^-\right]}{a_w}r_{H^+}r_{OH^-}$	1.010×10^{-14}	mole/kg	Kim et al.[1993]
$CaSO_4\cdot 2H_2O_{(s)} \longleftrightarrow Ca_{(aq)}^{2+} + SO_{4(aq)}^{2-} + 2H_2O_{(aq)}$	$\left[Ca^{2+}\right]\left[SO_4^{2-}\right]r_{Ca^{2+}}r_{SO_4^{2-}}a_w^2$	4.320×10^{-5}	$mole^2/kg^2$	Jacobson [1999]
$NH_4HSO_{4(aq)} \longleftrightarrow NH_{4(aq)}^+ + HSO_{4(aq)}^-$	$\left[NH_4^+\right]\left[HSO_4^-\right]r_{NH_4^+}r_{HSO_4^-}$	1.380×10^{2}	$mole^2/kg^2$	Jacobson [1999]
$\left(NH_4\right)_2 SO_{4(s)} \longleftrightarrow 2NH_{4(aq)}^+ + SO_{4(aq)}^{2-}$	$\left[NH_4^+\right]^2\left[SO_4^{2-}\right]r_{NH_4^+}^2 r_{SO_4^{2-}}$	1.820	$mole^3/kg^3$	Jacobson [1999]
$\left(NH_4\right)_3 H\left(SO_4\right)_{2(s)} \longleftrightarrow 3NH_{4(aq)}^+ + 2SO_{4(aq)}^{2-} + H_{(aq)}^+$	$\left[NH_4^+\right]^3\left[H^+\right]\left[SO_4^{2-}\right]^2 r_{NH_4^+}^3 r_{H^+}r_{SO_4^{2-}}^2$	2.930×10^{1}	$mole^5/kg^5$	Jacobson [1999]
$NaHSO_{4(s)} \longleftrightarrow Na_{(aq)}^+ + HSO_{4(aq)}^-$	$\left[Na^+\right]\left[HSO_4^-\right]r_{Na^+}r_{HSO_4^-}$	2.840×10^{2}	$mole^2/kg^2$	Jacobson [1999]
$Na_2SO_{4(s)} \longleftrightarrow 2Na_{(aq)}^+ + SO_{4(aq)}^{2-}$	$\left[Na^+\right]^2\left[SO_4^{2-}\right]r_{Na^+}^2 r_{SO_4^{2-}}$	4.800×10^{-1}	$mole^3/kg^3$	Jacobson [1999]

$Ca_3(PO_4)_{2(s)} \longleftrightarrow 3Ca^{2+}_{(aq)} + 2PO^{3-}_{4(aq)}$	$[Ca^{2+}]^3[PO_4^{3-}]^2 r^3_{Ca^{2+}} r^2_{PO_4^{3-}}$	2.109×10^{-33}	$mole^5/kg^5$	This study[a]
$CaHPO_{4(s)} \longleftrightarrow Ca^{2+}_{(aq)} + HPO^{2-}_{4(aq)}$	$[Ca^{2+}][HPO_4^{2-}] r_{Ca^{2+}} r_{HPO_4^{2-}}$	1.889×10^{-7}	$mole^2/kg^2$	This study[a]
$Ca(H_2PO_4)_2 \cdot H_2O_{(s)} \longleftrightarrow Ca^{2+}_{(aq)} + 2H_2PO^{-}_{4(aq)} + H_2O$	$[Ca^{2+}][H_2PO_4^{-}]^2 r_{Ca^{2+}} r^2_{H_2PO_4^{-}} a_w$	6.153×10^{-2}	$mole^3/kg^3$	This study[a]
$NH_4H_2PO_{4(s)} \longleftrightarrow NH^{+}_{4(aq)} + H_2PO^{-}_{4(aq)}$	$[NH_4^{+}][H_2PO_4^{-}] r_{NH_4^{+}} r_{H_2PO_4^{-}}$	7.106×10^{-1}	$mole^2/kg^2$	This study[a]
$(NH_4)_3PO_{4(s)} \longleftrightarrow 3NH^{+}_{4(aq)} + PO^{3-}_{4(aq)}$	$[NH_4^{+}]^3[PO_4^{3-}] r^3_{NH_4^{+}} r_{PO_4^{3-}}$	9.437×10^{-1}	$mole^4/kg^4$	This study[a]
$Na_3PO_{4(s)} \longleftrightarrow 3Na^{+}_{(aq)} + PO^{3-}_{4(aq)}$	$[Na^{+}]^3[PO_4^{3-}] r^3_{Na^{+}} r_{PO_4^{3-}}$	9.823×10^{-1}	$mole^4/kg^4$	This study[a]
$NaH_2PO_{4(s)} \longleftrightarrow Na^{+}_{(aq)} + H_2PO^{-}_{4(aq)}$	$[Na^{+}][H_2PO_4^{-}] r_{Na^{+}} r_{H_2PO_4^{-}}$	1.193×10^{1}	$mole^2/kg^2$	This study[a]
$Na_2HPO_{4(s)} \longleftrightarrow 2Na^{+}_{(aq)} + HPO^{2-}_{4(aq)}$	$[Na^{+}]^2[HPO_4^{2-}] r^2_{Na^{+}} r_{HPO_4^{2-}}$	6.879	$mole^3/kg^3$	This study[a]

[a] $K_{eq}(298.15\,\mathrm{K}) = \exp\left(-\frac{1}{R\times T}\sum_i k_i v_i \Delta G_i^o\right)$

R= 8.314 J/mole·K, T = 298.15 K, $k_i = +1$ for products and $k_i = -1$ for reactants, v_i = the dimensionless stoichiometric coefficient.

$\Delta G_i^o = \sum \Delta G^o{}_{products} - \sum \Delta G^o{}_{reactants}$, ΔG^o for each species is from Weast [1988].

Table 4-2. Median ion species concentrations of cascade impactor samples collected at the granulator on a scrub day ($\mu g/m^3$)

NO.	Mass	F^-	Cl^-	NO_3^-	PO_4^{3-}	SO_4^{2-}	Na^+	NH_4^+	K^+	Mg^{2+}	Ca^{2+}
PM_{23}	392	54	5	4	35	26	9	66	3	2	11
PM_{10}	331	42	5	6	23	22	8	58	3	1	7
$PM_{2.5}$	263	39	4	4	9	18	6	48	2	1	3

Table 4-3. Aerosol deposition fractions for 3 cases

	Size (μm)		Inhalable	Deposition fraction		
Case	Inhalable	Deposition	fraction	Head airway	Tracheobronchial region	Alveolar region
1a	2.6	2.6	0.99	0.70	0.06	0.11
1b	2.6	5.0	0.99	0.89	0.04	0.06
2a	6.2	6.2	0.94	0.87	0.03	0.04
2b	6.2	11.8	0.94	0.92	0.01	0.01
3	11.8	11.8	0.78	0.77	0.01	0.01

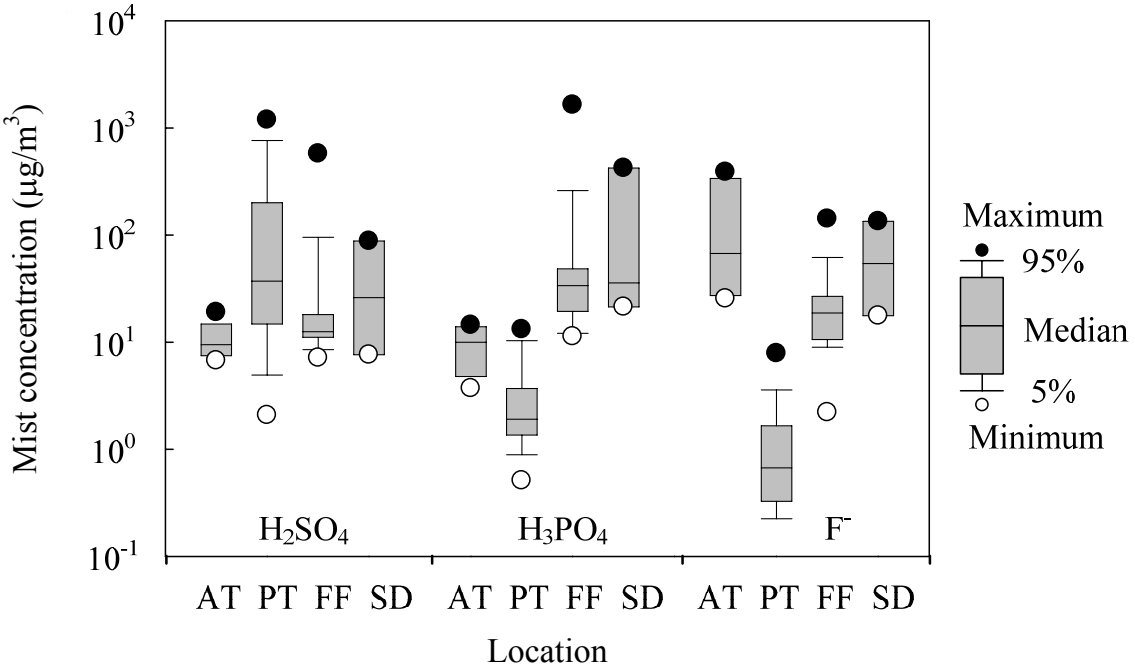

Figure 4-1. Sulfuric acid, phosphoric acid and fluoride concentrations at all locations. AT: attack tank area, PT: sulfuric acid pump tank area, FF: product filter floor, SD: the granulator plant on a scrub day

A

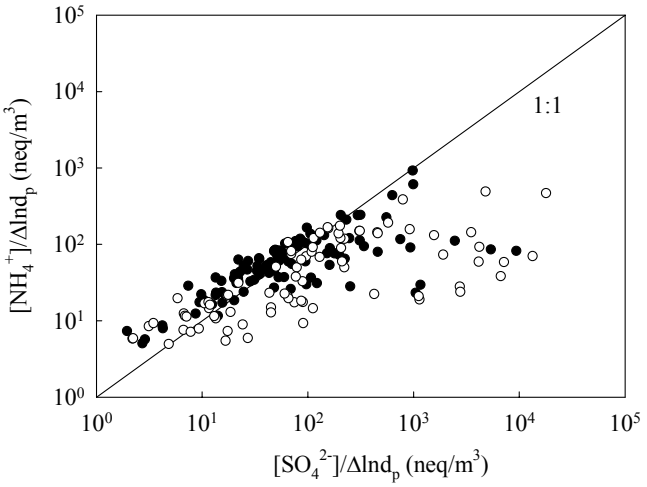

B

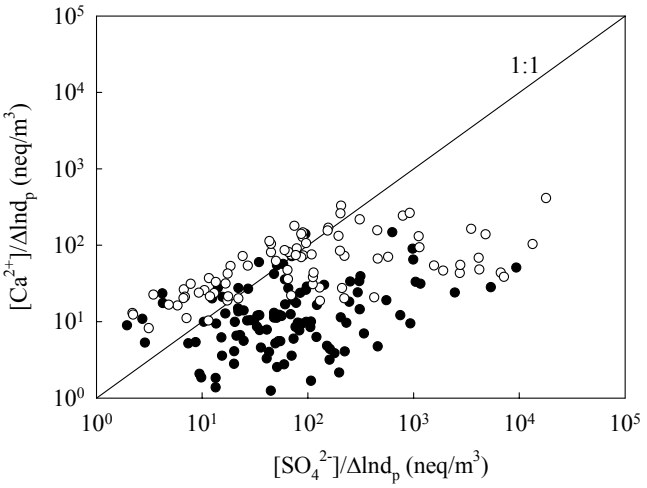

C

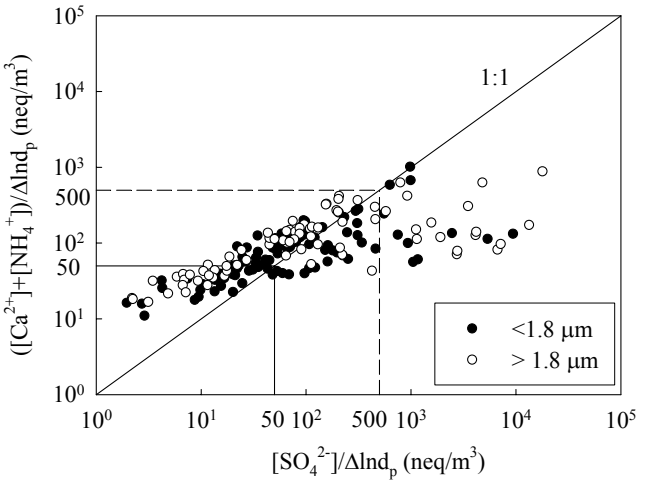

Figure 4-2. Relation between the major cations (ammonium and calcium) and sulfate concentrations at the sulfuric acid pump tank areas. A) Ammonium versus sulfate. B) Calcium versus sulfate. C) Ammonium and calcium versus sulfate

A

B

C

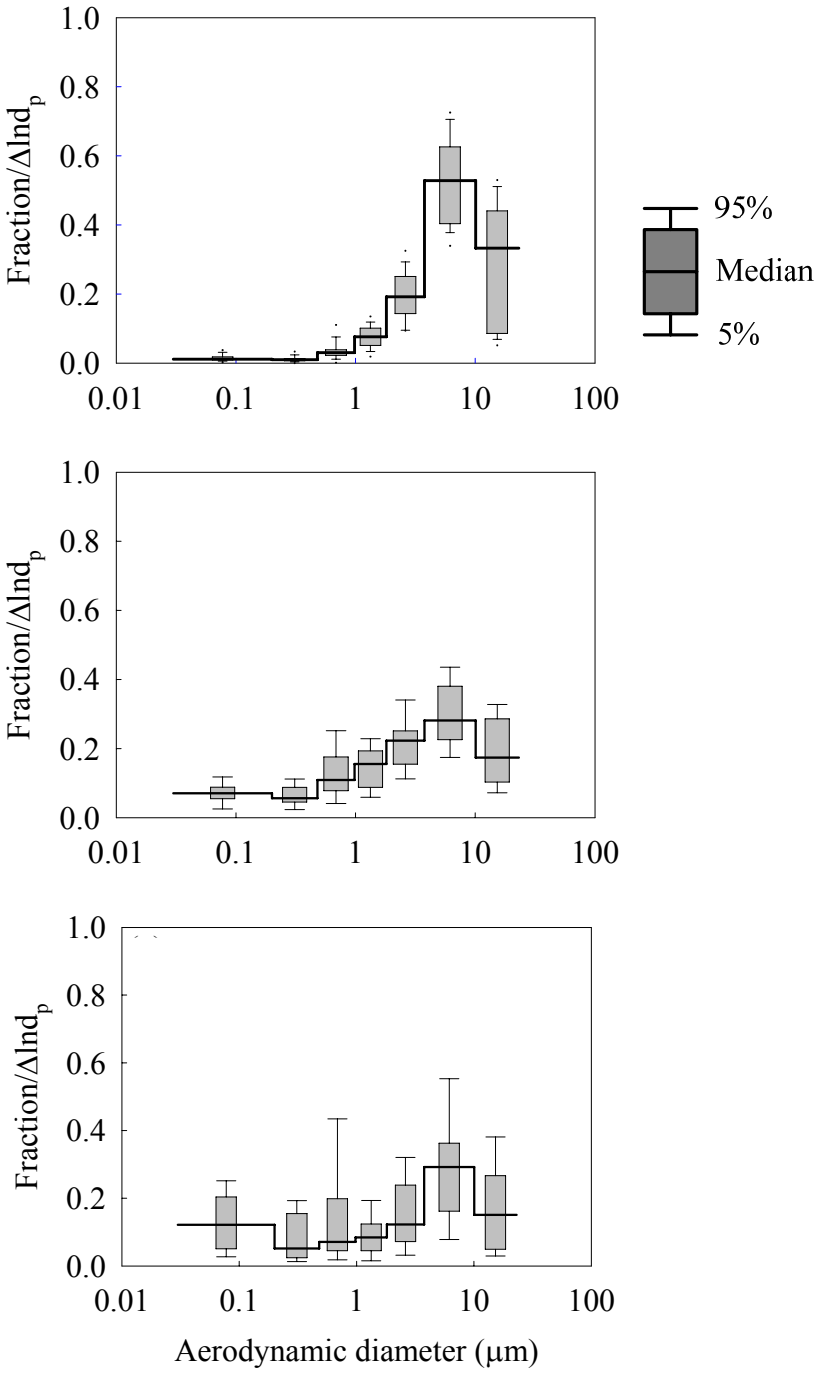

Figure 4-3. Aerosol size distributions at the product filter floors. A) Phosphoric acid mist. B) Aerosol mass. C) Particulate fluoride

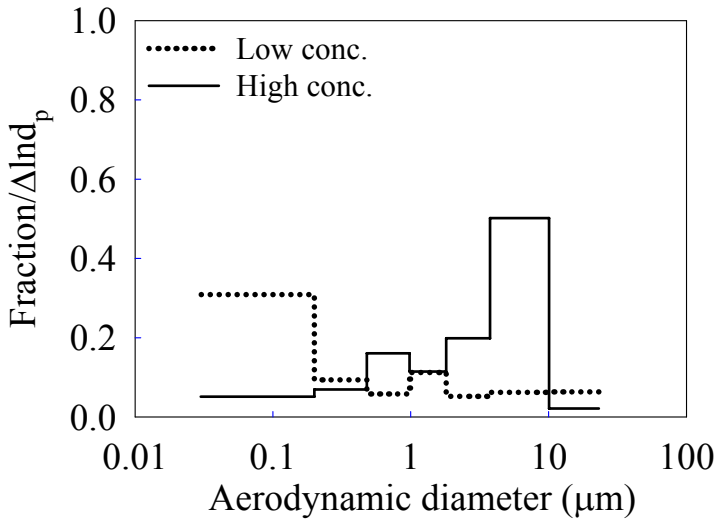

Figure 4-4. Particulate fluoride size distribution at the attack tank areas

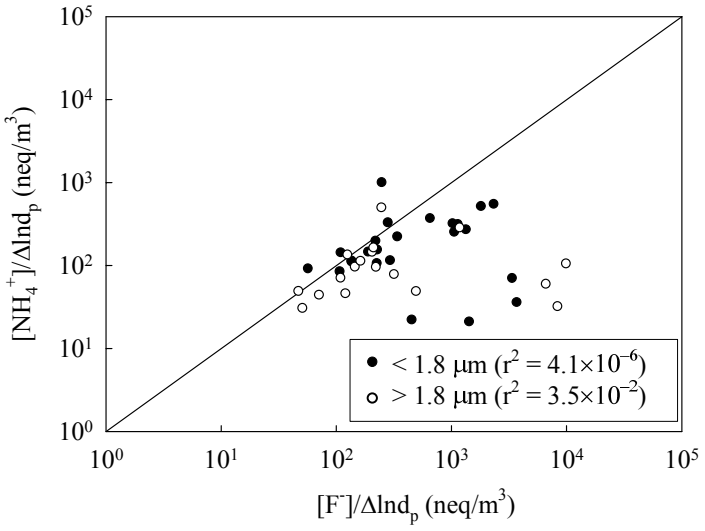

Figure 4-5. Relation between ammonium and fluoride concentrations at the attack tank areas

A

B

C

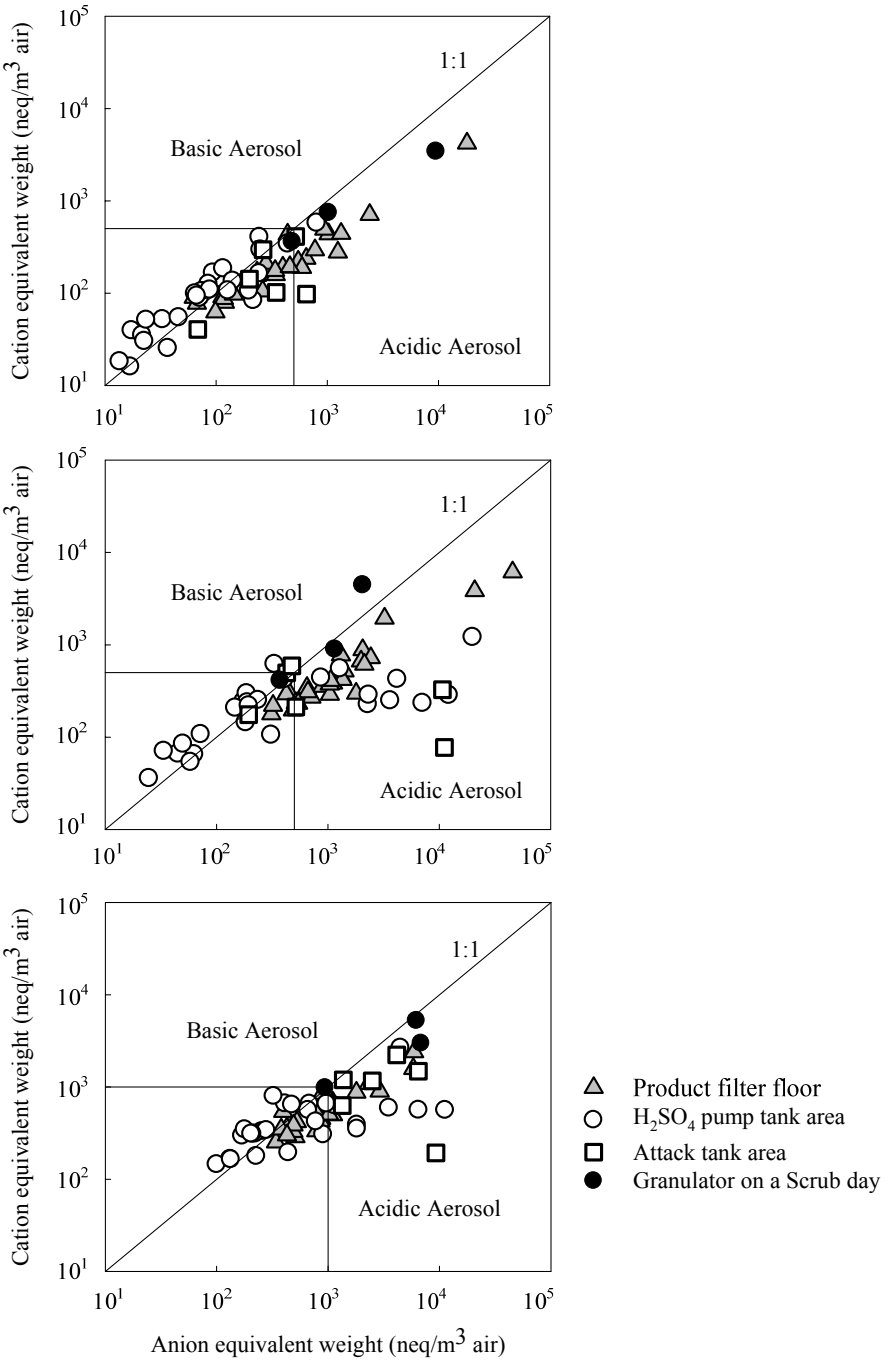

Figure 4-6. Relationship of cation equivalent weight and anion equivalent weight. A) For PM_{10-23}. B) For $PM_{2.5-10}$. C) For $PM_{2.5}$

A

B

C

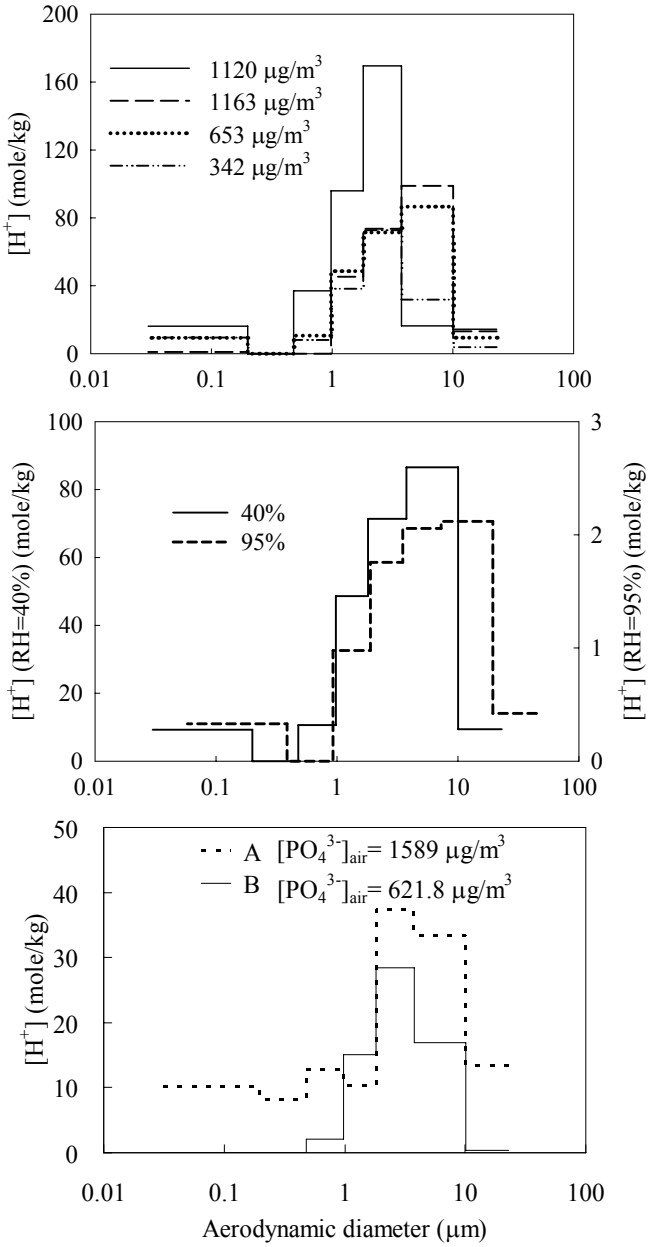

Figure 4-7. Aerosol hydrogen ion concentration size distribution. A) Aerosol H^+ concentration size distribution of samples with high sulfuric acid mist concentrations. B) Aerosol H^+ concentration size distributions for the sample with H_2SO_4 concentration of 653 $\mu g/m^3$ at RHs of 40% and 95%. C) Aerosol H^+ concentration size distribution of samples with high phosphoric acid mist concentrations

CHAPTER 5
POSITIVE SULFATE ARTIFACT FORMATION FROM SO_2 ADSORPTION IN THE SILICA GEL SAMPLER USED IN NIOSH METHOD 7903*

Background

NIOSH Method 7903 [*NIOSH*, 1994] is the approved method set by OSHA for measuring the total concentration of acidic aerosols and gases, including hydrogen fluoride, hydrogen chloride (HCl), hydrogen bromide (HBr), nitric acid (HNO_3), sulfuric acid and phosphoric acid. It is the method commonly used by the health and safety staff in the phosphate industry, as well as other occupational environments such as semiconductor industry, lead battery factories, aluminum smelting, machining, electroplating processes, and even disaster response [*Healy et al.*, 2001; *Hsu et al.*, 2007b; *Lue et al.*, 1998; *Tsai et al.*, 2001; *Wallingford and Snyder*, 2001]. The sampler of NIOSH Method 7903 consists of one section of glass fiber filter plug, followed by two sections of silica gel. The glass fiber filter plug is designed to filter out the majority of aerosols, whereas the silica gel sections are used mainly to adsorb acidic gases. The NIOSH recommended sampling flow rate range is 0.2–0.5 Lpm (except that less than 0.3 Lpm should be used for HF). The samples collected are extracted and then analyzed by IC. In evaluating the method, NIOSH researchers reported ~100% collection efficiency for acidic gases (HCl, HF and HNO_3) [*Cassinelli*, 1986; *Cassinelli and Taylor*, 1981]. For aerosols (H_2SO_4 and H_3PO_4), ~90% efficiency (94.8±4.8% for H_3PO_4 and 86±4.6% for H_2SO_4) was reported when the samples collected on the glass fiber filter section and the front silica gel section were combined. In Chapter 3 [*Hsu et al.*, 2007b], NIOSH Method 7903 was compared with cascade impactor sampling for sulfuric acid mist sampling at phosphate fertilizer manufacturing facilities. The

* Reprinted with permission from Hsu, Y.-M., Kollett, J., Wysocki, K., Wu, C.-Y., Lundgren, D. A., Birky, B. K., 2007. Positive Artifact Sulfate Formation from SO_2 Adsorption in the Silica Gel Sampler Used in NIOSH Method 7903. *Environ. Sci. Technol.* 41, 6205-6209.

results indicate that sulfuric acid mist concentration from the NIOSH method might be overestimated, because of the interference of SO_2.

Past studies have reported that glass fiber filter can adsorb SO_2, which can be subsequently transformed into a sulfite (SO_3^{2-}) species [*Chow*, 1995; *Coutant*, 1977; *Lee and Mukund*, 2001; *Watson and Chow*, 2001] on the moist-basic surface of glass fiber filter, as listed in Reaction 5-1 and Reaction 5-2.

$$SO_2 + OH^- \leftrightarrow HSO_3^- \quad (5\text{-}1)$$

$$HSO_3^- + OH^- \leftrightarrow SO_3^{2-} + H_2O \quad (5\text{-}2)$$

The glass fiber filter consists of borosilicate glass filaments, which have high alkalinity [*Chow*, 1995; *Coutant*, 1977; *Watson et al.*, 1995]. It also contains high concentrations of sodium, potassium, calcium, and other basic species that exhibit high alkalinities and pH values. These properties aid in the adsorption of SO_2, HNO_3 and acidic gases [*Chow*, 1995; *Lee and Mukund*, 2001; *Watson and Chow*, 2001]. To cause artifacts in sulfate measurement, subsequent oxidation to form sulfate is also critical. Oxidation of sulfite in solution is highly dependent on pH, and the half-life is 4–5 min for sodium sulfite solution at room temperature, if the oxygen supply is unlimited [*Schroeter*, 1963]. Coutant [1977] reported that the conversion on glass fiber filter is 90% within 2 h when air containing SO_2 passes though the filter. Penetration occurs when the alkalinity decreases below a certain value. Silica gel, a high surface area material, can also adsorb sulfur dioxide [*Fox and Jeffries*, 1979; *Kopac and Kocabas*, 2002; *Stratmann and Buck*, 1965]. The hydrophilic property of silica gel can effectively attract moisture, which can enhance the absorption of soluble species such as SO_2 [*Tsai et al.*, 2001]. As mentioned, this method is widely used in the workplace to characterize sulfuric acid mist concentrations, as a way to evaluate protection for workers. No study has examined and quantified the artifact

sulfate from the silica gel tube. Therefore, the objective of this chapter was to characterize the interference of SO_2 to determine the accurate sulfuric acid mist concentration. The oxidation of sulfur(IV) and SO_2 adsorption, following the NIOSH protocol, were investigated in this study.

Methods

Two groups of experiments were conducted: sulfur(IV) oxidation and SO_2 adsorption. Sulfur(IV) includes sulfite, bisulfite (HSO_3^-), and sulfurous acid (H_2SO_3). These experiments are described below.

Sulfur(IV) Oxidation

NIOSH Method 7903 specifies the use of IC eluent solution as the extraction solution, which is the 9 mM Na_2CO_3 solution used in this study. In addition, a water bath at 100 °C was used as specified in the method to enhance desorption of samples. To examine the effect of the extraction procedures on sulfur(IV) oxidation, experiments were performed for four combinations of eluent solution and water bath temperature, which were as follows:

(A) using DI water (Nanopure Diamond, Barnstead) of 18.2 MΩ cm as the extraction solution without a water bath,

(B) using DI water as the extraction solution with a water bath at 100 ^oC to investigate the effect of temperature,

(C) using 9 and 18 mM Na_2CO_3 solutions as the extraction solution without a water bath to examine the effect of the concentration of eluent, and

(D) using 9 mM Na_2CO_3 solution as the extraction solution with a water bath at 100 ^oC.

Sodium sulfite (Na_2SO_3) was used as the sulfite source. 3.7% formaldehyde (HCHO) solution was used to quench the sulfur(IV) oxidation [*Dong and Dasgupta*, 1986; *Munger et al.*, 1986] at the designated time. For the procedures, a 100 mL solution (DI water, 9 or 18 mM

Na_2CO_3 solution) was placed on the stirrer (Isotemp Magnetic Stirrer, Fisher) of 300 rpm at room temperature or 100 °C. The designated amount of Na_2SO_3 was then added into the solution. A 5 mL sample was taken out at a designated time and put into a glass tube with 5 mL HCHO solution. Sulfate concentration was then analyzed via IC (model ICS 1500, Dionex).

Preliminary experiments were conducted to suggest that the experimental time should be 1 h for tests without water bath and 10 min for tests with water bath. Measurements indicated that the sulfur(IV) oxidation was fast in the beginning. Hence, sulfate concentrations were measured every minute, for the first 5 min, for oxidation without water bath and every 20 s, for the first 5 min, for oxidation with a water bath.

Sulfur Dioxide Adsorption

The experimental setup is shown in Figure 5-1. SO_2 gas from a cylinder (10 ppm, relative uncertainty of ±5%) was mixed with zero air (Thermo Electron Instrument) to obtain the desired concentration. A bubbler was used to supply moisture, and the mixing ratio was used to adjust the humidity. The gas stream then passed though a silica gel tube, followed by an impinger containing 100 ml of a 9 mM Na_2CO_3 solution. Preliminary experiments showed the SO_2 collection efficiency of the impinger was 100%. The total molar concentration of SO_2 passing through the system was the sum of sulfate molar concentration from the silica gel tube and the impinger. Hydrogen peroxide (0.6%) (1 mL) was added into the impinger after the experiment, to oxidize collected sulfite to obtain sulfate concentration. The suggested flow rate range of NIOSH Method 7903 is 0.2–0.5 Lpm. Thus, the experimental condition for sampling flow rate was set in this range. According to past studies, SO_2 concentrations in sulfuric acid plants have been 0.12–15.9 ppm [*Englander et al.*, 1988; *Meng and Zhang*, 1990; *Yadav and Kaushik*, 1996]. Hence, SO_2 concentration used in this study was set in this range. Experimental conditions are

shown in Table 5-1. The adsorption of SO_2 on silica gel tube under various feed SO_2 concentrations, sampling flow rates, and sampling times was examined.

Results and Discussion

Sulfur(IV) Oxidation

Aqueous sulfur(IV) uncatalyzed oxidation is a first-order reaction which can be expressed by Equation 5-3 [*Larson et al.*, 1978]:

$$-\frac{d\left[SO_3^{2-}\right]}{dt} = k\left[SO_3^{2-}\right] \tag{5-3}$$

The analytical solution to Equation 5-3 can be obtained by integrating it from time $t = 0$ to time t and is shown in Equation 5-4. Sulfate was the species analyzed in this study; therefore, sulfite mass concentration was calculated using the measured sulfate mass concentration following Equation 5-5. The least-square fitting method (SigmaPlot, Version 8.0, SPSS Inc., Chicago, IL) with Equation 5-4 was used to calculate the rate constant (k) and the pre-exponent constant (a):

$$\frac{\left[SO_3^{2-}\right]_t}{\left[SO_3^{2-}\right]_o} = a\exp\left(-kt\right) \tag{5-4}$$

$$[SO_3^{2-}]_t = \frac{\left[SO_4^{2-}\right]_{Total} - \left[SO_4^{2-}\right]_t}{96} \times 80 \tag{5-5}$$

where $[SO_3^{2-}]_t$ is the sulfite concentration at time t, $[SO_3^{2-}]_o$ the initial sulfite concentration, $[SO_4^{2-}]_{Total}$ the total sulfate concentration, $[SO_4^{2-}]_t$ the sulfate concentration at time t, and t the time (expressed in seconds).

Figure 5-2 illustrates the normalized sulfite concentration ($[SO_3^{2-}]_t/[SO_3^{2-}]_o$) as a function of time. For the conditions expressed in panels (A) and (C), sulfur(IV) oxidation reached at least 85% in 1 h and 40 min, respectively. The means and standard deviations of the rate constants for

the conditions in panels (A) and (C) were 0.0003 ± 0.0001 and 0.0023 ± 0.0003 s^{-1}, respectively. As shown, the addition of Na_2CO_3 enhanced the kinetics, i.e., the application of Na_2CO_3 solution as the extraction solution can result in more effective conversion. For the conditions described in panel (B), sulfur(IV) oxidation reached at least 90% in 5–10 min and the mean ± standard deviation of the rate constants was 0.0198 ± 0.0144 s^{-1}. Comparing the results with that of conditions expressed in panel (A), it can be observed that the kinetics was significantly increased by the water bath designed to aid the desorption. Two Na_2CO_3 concentrations (9 and 18 mM) were tested; the results showed no discernible difference between these two. For condition (D), sulfur(IV) oxidation reached 100% in just 2—3 min and the mean ± standard deviation of the rate constants was 0.0508 ± 0.0274 s^{-1}. The condition shown in panel (D) is the exact sample extraction method specified by NIOSH Method 7903, which recommends a boiling time of 10 min. The results clearly show that SO_2 adsorbed by silica gel and glass fiber filter can be completely converted to sulfate during the extraction procedure.

Rate constants for uncatalyzed oxidation reactions of sulfur(IV) are summarized in Table 5-2. As shown, the reported values range widely. Indeed, many reaction rates of the uncatalyzed oxidation of sulfur(IV) are often too high, because traces of transition metals in the water enhance the uncatalyzed process [*Huss et al.*, 1978]. Clark and Radojevic [*Clarke and Radojevic*, 1983] obtained a rate constant that was 7 times slower for the uncatalyzed reaction, when using Milli-R/Q water instead of distilled water. Furthermore, the oxidation rates shown in Table 5-2 indicate that sulfur(IV) oxidation is strongly dependent on the pH. Radojevic [*Radojevic*, 1984] has recommended the uncatalyzed oxidation rate be given by Equation 5-6:

$$\frac{d\left[SO_4^{2-}\right]}{dt}(M/s) = 0.32\left[SO_3^{2-}\right]\left[H^+\right]^{1/2} \qquad (pH \le 7) \quad (5\text{-}6)$$

The oxidation rates for the conditions portrayed in panels (A) and (C) in this study are within this range. The oxidation rate for condition (C) was higher than that for condition (A) and the pH dependence can explain this difference.

Some may have concerns about potential oxidants or catalysts present in the solution that may change the oxidation rate. The IC extraction solution was prepared from fresh DI water; the hydrogen peroxide (H_2O_2) and ozone (O_3) concentrations are negligible in the samples. The concentrations of trace metals should be very low, because the DI water system provided the fresh water with a resistivity of 18.2 MΩ-cm, which is an ion-free solution (except H^+ and OH^-). The IC eluent solution used in this study was prepared by using commercially available sodium carbonate (EM Science). Based on the information provided by the supplier, the maximum iron content is 0.0005% (w/w). The corresponding iron concentration of the IC extraction solution is $<8.5\times10^{-8}$ M, and the effect at this concentration level, if any, is considered to be negligible.

Sulfur Dioxide Adsorption

If artifact SO_2 causes overestimation of sulfuric acid mist concentration, the degree of impact for a given sampling condition must be investigated. In the second group of experiments, SO_2 concentration, sampling flow rate, and sampling time were examined to assess their effects.

Sulfur dioxide concentration

Two runs of artifact sulfate concentrations under various SO_2 concentrations sampled at 0.3 Lpm for 2 h are displayed in Figure 5-3A. Runs A and B were conducted under the same conditions to examine the reproducibility. Results from these two runs had the same trend and the 10% variation of feed SO_2 concentration could explain the difference of artifact sulfate concentrations between these runs. The sulfate concentration, or the interference of SO_2, increased as the inlet SO_2 concentration increased. Figure 5-3A indicated that, when the inlet

SO_2 concentration was 0.8 ppm (±10%), the mean artifact sulfate concentration was 190 μg/m^3. To assess the relative amount adsorbed, time-weighted collection percentage (TWCP) was adopted, which is defined as the percentage of feed SO_2 concentration collected by the silica gel tube over the given sampling time, i.e., (collected sulfate concentration/total sulfate concentration) × 100%. The TWCP had the opposite trend, i.e., the TWCP was high when low SO_2 concentration was introduced. The adsorption isotherm dictates that the adsorbed amount increases but gradually plateaus as vapor concentration increases. For a linearly increasing concentration, the percentage therefore decreases. When low SO_2 concentration (0.2 ppm) was introduced, the TWCP reached 16% after 2 h of sampling at 0.3 Lpm, or equivalent to a 125 μg/m^3 sulfate artifact. As SO_2 concentration increased to 0.8 ppm, the TWCP reached 6%, which is equivalent to a 190 μg/m^3 sulfate artifact after 2 h of sampling.

Sampling flow rate

The artifact sulfate concentrations and the corresponding TWCPs with an inlet SO_2 concentration of 1.5 ppm (±10%) under various flow rates are exhibited in Figure 5-3B. The sulfate concentration at a low flow rate (0.2 Lpm) was 374 μg/m^3, whereas, at the higher flow rate, 0.5 Lpm, it was 163 μg/m^3. The TWCP at a low flow rate was also higher than that at a high flow rate. Collection by diffusion is a function of residence time, and it increases as residence time increases. As flow rate increased, the residence time decreased, resulting in a lower artifact sulfate concentration. The NIOSH method recommends a flow rate lower than 0.3 Lpm if HF is present. However, as shown, a low flow rate yielded a higher amount of sulfate artifact.

Sampling time

The artifact sulfate concentrations and the TWCP, as a function of sampling time, are shown in Figure 5-3C. The TWCP for 2 h of sampling of 0.8 ppm SO_2 were 16%, 9.2%, 5.4%, and 4.6% for 0.2, 0.3, 0.4, and 0.5 Lpm, respectively. At 0.2 Lpm (2 h sampling), 0.8 ppm SO_2 can cause artifact sulfate amount of 498 $\mu g/m^3$, which can significantly affect the accurate determination of sulfuric acid mist concentration. Increasing the sampling time to 8 h yielded an artifact at 0.2 Lpm of 172 $\mu g/m^3$. The artifact sulfate concentration decreased as sampling time increased. This was due to the decrease of adsorption rate as the effective adsorption sites were consumed over time. For the same reason, the TWCP also decreased.

Both glass fiber filter and silica gel can adsorb SO_2. The adsorptions of the glass fiber filter and the silica gel are displayed in Figure 5-4 using collection index (CI), which is defined as the artifact sulfate amount (given in micrograms) divided by the feed SO_2 concentration (expressed in units of pm). As shown, the adsorbed SO_2 amount increased as the sampling time increased for both glass fiber filter and silica gel, although the patterns were not the same. The adsorption of SO_2 on the glass fiber filter was very quick and accounted for the majority of the adsorption in the first few hours. However, it was saturated within 2–3 h and the amount increased only slightly after that. In contrast, the adsorbed amount of SO_2 on silica gel increased as the time increased.

The adsorbed SO_2 amounts under various SO_2 concentrations, flow rates, and sampling times indicate that SO_2 can cause significant interference. It can be as high as 500 $\mu g/m^3$ for 0.8 ppm SO_2 at a sampling time of 2 h and flow rate of 0.2 Lpm. The OSHA regulation for sulfuric acid mist concentration is 1 mg/m^3. The result indicates that the interference caused by SO_2 cannot be neglected when the mist concentration is low and SO_2 concentration is high (e.g., > 0.5

ppm). The artifact can affect the compliance status of a plant. Therefore, the silica gel sampler containing a glass fiber filter plug and two sections of silica gel is not suitable for sampling sulfuric acid mist under such conditions.

Sulfur Dioxide Adsorption Model

To estimate the artifact for a given sampling condition, a modified model based on a deactivation model [*Kopac and Kocabas*, 2002; *Yasyerli et al.*, 2001] that considers flow rate, sampling time and SO_2 concentration was developed, which is shown in Equation 5-7. The first-order deactivation rate constants (k_d, and k_sS_o) can be obtained by fitting experimental data.

$$\left[SO_4^{2-}\right]_t = \theta\left[SO_2\right]_O\left\{1-\exp\left[-\frac{k_sS_o}{Q}\times\exp\left(-k_dt\right)\right]\right\} \quad (5\text{-}7)$$

where $\left[SO_4^{2-}\right]_t$ is the artifact sulfate concentration (expressed in units of μg/m^3), θ the conversion factor of SO_2 to SO_4^{2-} (1.67), $[SO_2]_o$ the initial SO_2 concentration (expressed in unit of μg/m^3), k_sS_o the observed adsorption rate (expressed in unit of cm^3/min), Q the flow rate (given in units of cm^3/min), k_d the first-order deactivation rate constant (given in units of min^{-1}), and t the time (expressed in minutes).

Results of the regression analysis of the experimental data are given in Table 5-3, which shows a good relationship between the experimental data and the estimated values. The R^2 values for the regression were ≥0.81 for the silica gel section. Although this model was developed for the adsorption on silica gel, the adsorption on glass fiber filter also fit well. The R^2 value was > 0.92.

The relation between the measured sulfate concentration from the silica gel tube and the concentration from the model prediction is displayed in Figure 5-5. Most predictions are in the range of ±35% artifact sulfate concentration from the measurement. As demonstrated, the

deactivation model gives reasonably good predictions of artifact sulfate concentrations obtained in the silica gel tube. Thus, it can be used for correcting the artifacts in sulfuric acid sampling if the SO_2 concentration is available. The application of this model should be further investigate in a field sampling.

Summary

NIOSH Method 7903, which uses one section of glass fiber filter and two sections of silica gel, has been developed to determine the total concentrations of acid mists in workplace air although certain gases are suspected to cause interference. In this study, experiments were carried out to investigate the roles of S(IV) oxidation and sulfur dioxide (SO_2) adsorption in causing artifacts in sulfuric acid measurement. First, S(IV) oxidation under 4 combinations of water bath temperature and Na_2CO_3 solution concentration was examined to investigate the effect of the extraction process of NIOSH Method 7903. It was shown that S(IV) oxidation to form sulfate could reach 100% in just 2-3 min following the extraction process of NIOSH Method 7903. The results demonstrate that using the procedure, SO_2 adsorbed by the silica gel and the glass fiber filter easily yields sulfate artifact. Sulfur dioxide adsorption under various flow rates, SO_2 concentrations and sampling times was also investigated. The experimental data were fitted into a deactivation model to determine the adsorption rate constant and the deactivation rate constant. The model can serve as a tool for estimating the sulfate artifact if SO_2 concentration is available.

Table 5-1. Experimental conditions of SO_2 adsorption

Set	Flow Rate (Lpm)	Sampling Time (h)	[SO_2] (ppm)
1	0.3	2	0.2, 0.4, 0.6 and 0.8
2	0.4 and 0.5	3	0.2, 0.6, 1.1, 1.4 and 1.6
3	0.2, 0.3, 0.4 and 0.5	3 and 8	1.5
4	0.2, 0.3, 0.4 and 0.5	2, 3, 4, 8, 10 and 12	0.8

Table 5-2. Rate constants for uncatalyzed oxidation reaction of sulfur(IV) by oxygen

	Reaction conditions		
k (s^{-1})	pH	Temp, *T* (^oC)	Reference
1.18×10^{-7}	3.0	25	Tanaka [1987]
1.72×10^{-7}	4.0	25	Tanaka [1987]
9.19×10^{-7}	5.0	25	Tanaka [1987]
1.63×10^{-6}	6.0	25	Tanaka [1987]
1.3×10^{-5} [a]	8.2–8.9	25	Clarke and Radojevic [1983]
9.5×10^{-5} [b]	8.2–8.9	25	Clarke and Radojevic [1983]
1.7×10^{-3}	6.8	25	Scott and Hobbs [1967]
3.0×10^{-3}	2.0–4.0	25	Miller and Pena [1972]
1.3×10^{-2}	8.2–8.8	25	Fuller and Crist [1941]

[a] In Milli-R/Q Water. [b] In distilled water

Table 5-3. Rate parameters obtained using Equation 5-6

	Glass fiber filter			Silica gel		
Q	$k_s S_o$	k_d	R^2	$k_s S_o$	k_d	R^2
Lpm	mlpm	min^{-1}		mlpm	min^{-1}	
0.2	0.0254	0.0026	0.95	0.0119	0.0012	0.81
0.3	0.0226	0.0025	0.93	0.0114	0.0013	0.87
0.4	0.0169	0.0025	0.94	0.0096	0.0015	0.92
0.5	0.0160	0.0026	0.92	0.0089	0.0014	0.81
Mean	0.0202	0.0026		0.0104	0.0014	
Stdev[a]	0.0045	5.8×10^{-5}		0.0014	0.0001	

Stdev[a]: Standard deviation

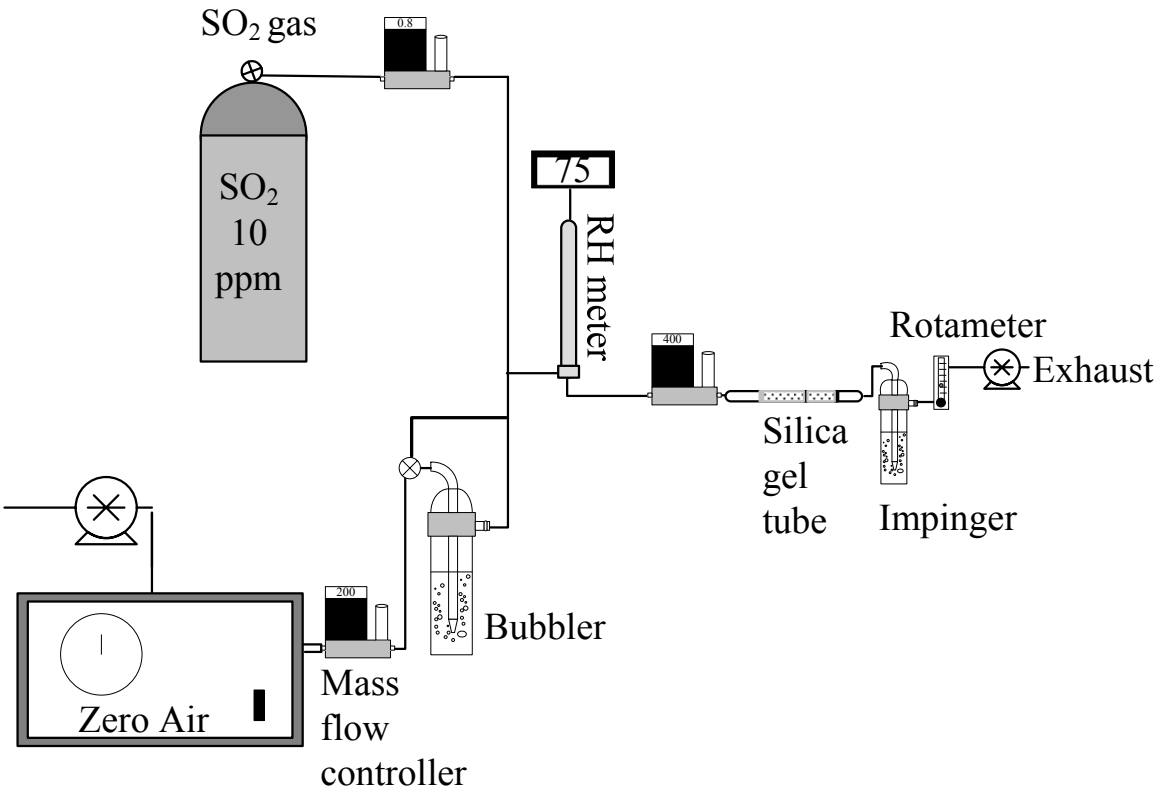

Figure 5-1. Experimental setup for sulfur dioxide adsorption

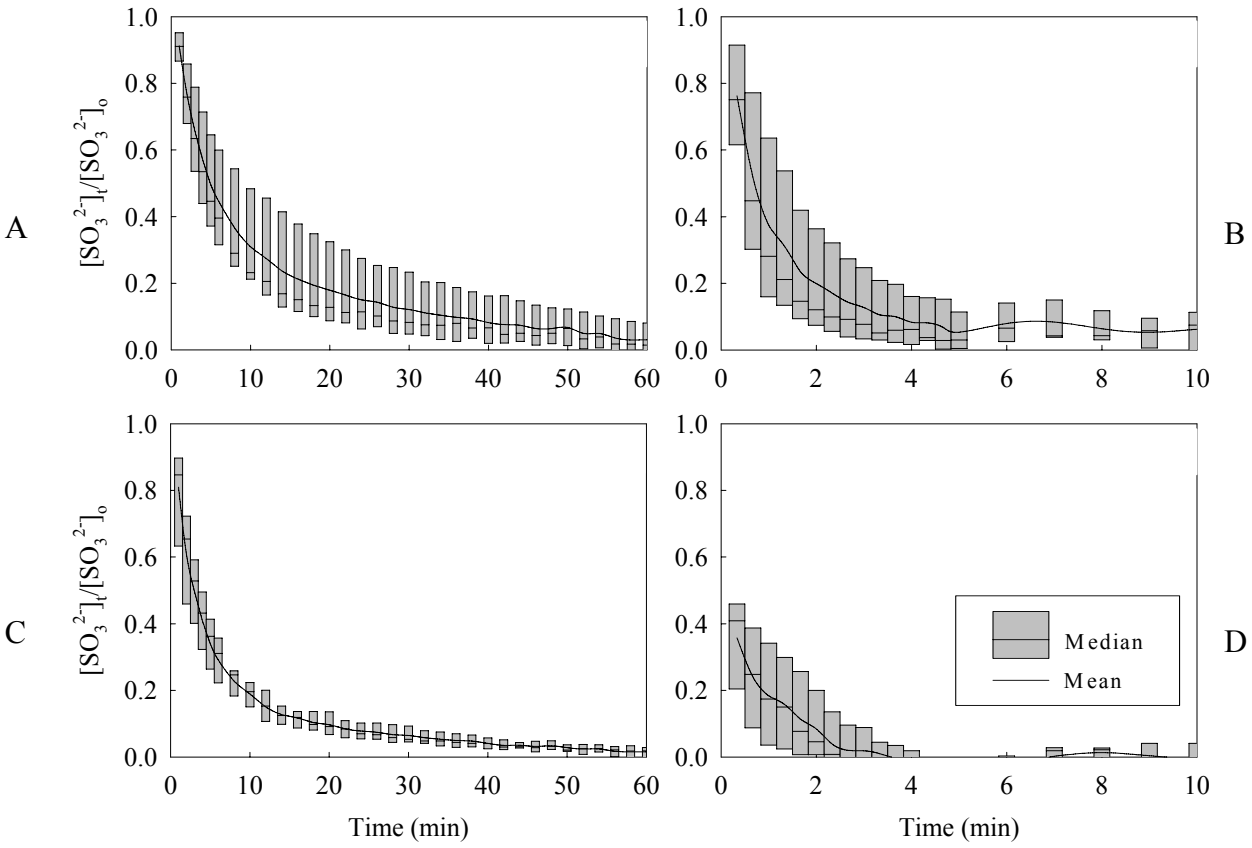

Figure 5-2. Sulfur(IV) oxidation under four conditions. A) DI water without a water bath. B) DI water with a water bath. C) 9 and 18 mM Na_2CO_3 solution without a water bath. D) 9 mM Na_2CO_3 solution with a water bath

A

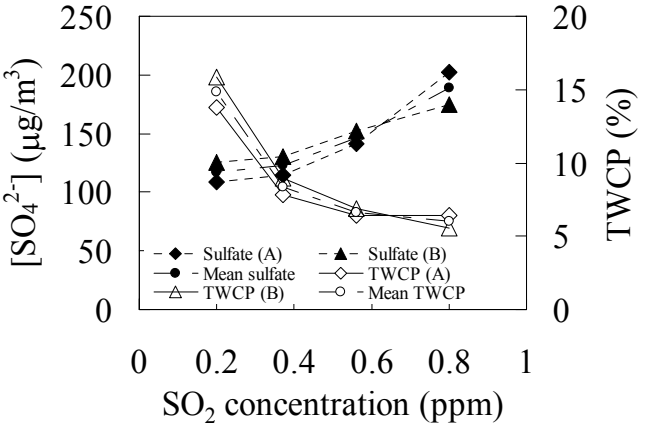

B

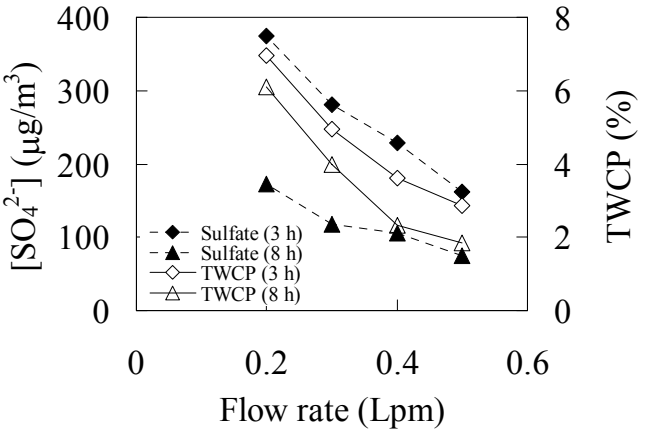

C

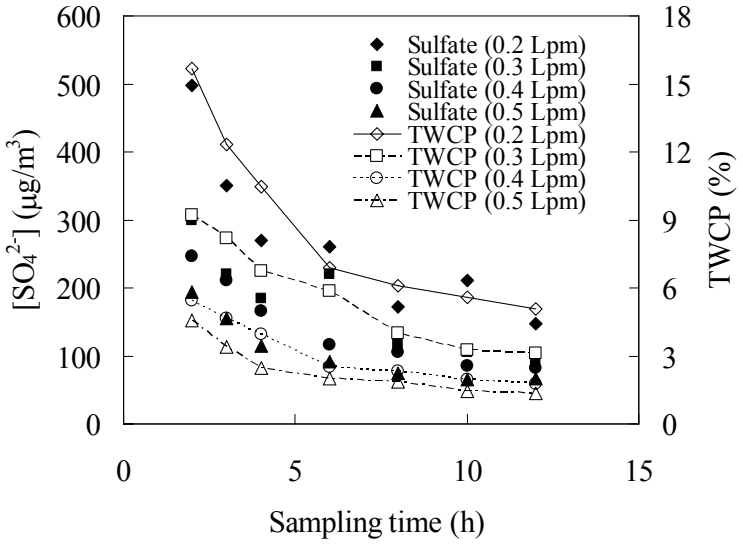

Figure 5-3. Artifact sulfate concentrations and time-weighted collection percentages (TWCPs). A) Various SO_2 concentrations with a flow rate of 0.3 Lpm and sampling time of 2 h. B) Various sampling flow rates. C) Various sampling times and sampling flow rates. Solid symbols represent artifact sulfate concentrations, and open symbols represent their corresponding TWCPs

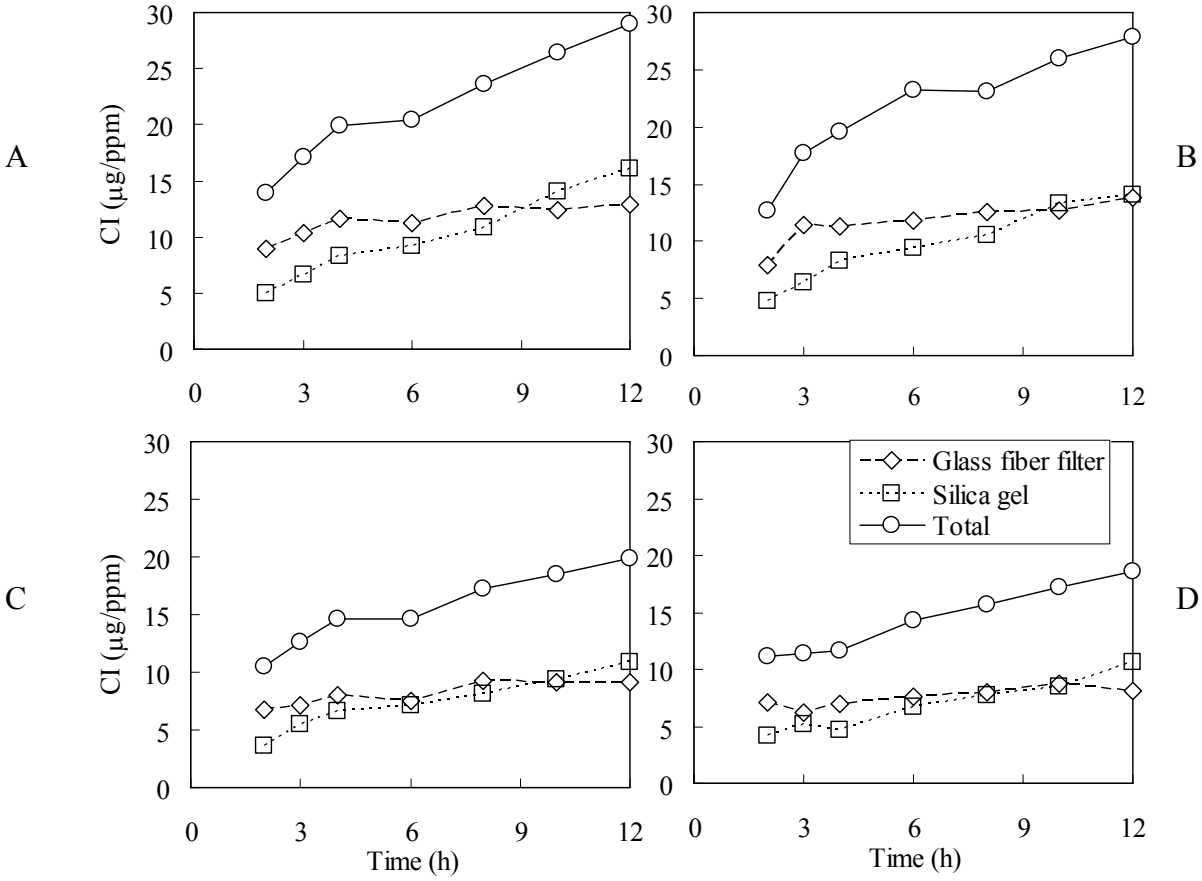

Figure 5-4. Collection index (CI) at four flow rates (Lpm). A) 0.2. B) 0.3. C) 0.4. D) 0.5

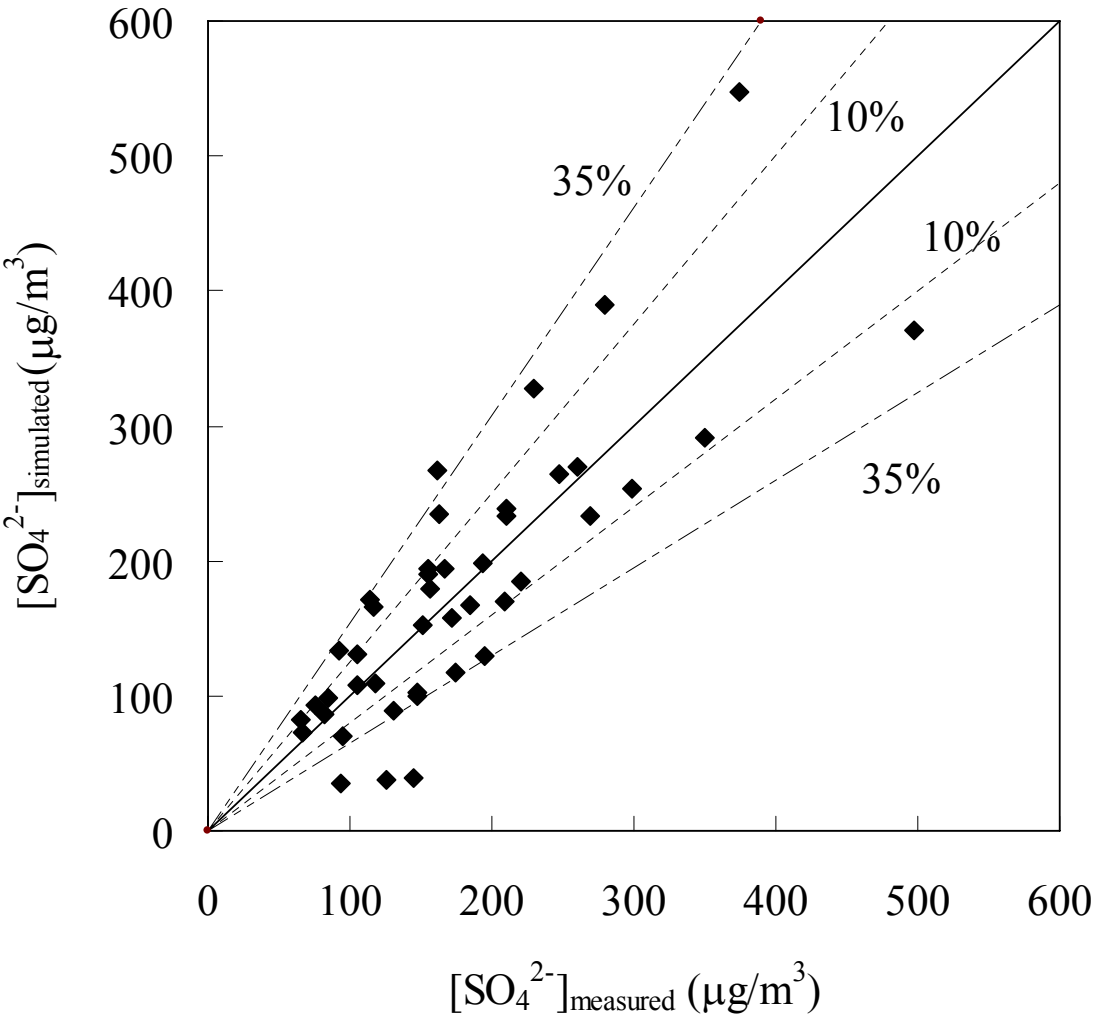

Figure 5-5. Relationship between sulfate concentrations from the measurement versus from the model

CHAPTER 6
MINIMIZATION OF ARTIFACTS IN SULFURIC ACID MIST MEASUREMENT USING NIOSH METHOD 7903

Background

NIOSH Method 7903 [*NIOSH*, 1994] is an approved method set by the OSHA for measuring the total concentration of acidic aerosols and gases, including HF, HCl, HBr, HNO_3, H_2SO_4 and H_3PO_4. It is the method commonly used by the health and safety staffs in the phosphate industry [*Hsu et al.*, 2007b] as well as other occupational environments such as the semiconductor industry, lead battery factories, aluminum smelting, machining, electroplating processes and even disaster response [*Healy et al.*, 2001; *Lue et al.*, 1998; *Tsai et al.*, 2001; *Wallingford and Snyder*, 2001]. The sampler used for NIOSH Method 7903, a silica gel tube, consists of one section of glass fiber filter plug followed by two sections of silica gel. The glass fiber filter plug is designed to filter out the majority of aerosols while the silica gel sections are used mainly to adsorb acidic gases. The NIOSH recommended sampling flow rate range is 0.2 – 0.5 Lpm, except that less than 0.3 Lpm should be used for HF. The collected samples are desorbed in eluent and the aliquots are analyzed by IC. In evaluating the method, NIOSH researchers reported nearly 100% collection efficiency for acidic gases (HCl, HF and HNO_3) [*Cassinelli*, 1986; *Cassinelli and Taylor*, 1981]. For aerosols (H_2SO_4 and H_3PO_4), around 90% efficiency (94.8±4.8% for H_3PO_4 and 86±4.6% for H_2SO_4) was reported when the samples collected on the glass fiber filter section and the front silica gel section were combined. Ortiz and Fairchild [1976] reported approximately 70% of the aerosol mass was collected by the glass fiber filter plug although the efficiency varied depending on the size distribution of the sampling aerosol [*Chen et al.*, 2002].

Sulfur dioxide is a species which can be adsorbed by the glass fiber filter [*Chow*, 1995; *Coutant*, 1977; *Lee and Mukund*, 2001; *Watson and Chow*, 2001] and the silica gel [*Fox and*

Jeffries, 1979; *Kopac and Kocabas*, 2002; *Stratmann and Buck*, 1965]. Once adsorbed, it is subsequently transformed into sulfate in the analytical process that causes an overestimate of sulfuric acid mist concentration [*Hsu et al.*, 2007c]. Hsu et al. [2007c] carried out experiments in a laboratory system that verified and quantified the artifacts resulting from the adsorption and conversion of interfering SO_2 into sulfate. A deactivation model [*Kopac and Kocabas*, 2002] was modified for estimating the artifact sulfate concentration based on the various SO_2 concentrations, flow rates and sampling times.

Denuder systems have been widely used for air sampling [*Acker et al.*, 2005; *Hayami*, 2005; *Huang et al.*, 2004; *Pathak and Chan*, 2005; *Sioutas et al.*, 1996; *Tsai et al.*, 2004]. Various types of denuders have been developed and are commercially available. The denuder's wall is coated with pertinent adsorbents depending on the gaseous species of interest. When air passes through the denuder, gas molecules with large diffusivity can diffuse to the wall and get adsorbed. Basic adsorbent (e.g. sodium carbonate (Na_2CO_3)/glycerol) can be used for acidic gases, such as HCl, HNO_3, SO_2 and HNO_2. Aerosols can be collected in the filter that follows. As a consequence, this design can reduce the interference of gaseous species on aerosols. The removal efficiency of SO_2 using an annular denuder system, depending on the operating flow rate, has been reported to be > 99% when operated at a low flow rate [*Possanzini et al.*, 1983]. The denuder system [*Koutrakis et al.*, 1993] has also been applied for ambient air sampling and can provide high SO_2 collection efficiency.

Accurate determination of sulfuric acid mist concentration in fertilizer manufacturing facilities is seminal to the evaluation of its occupational exposure. Minimizing the artifact due to SO_2 gas in the sampling process is essential in reaching this goal. The objectives of this chapter are twofold: (1) to explore the use of a denuder for removing SO_2 gas from the sampling volume

to reduce the artifact sulfate and, (2) to assess the applicability of the deactivation model for correcting the artifacts for the phosphate fertilizer production environment.

Methods

Two methods, a sampling system cooperating with a honeycomb denuder system (HDS) and a deactivation model, were applied to minimize the artifact sulfate. Field sampling was carried out to examine the artifact removal efficiency when the HDS was applied to remove the interfering SO_2 before entering the standard sampling train. Experiments were conducted to characterize SO_2 adsorption at high SO_2 concentrations encountered in the field sampling conditions. The deactivation model was used to estimate the artifact sulfate concentration based on known SO_2 concentrations.

Field Sampling

Field sampling was carried out on top of the sulfuric acid pump tank area at seven phosphate fertilizer plants in Florida [*Hsu et al.*, 2007c]. Four samples were acquired at each of six sites and five samples were collected at the one remaining plant. Sampling time was 8 h for each sample.

Silica gel tubes, a cascade impactor and a honeycomb denuder system were applied for the field sampling. Three sets of sampling trains, shown in Figure 6-1, were employed. (A) A silica gel tube – This method was used for total sulfuric acid mist concentration following NIOSH Method 7903 (N = 29). (B) The HDS followed by two silica gel tubes in parallel – The HDS (coating solution: 1% Na_2CO_3/glycerol) was used to remove SO_2 gas before the air entered the silica gel tubes. The measurement also provided SO_2 concentration. Two silica gel tubes were applied for replication (N = 29 for the HDS sample; N = 58 for the silica gel tube sample). (C) A cascade impactor (Mark III, U. Washington) with Zefluor membrane filters (P5PJ001, Pall

Corp.) – This sampling system was used for sulfuric acid mist concentration with size-resolved information (N = 29). Zefluor membrane filters can provide high aerosol collection efficiency with low interaction with acidic gases [*Chow*, 1995; *Watson and Chow*, 2001]. All three sampling trains were set side by side for parallel sampling.

All silica gel tube samples were analyzed following the sample preparation procedures outlined in NIOSH Method 7903 [*NIOSH*, 1994], including adding 9 mM Na_2CO_3 of 10 mL and a water bath at 100 °C for 10 min. The HDS sample was extracted by 10 mL DI water (Nanopure Diamond, Barnstead), and 1 mL hydrogen peroxide (0.6%) was then added into 1 mL sample solution to oxidize sulfite to sulfate for the analysis. The cascade impactor sample was extracted by 10 mL DI water with a 1-h ultrasonic bath. Sulfate concentrations of all samples were analyzed via IC (Model ICS 1500, Dionex).

Deactivation Model

A deactivation model [*Hsu et al.*, 2007c], Equation 6-1, has been developed to estimate the artifact sulfate concentration. In developing this model, experiments were conducted at SO_2 concentrations ranging from 0.2 to 1.6 ppm. Hence, the model can be applied for SO_2 concentrations in this range.

$$\left[SO_4^{2-}\right]_t = \theta\left[SO_2\right]_o \left\{1 - \exp\left[-\frac{k_s S_o}{Q} \times \exp\left(-k_d t\right)\right]\right\}$$

$$\text{for } 0.2 \text{ ppm} < \left[SO_2\right]_o < 1.6 \text{ ppm} \qquad (6\text{-}1)$$

$\left[SO_4^{2-}\right]_t$: artifact sulfate concentration ($\mu g/m^3$)

$\theta = 1571$, conversion factor

$\left[SO_2\right]_o$ = feed SO_2 concentration (ppm)

k_sS_o = observed adsorption rate (mLpm/min), 16 for the glass fiber filter and 8.9 for the silica gel at the flow rate of 500 mLpm

Q = flow rate (500 mLpm)

k_d = first order deactivation rate constant (min^{-1}), 0.0026 for the glass fiber filter and 0.0014 for the silica gel at the flow rate of 500 mLpm

t = time (min)

Sulfur Dioxide Adsorption

High SO_2 concentrations, 1.6 ppm to 5.6 ppm, were observed during the field sampling described in the previous section. However, the parameter values in the deactivation model have not been validated for the artifact estimate at high SO_2 concentrations. Therefore, experiments were conducted to quantify the SO_2 adsorption by the silica gel tube under high SO_2 concentrations ranging from 1.6 ppm to 5.6 ppm at 0.5 Lpm flow rate with 8 h of sampling time (condition employed for the field sampling). The experimental setup has been described in Hsu et al. [2007c]. SO_2 gas from a cylinder (10 ppm, relative uncertainty = ±5%) was mixed with zero air (Model 111, Thermo Electron Instrument) to obtain the desired concentration. SO_2 gas was then passed through the silica gel tube for the adsorption. An impinger with 100 mL of 9 mM Na_2CO_3 solution was employed downstream to collect the residual SO_2 gas. Sulfate concentration was determined following the analytical procedures described in the field sampling section. To evaluate residual sulfate of both glass fiber filter and silica gel, eighteen silica gel tubes as received were analyzed for their sulfate concentration following the sample preparation procedures of NIOSH Method 7903.

Results and Discussion

Field Sampling

Collection efficiency and concentration of SO_2

The HDS consists of two honeycomb denuders in series. Collection efficiency, η, was determined according to Equation 6-2:

$$\eta(\%) = \frac{[SO_2(HD1)] - [SO_2(HD2)]}{[SO_2(HD1)]} \times 100\% \quad (6\text{-}2)$$

where $[SO_2(HD1)]$ and $[SO_2(HD2)]$ are SO_2 concentrations collected by the first and second honeycomb denuders, respectively. The mean SO_2 collection efficiency ± standard deviation of the HDS was found to be 95.7 ± 6.8% (N = 29), demonstrating that the deployed HDS could effectively remove SO_2 gas from the sample gas.

Regarding the SO_2 concentration at the phosphate fertilizer plants, it ranged from 34 ppb to 5.6 ppm. Although it varied significantly from plant to plant, for each plant the SO_2 concentration level varied within a limited range during the sampling period. Table 6-1 displays the statistics of SO_2 concentrations at each plant. At plant F, sampling was conducted at two locations where SO_2 concentrations differed greatly. Hence, SO_2 concentrations at plant F are shown separately for each location.

Ratio of $S\text{-}SO_4^{2-}$/ $S\text{-}SO_2$

The deployment of the HDS was to collect SO_2 gas; however, sulfate aerosols might also be collected by the HDS which could cause an overestimate of SO_2 concentration. To determine if the presence of sulfate significantly affects the SO_2 concentration measurement, the $S\text{-}SO_4^{2-}$/$S\text{-}SO_2$ ratios (elemental sulfur from SO_4^{2-} collected by the silica gel tubes, SGHA and SGHB in the second sampling train, to elemental sulfur from SO_2 collected by the HDS) for all samples were calculated and are shown in Figure 6-2. As shown, the maximum was 0.13 and it occurred at a

very low SO_2 concentration. At high SO_2 concentrations where the focus of this study is, they were below 2%. The low ratios demonstrate that the honeycomb denuder system can be used for measuring SO_2 concentration accurately and the interference of particulate sulfate is negligible.

Aerosol loss of HDS

The aerosol loss in the HDS causes an underestimate of sulfate concentration. Two mechanisms causing the aerosol loss in the HDS are: (1) the aerosol with size larger than 10 μm can be removed by the impactor of the HDS, and (2) the aerosol can diffuse to the wall of the denuder. The aerosol concentration with size-resolved information from the cascade impactor (CI) can be employed to correct the first mechanism. The sulfate diffusional loss, $\left[SO_4^{2-}\right]_{DF}$, can be calculated by Equation 6-3.

$$\left[SO_4^{2-}\right]_{DF} = \sum_i DF_i \times \left[SO_4^{2-}\right]_{CI_i} \qquad (6\text{-}3)$$

DF_i : aerosol deposition fraction of aerosol size range i.

$\left[SO_4^{2-}\right]_{CI_i}$: sulfate concentration of aerosol size range i measured by the CI.

The aerosol deposition (DF) in the honeycomb denuder due to diffusion can be calculated according to Equation 6-4a and Equation 6-4b [*Hinds*, 1999].

$$DF_i = 5.5\mu_i^{2/3} - 3.77\mu_i \qquad \text{for } \mu < 0.009 \qquad (6\text{-}4a)$$

$$DF_i = 1 - 0.819\exp(-11.5\mu_i) - 0.0975\exp(-70.1\mu_i) \qquad \text{for } \mu \geq 0.009 \qquad (6\text{-}4b)$$

where $\mu_i = \dfrac{D_i LN}{Q}$

μ_i: dimensionless deposition parameter for particle size range i

D_i: diffusion coefficient of the particle size range i (cm^2/min)

L: the length of the tube (= 9.6 cm)

N : the number of tubes (= 160)

Q: the volume flow rate through the tube (= 500 mLpm)

Table 6-2 shows the mean ratio and its range of the sulfate diffusional loss, the sulfate loss due to the HDS' inner impactor ($\left[SO_4^{2-}\right]_{H_2SO_4 > 10\ \mu m}$, derived from the CI measurement) and the total sulfate loss ($\left[SO_4^{2-}\right]_{HD_{loss}} = \left[SO_4^{2-}\right]_{H_2SO_4 > 10\ \mu m} + \left[SO_4^{2-}\right]_{DF}$) to the total sulfate concentration from the CI ($\left[SO_4^{2-}\right]_{CI}$) at each plant.

The mean sulfate loss due to the aerosol diffusional loss at each plant ranged from 3.2% to 6.3%. For all plants, the mean loss was 4.8% demonstrating that the effect was minor. On the other hand, the sulfate loss due to the impactor, shown in Table 6-2, was highly significant. The mean loss ranged from 3% to 43% demonstrating that the loss varied remarkably. If the HDS impactor sample were analyzed in this study, the information can be used to directly correct the majority of the loss. The CI information is then no longer needed.

Sulfur Dioxide Adsorption

Figure 6-3 shows the artifact sulfate concentration as a function of SO_2 concentration. As feed SO_2 concentration increased, the artifact sulfate concentration increased. This is because more SO_2 can be adsorbed by the silica gel and the glass fiber filter, and the glass fiber filter and silica gel were not saturated yet. The relation between the feed SO_2 concentration (1.6—5.6 ppm) and the artifact sulfate concentration can be described by Equation 6-5. In this study, this equation was applied for SO_2 concentrations between 1.6 and 5.6 ppm while the deactivation model was applied for SO_2 concentrations from 0.2 to 1.6 ppm. The intercept in Equation 6-5 might be from the residual sulfate to be discussed in the next section. Since the ratio of the mean amount of residual sulfate of the second silica gel section to that of the first silica gel section was

2.1, shown in Table 6-3, outliers were defined as those with ratios exceeding 2.1. Theoretically, the first section should collect more SO_2 gas than the second section. However, the high residual sulfate artificially yields a higher sulfate concentration in the second section. Since the mean ratio of the sulfate concentration in the second section to that of the first section is 2.1, outliers are defined as exceeding this ratio.

$$\left[SO_4^{2-}\right]_t = 20.04 \times [SO_2]_o + 53.32 \qquad \text{for } 1.6 \text{ ppm} < [SO_2]_o < 5.6 \text{ ppm} \qquad (6\text{-}5)$$

$\left[SO_4^{2-}\right]_t$: artifact sulfate concentration ($\mu g/m^3$)

$[SO_2]_o$: feed SO_2 concentration (ppm)

To determine the effect of humidity, experiments were conducted for the relation between adsorbed water amount and sampling time. RHs of 35% and 85% for various sampling times and flowrates were investigated. It was found that the silica gel tube reached saturation quickly. Under these sampling flowrates and sampling times, the adsorbed water amount was around 0.2 g which is one-third of the silica gel weight. When 0.2 Lpm flowrate and RH of 35% were applied, the adsorbed water amount reached saturation in two hours. The results demonstrate that the sampling tube is generally operated under the saturation condition over a wide range of ambient RH.

Residual Sulfate in Silica Gel Tube

Due to the non-zero intercept in Equation 6-5, 18 silica gel tubes as received were analyzed for residual sulfate concentration. The statistical results of the residual sulfate concentrations in different sections for two batches purchased from the vendor are shown in Table 6-3. The first batch was used for the experiment conducted in this research while the second batch was purchased in 2004 and used for a prior study described in Chapter 3 [*Hsu et al.*, 2007b]. For the

first batch, the mean residual sulfate concentrations from the glass fiber filter, first and second sections of silica gel in the aliquots were 3.09, 5.23 and 10.77 μg, respectively, which are equivalent to 12.9, 21.8 and 44.9 $\mu g/m^3$ (in the air) at the sampling conditions of 8 h and 0.5 Lpm. Added together, the mean total sulfate concentration due to the residual was 79.5 $\mu g/m^3$. For the maximum residual sulfate concentration, the artifact sulfate concentration in the air was 439.3 $\mu g/m^3$. The total sulfate concentration in the air corresponding to the standard deviations of the sampler was 132 $\mu g/m^3$. This is higher than the mean residual sulfate concentration, indicating that the residual sulfate concentrations were quite variable. In contrast, the residual sulfate of the second batch was much lower than that of the first batch. Its mean total residual sulfate concentration was only 15.9 $\mu g/m^3$. In summary, the residual sulfate concentration can contribute greatly to the artifact sulfate concentration in the air and the impact of variation of residual sulfate in the silica gel tube should not be ignored. Therefore, NIOSH Method 7903 is not suitable for low sulfate concentration sampling, e.g., ambient air sampling.

Minimization of Artifact Sulfate

Two methods were applied to minimize the artifact sulfate and their effectiveness was evaluated. The first method was the SO_2 adsorption model described in Equation 6-1 and Equation 6-5. This method is based on using the known SO_2 concentration to calculate the artifact sulfate concentration. In this study, the SO_2 concentration was determined by the denuder as discussed earlier. The corrected sulfate concentration based on the model, $\left[SO_4^{2-}\right]_{model}$, can then be calculated according to Equation 6-6:

$$\left[SO_4^{2-}\right]_{model} = \left[SO_4^{2-}\right]_{SG} - \left[SO_4^{2-}\right]_t \qquad (6\text{-}6)$$

where $\left[SO_4^{2-}\right]_{SG}$: sulfate concentration from the SG, which includes artifact sulfate.

The second method used to minimize artifact sulfate was the HDS (sampling train 2). However, it has the potential to remove true sulfate aerosol. Therefore, the sulfate concentrations from SGHA and SGHB need to be corrected and the correcting equation is shown in Equation 6-7.

$$\left[SO_4^{2-}\right]_{\text{SGHAC (or SGHBC)}} = \left[SO_4^{2-}\right]_{\text{SGHA (or SGHB)}} + \left[SO_4^{2-}\right]_{HD_{loss}} \quad (6\text{-}7)$$

Figure 6-4 shows the sulfate concentrations from the SG, the SGHC (the average of the corrected SGHA (SGHAC) and the corrected SGHB (SGHBC)), the model and the CI as a function of SO_2 concentration. The sulfate concentrations from the SG were always higher than those from other samplers. For most samples, the sulfate concentration from the CI was the lowest and the sulfate concentrations from the model and SGHC were between the SG and the CI. For low SO_2 concentration, the sulfate concentrations from the SG and the model were similar due to the expected small artifact sulfate produced. The relative error (E) shown in Equation 6-8 was applied to evaluate the difference and the results are shown in Table 6-4.

$$E=\frac{\left|\left[SO_4^{2-}\right]_{sampler} - \left[SO_4^{2-}\right]_{CI}\right|}{\left[SO_4^{2-}\right]_{CI}} \quad (6\text{-}8)$$

$\left[SO_4^{2-}\right]_{sampler}$: sulfate concentration measured by SG, SGHAC and SGHBC.

The relative errors of the NIOSH method and the model were relatively large when SO_2 concentration was lower than 0.05 ppm; their mean values were 4.4 and 4.2, respectively. Between 0.1 and 2.7 ppm, the sulfate concentration from the SG can be 1 to 7 times higher than that from the CI. Meanwhile, both the model and the honeycomb denuder reduced the sulfate concentration, making them closer to the CI results. When high SO_2 concentration, ranging from 4.0 to 5.6 ppm, was observed, relative errors of all methods were low. However, it should be

addressed that the artifact sulfate concentration from the SG was still high and needed correction. For example, at SO_2 concentration of 4.7 ppm it was 287.6 $\mu g/m^3$.

The effectiveness, ε, for reducing artifact sulfate by the SGHAC/SGHBC and the model can be calculated by Equation 6-9.

$$\varepsilon(\%) = \frac{\text{reduced artifact sulfate}}{\text{true artifact sulfate}} = \frac{\left[SO_4^{2-}\right]_{SG} - \left[SO_4^{2-}\right]_{\text{SGHAC/SGHBC or model}}}{\left[SO_4^{2-}\right]_{SG} - \left[SO_4^{2-}\right]_{CI}} \times 100\% \qquad (6\text{-}9)$$

They were 70 ± 32% and 39 ± 36% for the SGHAC/SGHBC and the model, respectively. However, they were still higher than the CI values. One possible reason for the difference is the residual sulfate of the silica gel tube discussed earlier. Overall, the model and the HDS can be applied for the minimization of the artifact sulfate.

Aspiration Efficiency

The aspiration efficiencies ($\eta_{\text{asp, calm air}}$) for the cascade impactor, the silica gel tube and the honeycomb denuder system were calculated by Equation 6-10 (*Brockmann*, 2001).

$$\eta_{\text{asp, calm air}} = \frac{V_{ts}}{U} \cdot \cos(\varphi) + \exp\left[-\frac{4Stk^{1+\sqrt{\frac{V_{ts}}{U}}}}{1+2Stk}\right] \qquad (9\text{-}10)$$

for $0° \le \varphi \le 90°$, $10^{-3} \le V_{ts}/U \le 1$, and $10^{-3} \le Stk \le 100$.

V_{ts}: terminal settling velocity

U: inlet sampling velocity

$\varphi = 0°$ is upward facing, 90° is horizontal

Stk: Stokes number ($= \tau \cdot U/d$)

τ: the relaxation time of the particle

d: inlet diameter

The results with two orientations are shown in Figure 6-5. For the vertical (facing up) sampling, the aspiration efficiency of the silica gel tube is higher than others and the honeycomb denuder system and the cascade impactor have the similar aspiration efficiencies. In the field sampling, both the silica gel tube and the honeycomb denuder system were laid horizontially while the cascade impactor was placed vertically. The efficiencies for both samplers in this geometry are lower than the cascade impactor as shown in Figure 6-5 which indicates the cascade impactor should collect more aerosols than others. However, this result was not observed in this study. The aspiration efficiencies of three samplers were similar for aerosol smaller than 20 μm where most of the aerosols in the study were located. Hence, it is also reasonable to apply the cascade impactor measurements to the aerosol information for the honeycomb denuder system.

Sulfate Mass Balance

The sulfate mass balance between the silica gel tube in the first sampling train (SG) and the two silica gel tubes in the second train (SGHA or SGHB) in the parallel samples was checked. Ideally, they can be equated as Equation 6-11:

$$\left[SO_4^{2-}\right]_{SG} = \left[SO_4^{2-}\right]_{SGHA\ (or\ SGHB)} + \left[SO_4^{2-}\right]_t + \left[SO_4^{2-}\right]_{HD_{loss}} \qquad (6\text{-}11)$$

The sulfate mass balance is shown in Figure 6-6. Except for a few, most data points show good mass balance, i.e., most of them were within the standard deviation of the residual sulfate concentration of the silica gel tube. The large relative error of sulfate shown in Table 6-4 indicates the existence of artifact sulfate on the SG. The good sulfate mass balance between the SG and the SGHAC/SGHBC supports the conclusion that SO_2 gas is the key source of artifact sulfate.

Summary

A sampling train incorporating a honeycomb denuder system was applied for field sampling at seven phosphate fertilizer plants to evaluate its use for reducing the artifact sulfate concentration while preserving the actual sulfuric acid mist concentration. The denuder system was designed to remove SO_2 gas before the air entered the silica gel tube and to monitor SO_2 concentration at the same time. A deactivation model was also applied to correct for the presence of the artifact. The denuder system had 95.7 ± 6.8% collection efficiency for SO_2 gas, and the impact of sulfate aerosol on SO_2 collection was negligible. SO_2 concentrations at the seven plants ranged from 34 ppb to 5.6 ppm. Both the honeycomb denuder system and the deactivation model were shown to reduce the artifact sulfate concentration by 70% and 39%, respectively. However, they were still higher than the sulfate aerosol concentration measured by a cascade impactor. One possible reason is the residual sulfate in the glass fiber filter and the silica gel.

Table 6-1. Statistics of SO_2 concentrations (ppm)

Site	A	B	C	D	E	F-1	F-2	G
Mean	1.83	1.74	0.46	0.05	0.27	0.40	5.00	0.21
MIN	0.90	1.22	0.36	0.03	0.19	0.12	4.34	0.13
MAX	2.57	2.66	0.56	0.05	0.31	0.68	5.64	0.31
Sample no.	4	4	4	4	4	2	3	4

Table 6-2. Mean and standard deviation of the sulfate loss to the total sulfate concentration

	$\frac{[SO_4^{2-}]_{DF}}{[SO_4^{2-}]_{CI}}$ (%)	$\frac{[SO_4^{2-}]_{H_2SO_4 > 10\ \mu m}}{[SO_4^{2-}]_{CI}}$ (%)	$\frac{[SO_4^{2-}]_{HD_{loss}}}{[SO_4^{2-}]_{CI}}$ (%)	$[SO_4^{2-}]_{CI}$ (μg/m^3)
A	4.8 (4.0–5.3)	15.7 (8.3–26.8)	25.4 (19.0–34.8)	92.4 (53.2–142.6)
B	3.2 (2.5–3.9)	42.8 (31.6–52.6)	49.1 (39.4–57.7)	25.7 (21.1–32.3)
C	4.0 (3.0–5.4)	26.3 (16.7–33.6)	34.4 (22.7–44.4)	31.0 (21.1–43.5)
D	6.3 (5.9–6.6)	2.8 (1.3–6.6)	15.4 (14.4–18.4)	85.3 (21.3–134.1)
E	4.8 (4.0–5.4)	15.0 (4.4–34.9)	24.7 (14.6–42.9)	32.0 (5.6–61.3)
F-1	4.8 (4.8–4.8)	13.4 (10.3–16.4)	23.0 (19.9–26.1)	16.7 (11.7–21.6)
F-2	4.7 (4.6–4.8)	11.6 (10.7–12.5)	20.9 (20.2–21.7)	578.2 (412.7–686.3)
G	5.7 (5.3–6.3)	5.8 (1.0–11.3)	17.3 (13.7–21.9)	44.3 (10.3–108.7)
Total	4.8 (4.0–5.3)	15.7 (8.3–26.8)	25.4 (19.0–34.8)	92.4 (53.2–142.6)

Table 6-3. Statistical results of the residual sulfate concentrations of silica gel tubes

Sulfate (μg)	Mean	Standard deviation	MAX	MIN
1st Batch (N = 10)				
Glass fiber filter	3.1	2.3	9.0	1.1
Silica gel – 1st section	5.2	5.6	18.3	0.7
Silica gel – 2nd section	10.8	23.9	78.1	0.9
$\frac{\text{2nd section}}{\text{1st section}}$	2.1	4.3	4.3	1.3
2nd Batch (N = 8)				
Glass fiber filter	0.6	0.6	1.9	0.0
Silica gel – 1st section	2.0	0.5	2.6	1.2
Silica gel – 2nd section	1.3	0.6	2.8	0.9
$\frac{\text{2nd section}}{\text{1st section}}$	0.6	1.4	1.1	0.7

Table 6-4. Relative error of 4 samplers

	Relative Error			
	SG	SGHAC	SGHBC	Model
$[SO_2]$ < 1.6 ppm (N=21)				
mean	4.46	1.73	1.86	3.30
stdev*	2.12	1.59	1.48	2.23
min	0.47	0.06	0.14	0.07
max	8.56	5.76	5.49	7.87
1.6 ppm < $[SO_2]$ < 5.6 ppm (N=8)				
mean	1.90	0.48	0.63	0.82
stdev	2.00	0.23	0.44	1.02
min	0.02	0.20	0.20	0.17
max	5.78	0.94	1.30	3.10

Stdev*: standard deviation.

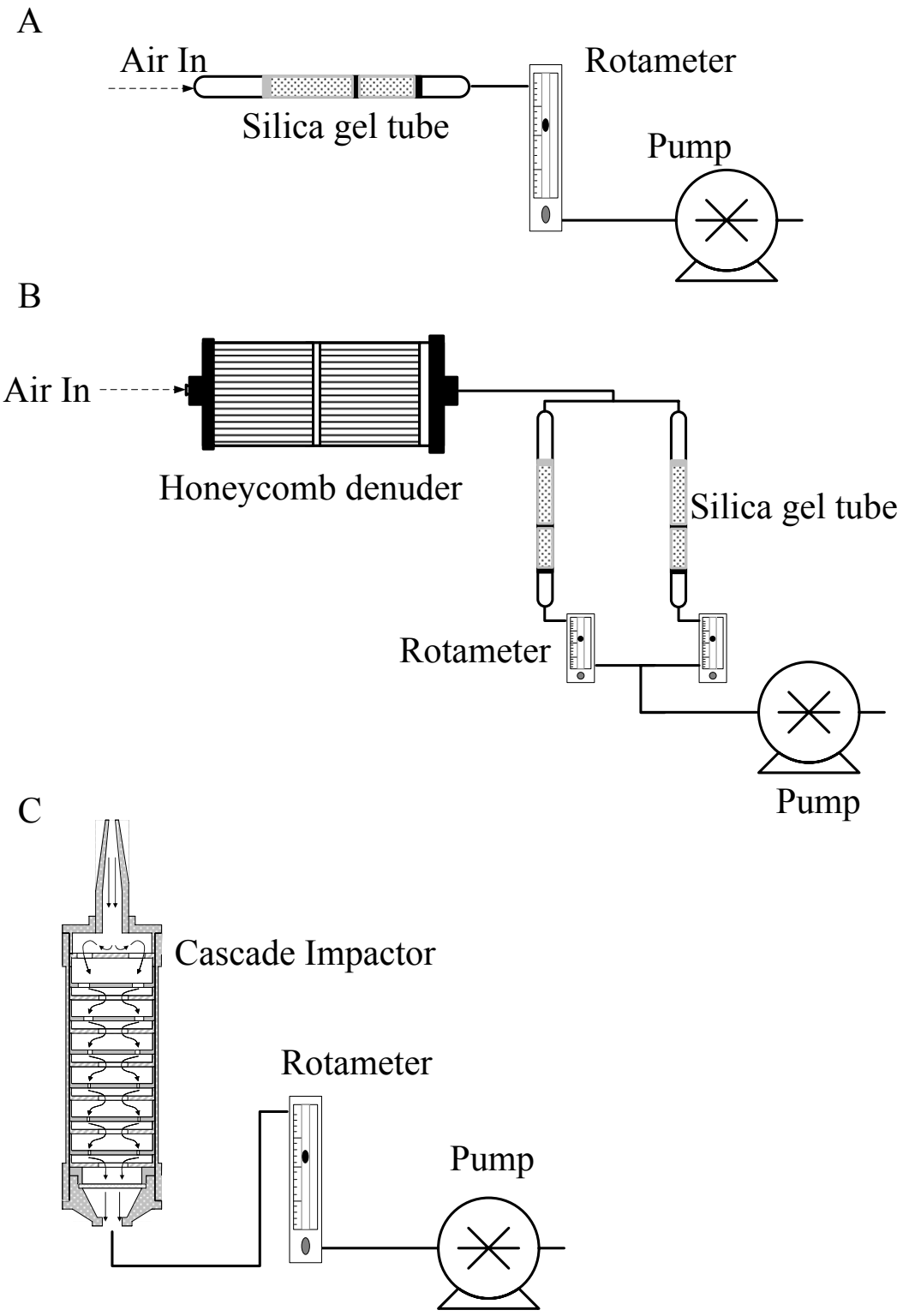

Figure 6-1. Three sampling trains. A) NIOSH Method 7903. B) Modified NIOSH Method 7903. C) Cascade impactor sampling system

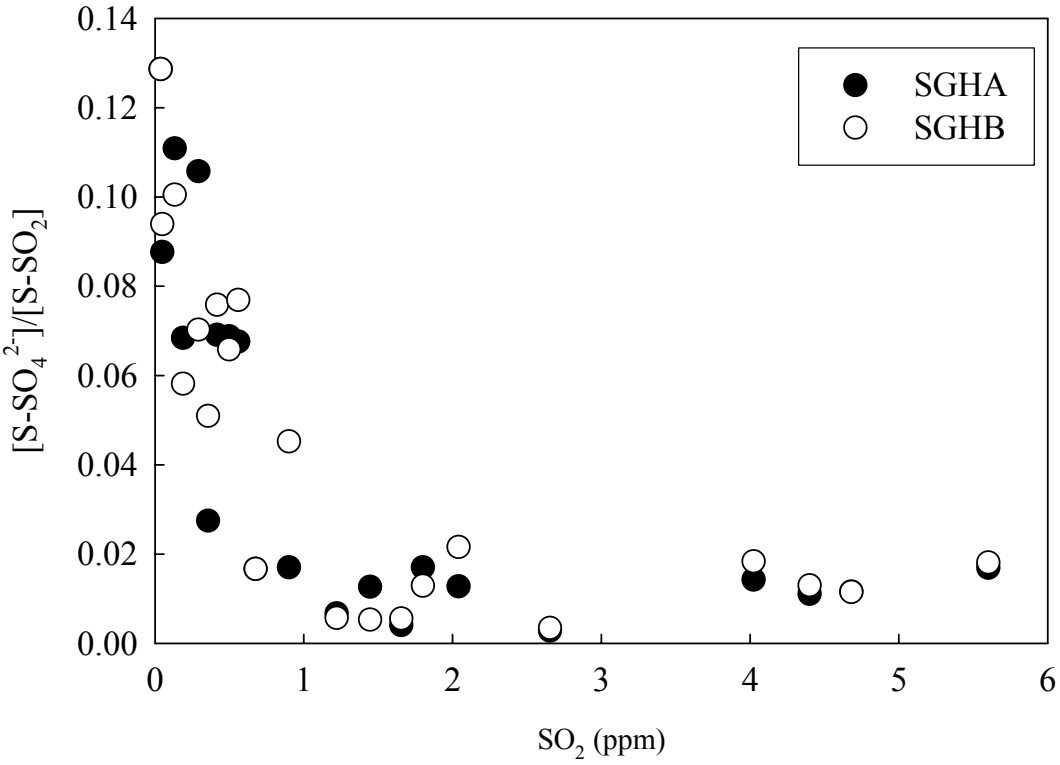

Figure 6-2. $S\text{-}SO_2/S\text{-}SO_4^{2-}$ as a function of SO_2 concentration. SGHA and SGHB are the silica gel tubes in the second sampling train

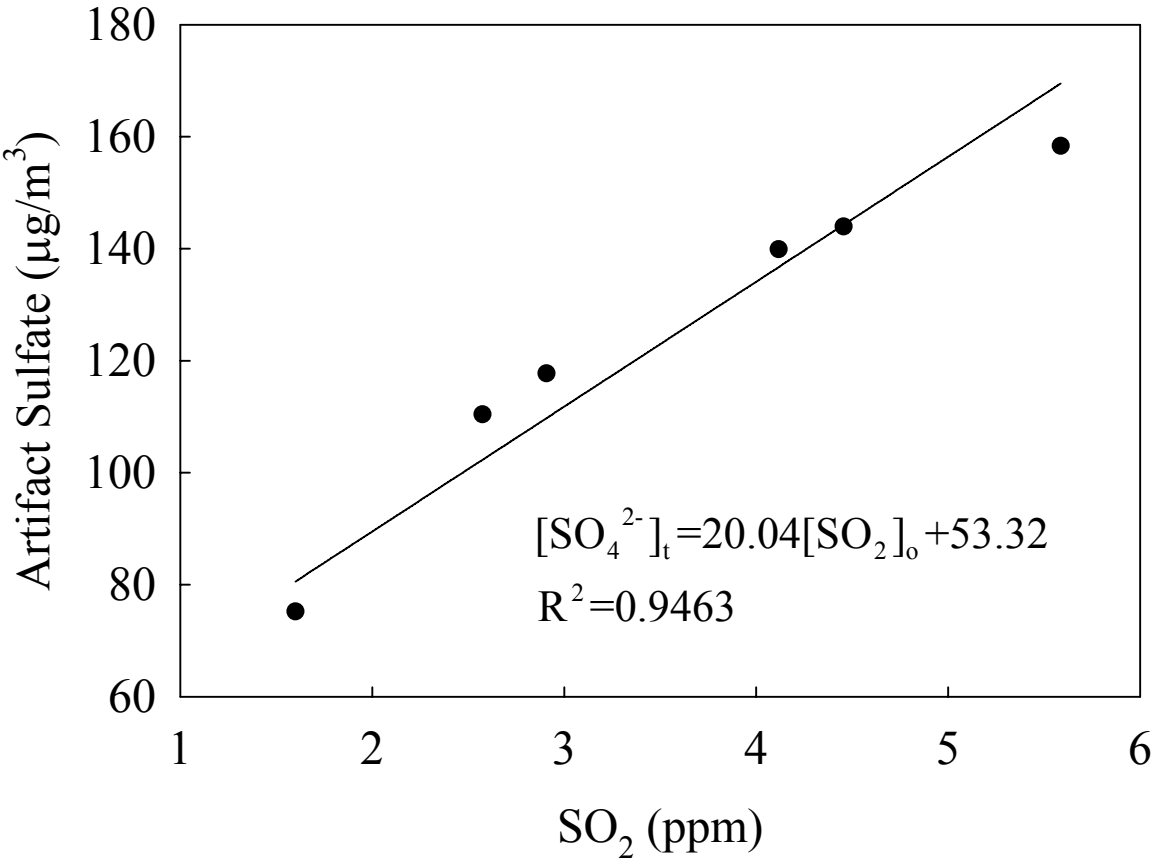

Figure 6-3. Artifact sulfate concentration as the function of SO_2 concentration

A

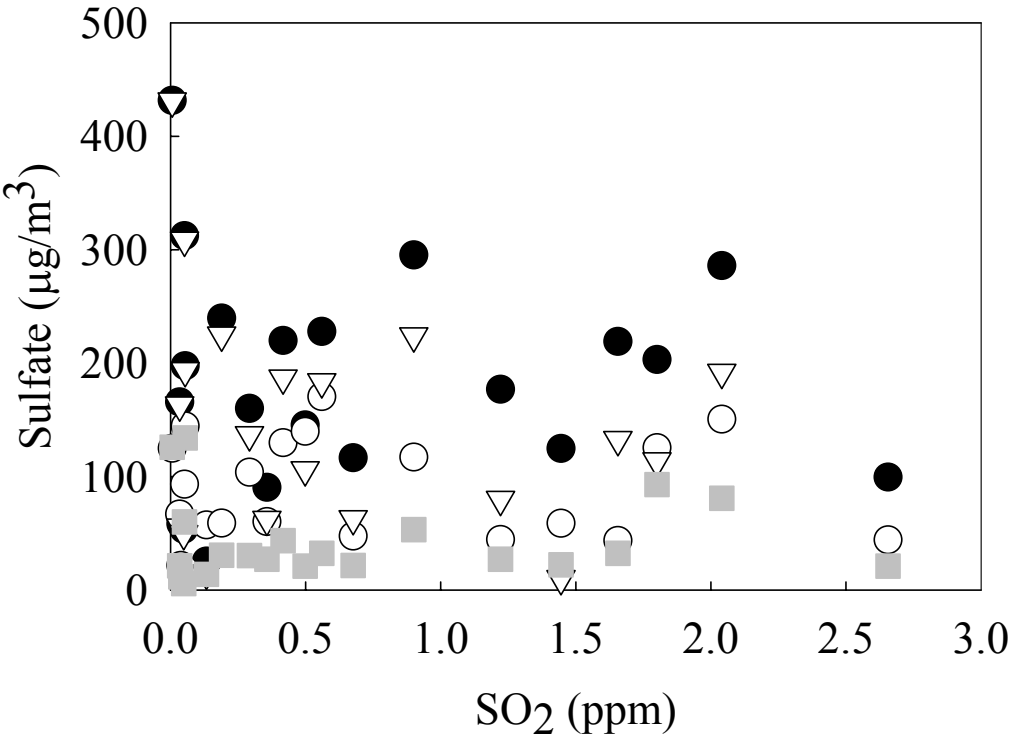

B

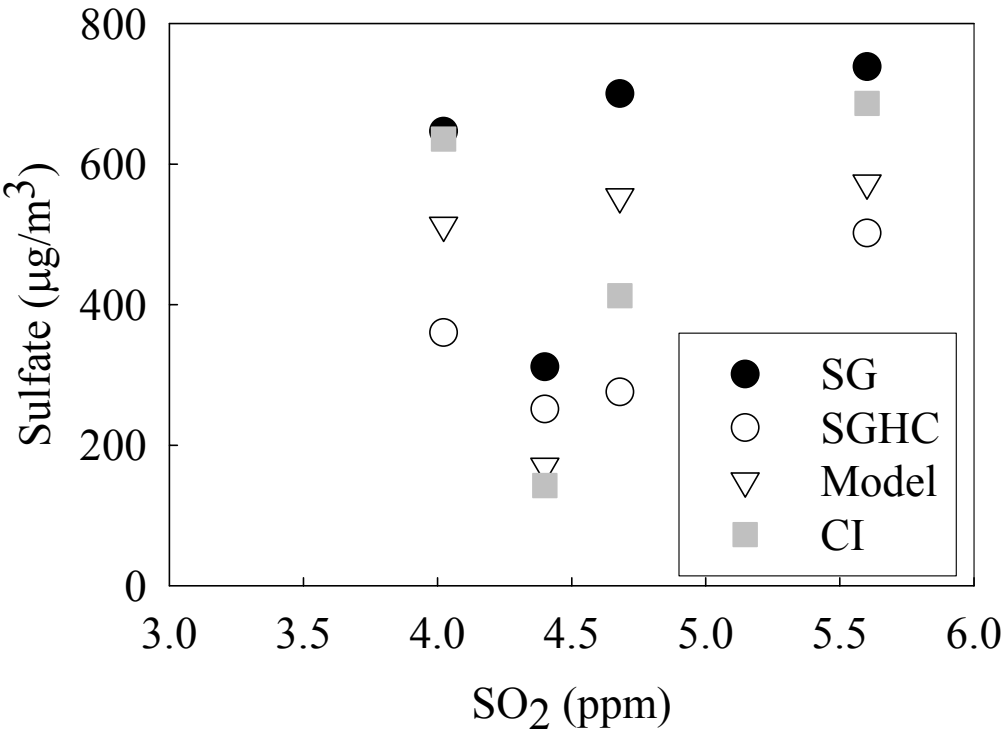

Figure 6-4. Comparison of the sulfate concentrations from the CI, SG, SGHAC and SGHBC. A) SO_2 concentration lower than 3 ppm. B) SO_2 concentration higher than 3 ppm.

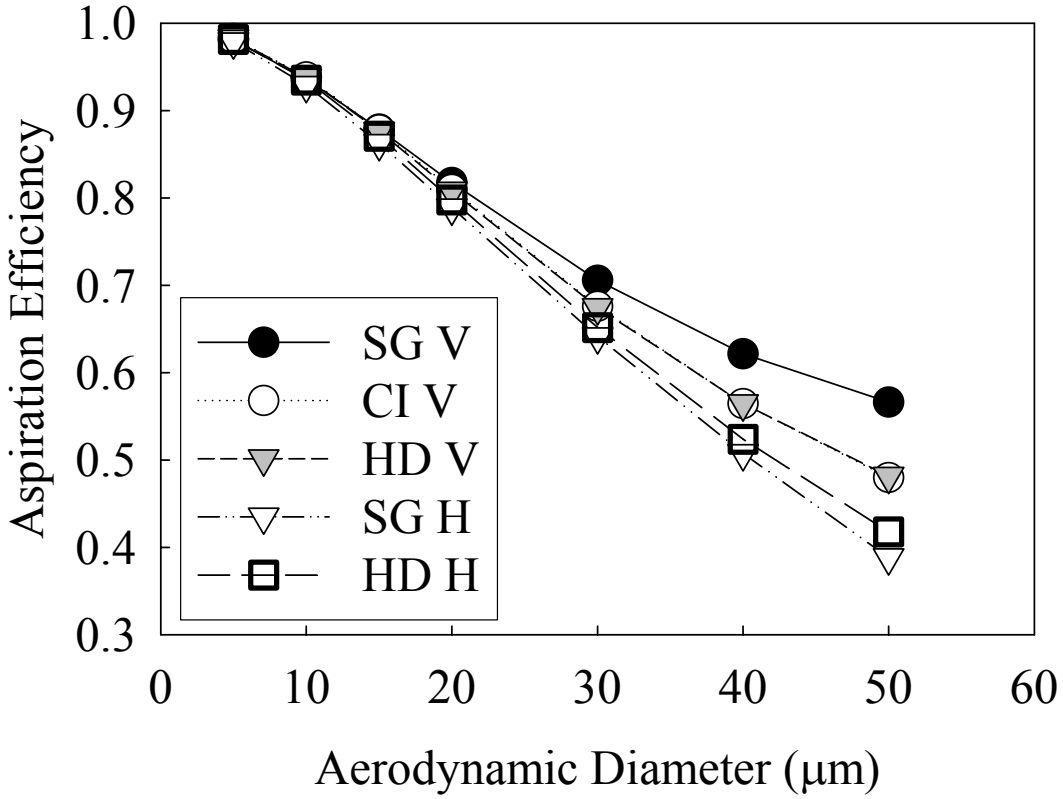

Figure 6-5. Aspiration efficiency of three samplers. (SG: silica gel tube, CI: Cascade impactor; HD: honeycomb denuder system, V: vertical; H: horizontal)

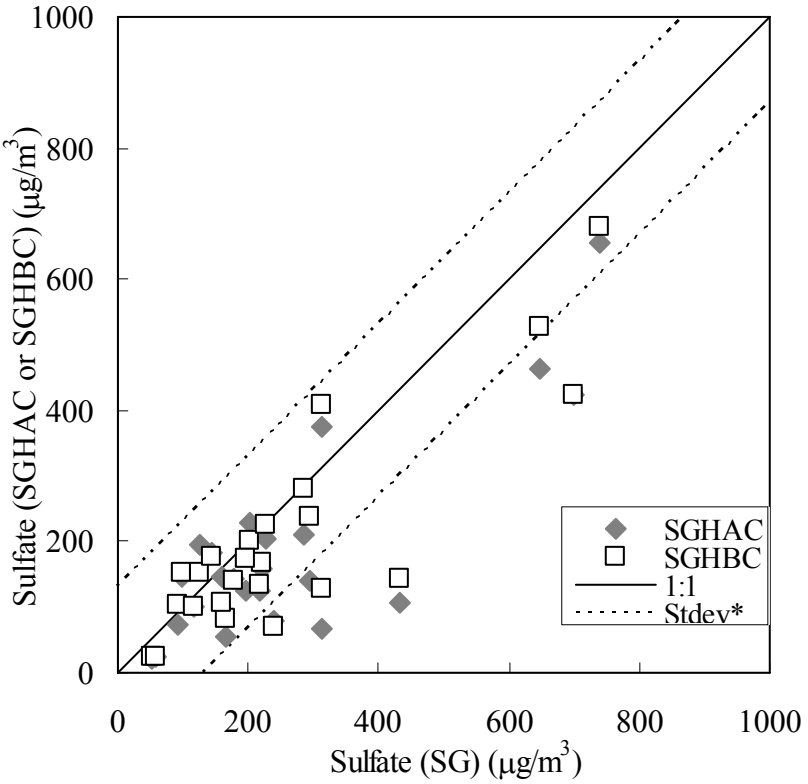

Figure 6-6. Sulfate mass balance between SG and SGHAC/SGHBC (Stdev*: standard deviation of the residual sulfate)

CHAPTER 7
CONCLUSIONS

Aerosol sampling using the dichotomous sampler, NIOSH Method 7903, and a cascade impactor was carried out at five types of locations at eight phosphate plants and two background sites to determine the worker exposure to sulfuric acid mist concentration in phosphate fertilizer plants. Artifact sulfate observed in using NIOSH Method 7903 for sampling in phosphate fertilizer manufacture process was also investigated in this study. To minimize the artifact sulfate, two methods were developed. Five conclusions can be drawn from this study.

Conclusion 1

The highest sulfate concentration, 0.185 mg/m^3, in the plants was obtained at the sulfuric acid pump tank area. Should monitoring of personal exposure to sulfuric acid mist be required, efforts should focus on workers with activities in this area where concentrations approach than the TLV-TWA standard of 0.2 mg/m^3 recommended by ACGIH for the thoracic fraction of sulfuric acid aerosol. At the attack tank area, fluoride was the dominant species and the maximum fluoride concentration in PM_{10} was 462 $\mu g/m^3$. At the rotating table/belt filter floor, phosphoric acid is separated from gypsum by rotating table/belt filter and the high temperature is favorable for the evaporation of phosphoric acid and the maximum phosphate concentration in PM_{10} was 170 $\mu g/m^3$. On a scrub day, a weak sulfuric acid solution is used to clean the piping and ductwork of the granulator for an average of 4 hours per day. Particulate sulfate concentrations were low during the scrubbing activity. At the truck loading/unloading station, the possible emission period is around 2-3 h/day, and this emission is not continuous. The concentration levels at the loading/unloading station were low and were greatly influenced by outdoor conditions.

Conclusion 2

Based on cascade impactor sampling, sulfuric acid pump tank areas still had higher sulfuric acid mist concentrations than other types of locations, and sulfuric acid was the dominant chemical species. When high sulfuric acid concentrations were identified, the aerosols were dominantly in the coarse mode. The most likely cause for high sulfuric acid concentrations at this location is the leakage of SO_3. According to the impactor sampling results, 7 samples (total: 72) exceeded the ACGIH recommendation (0.2 mg/m^3, thoracic fraction), and 2 samples (total: 72) were above the OSHA regulation (1 mg/m^3, total concentration). Meanwhile, there were 7 samples (total: 78) by the NIOSH method that exceeded the OSHA regulation. The sulfuric acid mist concentrations from the NIOSH method were higher than those from the cascade impactor for the dominating majority of samples. The possible reason for this variation is the interaction between SO_2 and silica gel/glass fiber.

Conclusion 3

In phosphate fertilizer facilities, phosphoric acid and sulfuric acid mists were the major aerosol components for the product filter floors and the sulfuric acid pump tank areas, respectively. The possible source of phosphoric acid was evaporation and then condensation when it encountered cooler air. The current OSHA 8-hour TWA - PEL of phosphoric acid and sulfuric acid mist set at 1 mg/m^3 was not exceeded on average, but could be exceeded at the product filter floors and the pump tank areas, respectively. It should be noted that workers spend much less than 8 hours per day in the area, and thus the true time-weighted exposure level can be expected to be lower. Calcium and ammonium were the major species to neutralize the aerosol acidity at the sulfuric pump tank areas when acid loading was low. The aerosol thermodynamic model showed the modes of aerosol H^+ concentration in 1.8 –3.8 μm and 3.8 –10 μm for the aerosols with high sulfuric acid mist concentrations. These hygroscopic acid mists can grow in

the high humidity condition in the upper respiratory system, and aerosols with high H^+ concentrations mainly deposit in the upper respiratory system. Sulfuric acid was found to play a much more prominent role than phosphoric acid. The respiratory deposition projection of sulfuric acid mists is consistent with that of H^+ ion and both components mainly deposit in the human head airway. However, extensive epidemiological studies of phosphate industry workers have not shown an increased incidence of any type of cancer resulting from these exposures.

Conclusion 4

The artifact sulfate of NIOSH Method 7903 originating from SO_2 gas was confirmed. SO_2 can be adsorbed by the glass fiber filter and the silica gel and the adsorbed SO_2 can be oxidized and transformed into sulfate during the extraction procedures of NIOSH Method 7903. The interference from SO_2 cannot be neglected when the sulfuric acid mist concentration is low and SO_2 concentration is high (> 0.5 ppm). The artifact sulfate can affect the compliance status of a facility and should be corrected. A deactivation model was developed to estimate the artifact sulfate concentration.

Conclusion 5

Two methods, a honeycomb denuder system and a deactivation model, were applied to minimize the artifact sulfate concentration. The honeycomb denuder system efficiently adsorbed SO_2 before it entered the silica gel tube while the deactivation model was employed to calculate the artifact sulfate concentration. Both methods were proven to reduce the artifact. However, the sulfate concentrations from both methods were still higher than the sulfate concentration from the cascade impactor. One likely reason is the residual sulfate from the silica gel tube, which yields a mean artifact sulfate equivalent to 79.5 $\mu g/m^3$ for 8-h sampling.

LIST OF REFERENCES

ACGIH (2004), Sulfuric acid. TLV Chemical Substances. 7th Edition Documentation, 1-12.

Acker, K., D. Moller, R. Auel, and D. Kalass (2005), Concentrations of nitrous acid, nitric acid, nitrite and nitrate in the gas and aerosol phase at a site in the emission zone during ESCOMPTE 2001 experiment, *Atmos. Res.*, *74*, 507-524.

Apol, A. G., and M. Singal (1987), Health Hazard Evaluation, J. R. Simplot Company, Pocatello, ID, National Institute for Occupational Safety and Health, Cincinnati, Ohio.

Baron, P. A., and K. Willeke (2001), *Aerosol Measurement: Principles, Techniques, and Applications*, 2nd ed., 1131 pp., Wiley, New York.

Bassett, M., and J. H. Seinfeld (1983), Atmospheric equilibrium-model of sulfate and nitrate aerosols, *Atmos. Environ.*, *17*, 2237-2252.

Becker, P. (1989), Industry process chemistry. Chapter 2., in *Phosphates and Phosphoric Acid: Raw Materials, Technology, and Economics of the Wet Process*, edited by P. Becker, pp. 43-177, Marcel Dekker, New York.

Becker, P. (1989), *Phosphates and Phosphoric Acid: Raw Materials, Technology, and Economics of the Wet Process*, 2nd ed., 740 pp., Marcel Dekker, Inc., New York.

Benjamin, M. M. (2002), *Water Chemistry*, 668 pp., McGraw-Hill, Boston.

Bhaskaran, R., N. Palaniswamy, N. S. Rengaswamy, and M. Jayachandran (2004), Cost of corrosion in fertilizer industry - A case study, *Mater. Corros.*, *55*, 865-871.

Blair, A., and N. Kazerouni (1997), Reactive chemicals and cancer, *Cancer Causes Control*, *8*, 473-490.

Block, G., G. M. Matanoski, R. Seltser, and T. Mitchell (1988), Cancer morbidity and mortality in phosphate workers, *Cancer Res.*, *48*, 7298-7303.

Brockmann, J. E. (2001), Sampling and Transport of Aerosols, in *Aerosol Measurement: Principles, Techniques, and Applications*, edited by P. A. Baron and K. Willeke, pp. 143-195, Wiley, New York.

Cassady, M. E., H. Donaldson, and S. Gentry. (1975), Industrial hygiene survey report of Agrico Chemical Company, Pierce, Florida, June 22-26, 1975., National Institute for Occupational Safety and Health, Cincinnati, OH.

Cassinelli, M. E. (1986), Laboratory evaluation of silica-gel sorbent tubes for sampling hydrogen-fluoride, *Am. Ind. Hyg. Assoc. J.*, *47*, 219-224.

Cassinelli, M. E., and D. G. Taylor (1980), Monitoring for airborne inorganic acids, *Abstracts of Papers of the American Chemical Society*, *180*, 39.

Cassinelli, M. E., and D. G. Taylor (1981), Monitoring for airborne inorganic acids, *Am. Chem. Soc. Symp. Ser.*, *149*, 137-152.

Cassinelli, M. E., and P. M. Eller (1979), Ion chromatographic determination of hydrogen fluoride, paper presented at Annual Conference, American Industrial Hygiene Conference and Exposition, Chicago, IL, 27 May - 1 June.

CFR Table Z-1 Limits for Air Contaminants, CFR (Code of Federal Regulation).

Checkoway, H., R. M. Mathew, J. L. S. Hickey, C. M. Shy, R. L. Harris, E. W. Hunt, and G. T. Waldma (1985a), Mortality among workers in the Florida phosphate industry.1. Industry-wide cause-specific mortality patterns, *J. Occup. Environ. Med.*, *27*, 885-892.

Checkoway, H., R. M. Mathew, J. L. S. Hickey, C. M. Shy, R. L. Harris, E. W. Hunt, and G. T. Waldma (1985b), Mortality among workers in the Florida phosphate industry.2. Cause-specific mortality relationships with work areas and exposures, *J. Occup. Environ. Med.*, *27*, 893-896.

Checkoway, H., N. J. Heyer, and P. A. Demers (1996), An updated mortality follow-up study of Florida phosphate industry workers, *Am. J. Ind. Med.*, *30*, 452-460.

Chen, C. C., C. H. Wu, S. H. Huang, and Y. M. Kuo (2002), Aerosol penetration through silica gel tubes, *Aerosol Sci. Technol.*, *36*, 457-468.

Chow, J. C. (1995), Measurement methods to determine compliance with ambient air-quality standards for suspended particles, *J. Air Waste Manage. Assoc.*, *45*, 320-382.

Clarke, A. G., and M. Radojevic (1983), Chloride-ion effects on the aqueous oxidation of SO_2, *Atmos. Environ.*, *17*, 617-624.

Coutant, R. W. (1977), Effect of environmental variables on collection of atmospheric sulfate, *Environ. Sci. Technol.*, *11*, 873-878.

Denzinger, H. F. J., H. J. Konig, and G. E. W. Kruger (1979), Fluorine recovery in the fertilizer industry - a review, *Phosphor. Potassium*, *103*, 33-39.

Dibb, J. E., R. W. Talbot, G. Seid, C. Jordan, E. Scheuer, E. Atlas, N. J. Blake, and D. R. Blake (2002), Airborne sampling of aerosol particles: Comparison between surface sampling at Christmas Island and P-3 sampling during PEM-Tropics B, *J Geophys Res-Atmos*, *108*, Art. No. 8230.

Divita, F., J. M. Ondov, and A. E. Suarez (1996), Size spectra and atmospheric growth of V-containing aerosol in Washington, DC, *Aerosol Sci. Technol.*, *25*, 256-273.

Dong, S., and P. K. Dasgupta (1986), On the formaldehyde-bisulfite-hydroxymethane-sulfonate equilibrium, *Atmos. Environ.*, *20*, 1635-1637.

Englander, V., A. Sjoberg, L. Hagmar, R. Attewell, A. Schutz, T. Moller, and S. Skerfving (1988), Mortality and cancer morbidity in workers exposed to sulfur-dioxide in a sulfuric-acid plant, *Int. Arch. Occ. Env. Hea.*, *61*, 157-162.

FDEP (2003), Florida Air Monitoring Report 2003, edited by A. R. Management, pp. 7.1-7.10, Florida Department of Environmental Protection, Tallahassee, Florida.

Finlayson-Pitts, B. J., and J. N. Pitts (2000), *Chemistry of the Upper and Lower Atmosphere: Theory, Experiments and Applications*, 969 pp., Academic Press, San Diego, Cali.

FIOH (1990), Industrial hygiene measurements, 1950-69 (data base), Finnish Institute of Occupational Health, Helsinki (Finland).

Fox, D. L., and H. E. Jeffries (1979), Air-Pollution, *Anal. Chem.*, *51*, R22-R34.

Fuller, E. C., and R. H. Crist (1941), The rate of oxidation of sulfite ions by oxygen, *J. Amer. Chem. Soc.*, *63*, 1644 - 1650.

Hagmar, L., T. Bellander, C. Andersson, K. Linden, R. Attewell, and T. Moller (1991), Cancer morbidity in nitrate fertilizer workers, *Int. Arch. Occup. Environ. Health.*, *63*, 63-67.

Hayami, H. (2005), Behavior of secondary inorganic species in gaseous and aerosol phases measured in Fukue Island, Japan, in dust season, *Atmos. Environ.*, *39*, 2243-2248.

Healy, J., S. D. Bradley, C. Northage, and E. Scobbie (2001), Inhalation exposure in secondary aluminium smelting, *Ann. Occup. Hyg.*, *45*, 217-225.

Hinds, W. C. (1999), *Aerosol Technology: Properties, Behavior, and Measurement of Airborne Particles*, 2nd ed., 483 pp., John Wiley & Sons, Inc., New York.

Hodge, C. A., and N. N. Popovici (1994), *Pollution Control in Fertilizer Production*, Marcel Dekker, Inc., New York.

Horton, K. D., and J. P. Mitchell (1989), Water droplet fragmentation in an Andersen Mark-III in-stack cascade impactor, *J. Aerosol Sci.*, *20*, 1585-1588.

Howell, S., A. A. P. Pszenny, P. Quinn, and B. Huebert (1998), A field intercomparison of three cascade impactors, *Aerosol Sci. Technol.*, *29*, 475-492.

Hsu, Y. M., C. Y. Wu, D. A. Lundgren, and B. K. Birky (2007a), Chemical characteristics of aerosol mists in phosphate fertilizer manufacturing facilities, *J. Occup. Environ. Hyg.*, *4*, 17-25.

Hsu, Y. M., C. Y. Wu, D. A. Lundgren, and B. K. Birky (2007b), Size-resolved sulfuric acid mist concentrations at phosphate fertilizer manufacturing facilities in Florida, *Ann. Occup. Hyg.*, *51*, 81-89.

Hsu, Y. M., J. Kollett, K. Wysocki, C. Y. Wu, D. A. Lundgren, and B. K. Birky (2007c), Positive artifact sulfate formation from SO_2 adsorption in the silica gel sampler used in NIOSH Method 7903, *Environ. Sci. Technol.*, *41*, 6205-6209.

Huang, Z., R. M. Harrison, A. G. Allen, J. D. James, R. M. Tilling, and J. X. Yin (2004), Field intercomparison of filter pack and impactor sampling for aerosol nitrate, ammonium, and sulphate at coastal and inland sites, *Atmos. Res.*, *71*, 215-232.

Huss, A., P. K. Lim, and C. A. Eckert (1978), Uncatalyzed oxidation of sulfur(IV) in aqueous-solutions, *J. Amer. Chem. Soc.*, *100*, 6252-6253.

IARC (1992), IARC Monograph on the Evaluation of Carcinogenic Risks to Humans, Vol. 54, *Occupational Exposures to Mists and Vapours from Strong Inorganic Acids; and Other Industrial Chemicals*, 336 pp., International Agency for Research on Cancer (IARC). Lyon, France.

ICRP (1994), *Human Respiratory Tract Model for Radiological Protection*, Elsevier Science, Tarrytown, NY.

Jacobson, M. Z. (1999), Chemical equilibrium and dissolution processes, in *Fundamentals of Atmospheric Modeling*, edited, pp. 553-597, Cambridge University Press, New York.

Jiang, C. F. (1996), Thermodynamics of aqueous phosphoric acid solution at 25 degrees C, *Chem. Eng. Sci.*, *51*, 689-693.

Jonnalagadda, S. B., M. Nyagani, P. Sawunyama, and R. Baloyi (1991), Studies on the levels of sulfur-dioxide, nitrogen-dioxide, ammonia, and hydrogen-chloride in ambient air of Harare, Zimbabwe, *Environ. Int.*, *17*, 461-467.

Kim, Y. P., J. H. Seinfeld, and P. Saxena (1993), Atmospheric gas-aerosol equilibrium.2. Analysis of common approximations and activity-coefficient calculation methods, *Aerosol Sci. Technol.*, *19*, 182-198.

Kopac, T., and S. Kocabas (2002), Adsorption equilibrium and breakthrough analysis for sulfur dioxide adsorption on silica gel, *Chem. Eng. Process.*, *41*, 223-230.

Koutrakis, P., C. Sioutas, S. T. Ferguson, J. M. Wolfson, J. D. Mulik, and R. M. Burton (1993), Development and evaluation of a glass honeycomb denuder filter pack system to collect atmospheric gases and particles, *Environ. Sci. Technol.*, *27*, 2497-2501.

Larson, T. V., N. R. Horike, and H. Harrison (1978), Oxidation of sulfur-dioxide by oxygen and ozone in aqueous-solution - kinetic study with significance to atmospheric rate processes, *Atmos. Environ.*, *12*, 1597-1611.

Lee, K. W., and R. Mukund (2001), Filter collection, in *Aerosol Measurement: Principles, Techniques, and Applications*, edited by P. A. Baron and K. Willeke, pp. 197-220, Wiley, New York.

Lue, S. J., T. Wu, H. Hsu, and C. Huang (1998), Application of ion chromatography to the semiconductor industry I. Measurement of acidic airborne contaminants in cleanrooms, *J. Chromatogr. A*, *804*, 273-278.

Lunsford, J. H. (1979), Surface Reactions of Oxides of Sulfur, U.S. Environmental Protection Agency, Research Triangle Park, NC.

Mann, H. C. (1992), Ammonium phosphates, in *Air Pollution Engineering Manual*, edited by A. J. Buonicore and W. T. Davis, pp. 574-576, Van Nostrand Reinhold, New York.

Meng, Z. Q., and B. Zhang (1997), Chromosomal aberrations and micronuclei in lymphocytes of workers at a phosphate fertilizer factory, *Mutat. Res.*, *393*, 283-288.

Meng, Z. Q., and L. Z. Zhang (1990), Chromosomal-aberrations and sister-chromatid exchanges in lymphocytes of workers exposed to sulfur-dioxide, *Mutat. Res.*, *241*, 15-20.

Meng, Z. Q., H. Q. Meng, and X. L. Cao (1995), Sister-chromatid exchanges in lymphocytes of workers at a phosphate fertilizer factory, *Mutat. Res.*, *334*, 243-246.

Meng, Z. Y., and J. H. Seinfeld (1996), Time scales to achieve atmospheric gas-aerosol equilibrium for volatile species, *Atmos. Environ.*, *30*, 2889-2900.

Messnaoui, B., and T. Bounahmidi (2005), Modeling of excess properties and vapor - liquid equilibrium of the system H_3PO_4 - H_2O, *Fluid Phase Equilib.*, *237*, 77-85.

Miller, J. M., and R. G. D. Pena (1972), Contribution of scavenged sulfur-dioxide to sulfate content of rain water, *J. Geophys. Res.*, *77*, 5905-5916.

Muller, T. L. (1992), Sulfuric acid, in *Air Pollution Engineering Manual*, edited by A. J. Buonicore and W. T. Davis, pp. 469-476, Air & Waste Management Association, Pittsburgh, PA.

Munger, J. W., C. Tiller, and M. R. Hoffmann (1986), Identification of hydroxymethanesulfonate in fog water, *Science*, *231*, 247-249.

NIOSH (1994), NIOSH Method No. 7903, in *NIOSH Manual of Analytical Methods*, edited by P.C. Schlecht and P.F. O'Connor, National Institute for Occupational Safety and Health (NIOSH), Cincinnati, OH.

Ortiz, L. W., and C. I. Fairchild (1976), Aerosol Research and Development Related to Health Hazard Analysis, US Energy Research and Development Administration.

Ostro, B. D., M. J. Lipsett, M. B. Wiener, and J. C. Selner (1991), Asthmatic responses to airborne acid aerosols, *Am. J. Public Health*, *81*, 694-702.

Palm, G. F. (1992), Phosphoric acid manufacturing, in *Air Pollution Engineering Manual*, edited by A. J. Buonicore, et al., pp. 439-446, Van Nostrand Reinhold, New York.

Parish, W. R. (1994), Phosphoric acid by wet process: recovery of fluorine-containing gases, in *Pollution control in fertilizer production*, edited by C. A. Hodge and N. N. Popovici., pp. 197-208, Dekker, New York.

Pathak, R. K., and C. K. Chan (2005), Inter-particle and gas-particle interactions in sampling artifacts of $PM_{2.5}$ in filter-based samplers, *Atmos. Environ.*, *39*, 1597-1607.

Pauluhn, J. (2005), Retrospective analysis of acute inhalation toxicity studies: Comparison of actual concentrations by filter and cascade impactor analyses, *Regul. Toxicol. Pharm.*, *42*, 236-244.

Petrov, G. A. (1987), Sanation of working-conditions and environment for the process of sulfuric acid manufacture from metallurgical gases (Russ), *Gig Sanit*, 70-71.

Possanzini, M., A. Febo, and A. Liberti (1983), New design of a high-performance denuder for the sampling of atmospheric pollutants, *Atmos. Environ.*, *17*, 2605-2610.

Radojevic, M. (1984), On the discrepancy between reported studies of the uncatalyzed aqueous oxidation of SO_2 by O_2, *Environ. Technol. Lett.*, *5*, 549-566.

Ridler, E. S. (1959), Chamber process for the manufacture of sulfuric acid, in *The Manufacture of Sulfuric Acid*, edited by W. W. Dueker and J. R. West, Reinhold Publishing Corporation, New York.

Sathiakumar, N., E. Delzell, Y. Amoateng-Adjepong, R. Larson, and P. Cole (1997), Epidemiologic evidence on the relationship between mists containing sulfuric acid and respiratory tract cancer, *Crit. Rev. Toxicol.*, *27*, 233-251.

Schlesinger, R. B. (1984), Comparative irritant potency of inhaled sulfate aerosols - effects on bronchial mucociliary clearance, *Environ. Res.*, *34*, 268-279.

Schlesinger, R. B. (1989), Factors affecting the response of lung clearance systems to acid aerosols - role of exposure concentration, exposure time, and relative acidity, *Environ. Health Perspect.*, *79*, 121-126.

Schlesinger, R. B., and L. C. Chen (1994), Comparative biological potency of acidic sulfate aerosols - Implications for the interpretation of laboratory and field studies, *Environ. Res.*, *65*, 69-85.

Schlesinger, R. B., L. C. Chen, I. Finkelstein, and J. T. Zelikoff (1990a), Comparative potency of inhaled acidic sulfates - speciation and the role of hydrogen ion, *Environ. Res.*, *52*, 210-224.

Schlesinger, R. B., A. F. Gunnison, and J. T. Zelikoff (1990b), Modulation of pulmonary eicosanoid metabolism following exposure to sulfuric acid, *Fundam. Appl. Toxicol.*, *15*, 151-162.

Schroeter, L. C. (1963), Kinetics of air oxidation of sulfurous acid salts, *J. Pharm. Sci.*, *52*, 559-563.

Scott, W. D., and P. V. Hobbs (1967), Formation of sulfate in water droplets, *J. Atmos. Sci.*, *24*, 54-57.

Seinfeld, J. H., and S. N. Pandis (1998), Thermodynamics of aerosols, in *Atmospheric Chemistry and Physics from Air Pollution to Climate Change*, pp. 491-544, John Wiley, New York.

Sioutas, C., P. Y. Wang, S. T. Ferguson, P. Koutrakis, and J. D. Mulik (1996), Laboratory and field evaluation of an improved glass honeycomb denuder filter pack sampler, *Atmos. Environ.*, *30*, 885-895.

Skyttä, E. (1978), Tilasto työhygieenisistä mittauksista v. 1971-1976 [Statistics of industrial hygiene measurements in 1971-1976]. Institute of Occupational Health, Helsinki (Finland).

Stayner, L., A. B. Smith, G. Reeve, L. Blade, L. Elliott, R. Keenlyside, and W. Halperin (1985), Proportionate mortality study of workers in the Garment Industry exposed to formaldehyde, *Am. J. Ind. Med.*, *7*, 229-240.

Steenland, K. (1997), Laryngeal cancer incidence among workers exposed to acid mists (United States), *Cancer Causes Control*, *8*, 34-38.

Stephenson, F., M. Cassady, H. Donaldson, and T. Boyle (1977), Industrial Hygiene Survey, CF Chemicals, Inc., Bartow, FL, August 9-12, 1976., National Institute for Occupational Safety and Health, Cincinnati, OH.

Stephenson, F., M. Cassady, H. Donaldson, and T. Boyle (1977), Industrial Hygiene Survey, IMC, Phosphate Chemical Complex, New Wales, Florida, National Institute for Occupational Safety and Health, Cincinnati, OH.

Stratmann, H., and M. Buck (1965), Comparative measurements using silica-gel and TCM procedures for determining-sulfur-dioxide in the atmosphere, *Ai.r Water. Pollut.*, *9*, 199-218.

Swenberg, J. A., and R. O. Beauchamp (1997), A review of the chronic toxicity, carcinogenicity, and possible mechanisms of action of inorganic acid mists in animals, *Crit. Rev. Toxicol.*, *27*, 253-259.

Swietlicki, E., H. C. Hansson, B. Martinsson, B. Mentes, D. Orsini, B. Svenningsson, A. Wiedensohler, M. Wendisch, S. Pahl, P. Winkler, R. N. Colvile, R. Gieray, J. Luttke, J. Heintzenberg, J. N. Cape, K. J. Hargreaves, R. L. StoretonWest, K. Acker, W. Wieprecht, A. Berner, Kruisz, C., M. C. Facchini, P. Laj, S. Fuzzi, B. Jones, and P. Nason (1997), Source identification during the Great Dun Fell Cloud Experiment 1993, *Atmos. Environ.*, *31*, 2441-2451.

Tadzhibaeva, N. S., and I. V. Gol'eva (1976), Industrial hygiene and condition of the upper respiratory tract of people working in the production of superphosphate in Uzbekistan, Russia, *Med. Zh. Uzb.*, *4*, 57-59.

Tanaka, S., K. Yamanaka, and Y. Hashimoto (1987), Measurement of concentration and oxidation rate of S(IV) in rainwater in Yokohama, Japan, *Am. Chem. Soc. Symp. Ser.*, *349*, 158-169.

Tsai, C. J., C. H. Huang, and S. H. Wang (2001), Collection efficiency and capacity of three samplers for acidic and basic gases, *Environ. Sci. Technol.*, *35*, 2572-2575.

Tsai, C. J., C. H. Huang, and H. H. Lu (2004), Adsorption capacity of a nylon filter of filter pack system for HCl and HNO_3 gases, *Sep. Sci. Technol.*, *39*, 629-643.

USDHHS (2005), *Report on Carcinogens*, Eleventh ed., U.S. Department of Health and Human Services, Public Health Service, National Toxicology Program, Research Triangle Park, NC.

USEPA (1995), *Compilation of Air Pollutant Emissions Factors Volume 1: Stationary Point and Area Sources, Fifth Edition with Supplements, Document No. AP-42.*, U.S. Environmental Protection Agency, Research Triangle Park, NC.

Wagner, J., and D. Leith (2001), Passive aerosol sampler. Part II: Wind tunnel experiments, *Aerosol Sci. Technol.*, *34*, 193-201.

Wallingford, K. M., and E. M. Snyder (2001), Occupational exposures during the World Trade Center disaster response, *Toxicol. Ind. Health*, *17*, 247-253.

Watson, J. G., and J. C. Chow (2001), Ambient air sampling, in *Aerosol Measurement: Principles, Techniques and Applications*, edited by P. A. Baron and K. Willeke, pp. 821-844, Wiley, New York.

Watson, J. G., G. Thurston, N. Frank, J. P. Lodge, R. W. Wiener, F. F. McElroy, M. T. Kleinman, P. K. Mueller, A. C. Schmidt, F. W. Lipfert, R. J. Thompson, P. K. Dasgupta, D. Marrack, R. A. Michaels, T. Moore, S. Penkala, I. Tombach, L. Vestman, T. Hauser, and J. C. Chow (1995), 1995 Critical-review discussion - measurement methods to determine compliance with ambient air-quality standards for suspended particles, *J. Air Waste Manage. Assoc.*, *45*, 666-684.

Weast, R. C. (1988), CRC Handbook of Chemistry and Physics, edited, CRC Press, Boca Raton, Fla.

Wu, C. Y., and P. Biswas (1998), Particle growth by condensation in a system with limited vapor, *Aerosol Sci. Technol.*, *28*, 1-20.

Yadav, J. S., and V. K. Kaushik (1996), Effect of sulphur dioxide exposure on human chromosomes, *Mutat. Res.-Envir. Muta.*, *359*, 25-29.

Yao, X. H., T. Y. Ling, M. Fang, and C. K. Chan (2006), Comparison of thermodynamic predictions for in situ pH in $PM_{2.5}$, *Atmos. Environ.*, *40*, 2835-2844.

Yao, X. H., T. Y. Ling, M. Fang, and C. K. Chan (2007), Size dependence of in situ pH in submicron atmospheric particles in Hong Kong, *Atmos. Environ.*, *41*, 382-393.

Yasyerli, S., G. Dogu, I. Ar, and T. Dogu (2001), Activities of copper oxide and Cu-V and Cu-Mo mixed oxides for H_2S removal in the presence and absence of hydrogen and predictions of a deactivation model, *Ind. Eng. Chem. Res.*, *40*, 5206-5214.

BIOGRAPHICAL SKETCH

Yu-Mei Hsu was born in 1975 in Hsin-Chu, Taiwan. She received her B.S. degree in environmental engineering in June 1999 at National Cheng-Kung University, Taiwan. She was awarded the Phi Tau Phi Scholastic Honor which awarded the first ranking student among 53 students. She also earned her M.S. degree in environmental engineering sciences in June 2001 at National Taiwan University, Taiwan. Her master's thesis, the Chloride Loss of Sea-Salt Aerosols, was awarded the Outstanding Master's Thesis Award from National Taiwan University and National Science Council, Taiwan.

She joined the research group of Dr. Chang-Yu Wu at the University of Florida in 2004 and started pursuing her Ph.D. degree in the Department of Environmental Engineering Sciences. Her research focused on the sulfuric acid mist sampling at the phosphate fertilizer plants. Yu-Mei Hsu was the vice-president, secretary, and webmaster of the student chapter of Air & Waste Management Association (A&WMA) at the University of Florida from 2005 to 2007. She was awarded the Axel Hendrickson Scholarship Award from Florida Section A&WMA in 2006, and also was awarded the AWMA Scholarship (2^{nd} place in air quality) from A&WMA in 2007.